X-622-74-238
PREPRINT
NASA TM X- 70735

FOURIER SPECTROSCOPY IN PLANETARY RESEARCH

R. A. HANEL
V. G. KUNDE

AUGUST 1974

GODDARD SPACE FLIGHT CENTER
GREENBELT, MARYLAND

FOURIER SPECTROSCOPY

AND

PLANETARY RESEARCH

R. A. Hanel and V. G. Kunde

Goddard Space Flight Center
Greenbelt, Maryland

ABSTRACT

The application of Fourier Transform Spectroscopy (FTS) to planetary research is reviewed. The survey includes FTS observations of the Sun, all the planets except Uranus and Pluto, the Galilean satellites and Saturn's rings. Instrumentation and scientific results are considered. The prospects and limitations of FTS for planetary research in the forthcoming years are discussed.

Table of Contents

1. INTRODUCTION

At first it may seem strange to simultaneously review a particular instrumental technique in spectroscopy and a particular area of astronomical research. However, both subjects are more closely associated with each other than one might suspect. Much of the motivation for advancing Fourier Transform Spectroscopy (FTS) has originated from research in astronomy; in particular, observations of the planets have permitted full exploitation of the well known advantages of this technique. Many of the advances in planetary exploration during recent years have been made with Fourier spectrometers, mostly from ground-based observatories, but also from aircraft and space vehicles. Therefore, it is not surprising that both subjects have often been discussed together. Planetary research and Fourier spectroscopy have been previously reviewed by Hunten (1968) and by Connes (1970). The purpose of this paper is to review progress made in the exploration of the solar system by means of Fourier spectroscopy between approximately 1968 and 1973, although some references are as recent as 1974. The application of Fourier Transform Spectroscopy to chemical emission spectroscopy, nuclear magnetic resonance spectroscopy and other disciplines may be found in reviews by Becker and Farrar (1972) and Griffiths, et al., (1972).

Some readers may be surprised to find in this review no discussion of the basic concepts of Fourier spectroscopy. We feel the principles are now well established, well documented and need not be repeated. At this time, a review of the subject does not even have to elaborate explicitly on the advantages of Fourier spectroscopy; however, the advantages become apparent in the discussions of the results and prospects for the future.

The reader primarily interested in the basic theories and techniques of FTS is referred to the thesis of Madame Connes (1961), the review paper by Vanasse and Sakai (1967), the books by Mertz (1965), Bell (1972), and Brigham (1974), and the Proceedings of the 1970 Aspen International Conference on Fourier Spectroscopy, (Vanasse , et al. 1971) which contains several tutorial articles as well as papers reflecting the state of the art about 1970. A comprehensive treatment of the theoretical aspects of FTS is contained in the thesis by Pilcher (1973).

The reader primarily interested in planetary research may find summaries on the present knowledge of the planets in the following review papers and conference reports. Text books on the subject are fairly well out of date due to the wealth of data obtained from ground-based and space probe measurements during recent years. Recent information on Mercury is available in Science (185, 1974). A summary of the knowledge of Venus before Mariner 10 is given by Marov (1972); preliminary results from Mariner 10 are presented in Science (183, 1974). Earth has recently been discussed by Houghton and Taylor (1973). Up to date summaries on Mars may be found in the papers presented at the Symposium on Planetary Atmospheres and Surfaces, Madrid, Spain, 10-13 May 1972, published in ICARUS, 17, (1972) and 18, (1973), and in the Mariner 9 results published in JGR, 78, July 10, (1973). The outer planets have been reviewed by Newburn and Gulkis (1973) and all planets by Hunten (1971), Sagan et al. (1971), and Fox (1972).

To review the subject matter, we summarize in Chapter 2 planetary observations obtained by means of Fourier spectroscopy.

It is apparent from this review that the field has grown substantially within the last few years. Several astronomical observatories now routinely use Fourier spectrometers in their planetary observation program and a Michelson interferometer has been carried as far as Mars by the Mariner 9 spacecraft. In the review of planetary observations we include measurements of the Earth when it has been observed from space. We omit, however, laboratory work although it is often relevant to planetary research. Some measurements in the Earth's atmosphere have also been included particularly when they can be interpreted in terms of the transmission and emission properties of the atmosphere, because both parameters play an important role in the planning of future observations of the planets from the ground, from aircraft, and from balloons as well. The numerous investigations of infrared airglow with Fourier spectrometers are considered to be beyond the scope of this review; summaries of developments in this field have been given by Vanasse, et al. (1971) and Jones (1973).

The third chapter deals with instrumentation. It is rather difficult to categorize the great variety of techniques in use today; however, certain patterns have developed, and certain questions may be discussed. For example, the relative merits of cat's eye retroreflectors and flat mirrors, of the stepping mode and the continuous mode of mirror motion, and of internal modulation.

The fourth chapter discusses the significance of results obtained by Fourier spectroscopy. FTS observations have been reported for the Sun, all the planets except Uranus and Pluto, the Galilean satellites

and Saturn's rings. The scientific results will be reviewed separately for each of the above objects. The last chapter of this review is devoted to a discussion of the potential and the limitations of FTS.

2. OBSERVATIONS

In the last several years planetary science has been advanced by the interpretation of a large body of new and exciting observational information. A substantial fraction of this new evidence was derived from infrared planetary spectra taken with Fourier spectrometers. FTS is particularly successful in the infrared because the available detectors in this region are limited mostly by noise which is independent of the incident flux and therefore the multiplex advantage can fully be exploited (Felgett, 1958). Improvement factors over conventional techniques of up to several hundred have been realized from the multiplex advantage alone. The area times solid angle ($A\Omega$, throughput, or etendue) advantage of the Michelson interferometer is also substantial (Jacquinot, 1960), but in many cases Earth based observers have been limited in $A\Omega$ by the telescope rather than by the interferometer. Considering also the wavenumber precision and the radiometric accuracy inherent in interferometers, it is not surprising that substantial advances in planetary observations can now be reviewed. Not all the credit for these advances can be claimed by the multiplex and $A\Omega$ advantages of FTS; partial credit must be given to simultaneous improvements in detector technology. In particular, the development of helium cooled bolometers by Low (1961) helped advance observations in the far and intermediate-infrared while perfection of photoconductors has helped in the near-infrared region.

For purposes of this paper the spectral range is subdivided into the far-infrared (10 to 200 cm^{-1} or 50 to 1000 μm), the intermediate-infrared (200 to 2000 cm^{-1} or 5 to 50 μm), and the near-infrared (2000 to 10000 cm^{-1} or 1 - 5 μm). Below 10 cm^{-1} radio frequency techniques are more applicable and narrow band receivers of high sensitivity are available. The boundary between far and intermediate-infrared has been chosen rather arbitrarily; primarily by considerations of technique rather than by physical processes. In the intermediate-infrared beam-splitters are normally deposited on transparent substrates such as potassium bromide (KBr) or cesium iodide (CsI) while in the far-infrared quarter-wave diaphragms of mylar or of similar materials or wire grids are preferred. The boundary between near and intermediate-infrared (2000 cm^{-1}) corresponds approximately to the division between preponderance of thermal emission and reflected solar radiation in planetary spectra, (see Figure 1).

The region above approximately 10,000 cm^{-1} (below 1 μm), the visible and the immediately adjacent infrared, has traditionally been the domain of the photographic plate and the photomultiplier. The photographic plate offers the multiplex advantage with a conventional prism or grating spectrometer, and the photomultiplier, particularly in the photon counting mode, is limited by noise proportional to the incoming flux. In that case, the multiplex advantage of Fourier spectrometers does not yield an improvement over conventional methods. Other considerations, such as wavenumber precision, for example, make Fourier spectroscopy still attractive even in the visible and possibly in the ultraviolet, but so

far the most spectacular results have been obtained in the infrared.

Fourier spectroscopy has been applied to planetary research by a large number of observers located at several institutions primarily in England, France, and the U.S. Observational programs in the far, intermediate, near-infrared, and visible spectral regions are summarized in Tables 1 to 4, respectively. Each table is organized around the various organizations active in infrared research with the observations by each organization listed chronologically. The tables are not inclusive with respect to references to instrumentation or results; these areas are treated fully in the appropriate sections.

The extensive effort in interferometry by the Air Force Cambridge Research Laboratories (AFCRL) group has not been included in this review as their major emphasis has been upper atmosphere physics, airglow and aurora, and laboratory spectroscopy. Some data on terrestrial transmission and emission observed from a KC-135 aircraft and spectra of the 7 March 1970 solar eclipse have been reported by Stair, et al. (1971). An overview of the Fourier spectroscopy program at AFCRL is also given in Stair, et al. (1971).

The observations are also summarized schematically in Figure 2; measurements of the Galilean satellites and the rings of Saturn are included under the associated planets. For the purpose of orientation, the transmission properties of the Earth's atmosphere from the ground at low spectral resolution are displayed at the top of Figure 2. At the operating altitudes of aircraft and balloons, the atmospheric windows are substantially larger and more transparent.

The coverage of the far-infrared region is extensive for the Earth with only a few observations existing for the Sun and none for the other planets. In the intermediate-infrared, observations by Fourier spectrometers are available for most of the planets with the general exception of the 100-400 cm^{-1} region which has not been observed from the ground due to water vapor absorption in the Earth's atmosphere. Absorption by telluric CO_2 prevents ground based observations in the 550-750 cm^{-1} region; however, observations from spacecraft exist in this range for Earth and Mars. Planetary radiation in the 1000-1200 cm^{-1} range is difficult to observe due to the low radiance levels associated with this crossover region between reflected and emitted radiation, although adequate spectra exist for Venus, Earth and Mars recorded with integration times of minutes or less. Radiance levels for Jupiter and Saturn decrease by several orders of magnitude from those of the terrestrial planets in this spectral region, as shown in Figure 1. Even with the advantage of Fourier spectrometers, long integration times are required to obtain spectra with adequate signal to noise ratios.

Surprising is the absence of spectra taken with the intent to investigate the Moon; all lunar observations have been recorded for the purpose of assessing the transmission characteristics of the Earth atmosphere. Also surprising is the absence of near infrared spectra of the Earth, although they would be useful for the detection of pollutants. Before discussing in detail the results obtained by these observations, we turn to a review of the instrumentation used in making such measurements.

3. INSTRUMENTATION

A large number of different Fourier spectrometers has been applied to planetary research. Size, degree of sophistication, performance and cost of these instruments vary over wide ranges. It is again convenient to subdivide the discussion into sections on the far, intermediate and near-infrared region; however, certain characteristics which are common to all spectral ranges are discussed first.

3.1 General Design Considerations

With the exception of the balloon measurements of Stettler et al., (1974), who used a laminar grating interferometer, and the aircraft and ground observations, respectively, of Thekhakara et al., (1969) and A'Hearn et al., (1974), who used polarization interferometers, all observations pertinent to this review have been carried out with Michelson interferometers. The laminar grating interferometer has been used only in the far-infrared ($\nu \lesssim 100$ cm^{-1}) where it is very efficient

(Richards, 1964) since it operates with reflecting surfaces only. Without the need to change beamsplitters, the laminar grating interferometer can be constructed to cover a wide useful spectral range. The problems associated with laminar grating interferometers are discussed by Strong and Vanasse (1960), Dowling (1971), Steel (1971) and Bell (1972). The polarization interferometer (Mertz, 1958, 1965; Steel, 1967; A'Hearn, et al. 1974) is restricted to spectral regions where birefringent materials are available. Instruments built so far have shown only a low resolving power. Advantages of the birefringent interferometer include the measurement of the spectrum in two orthogonal planes of linear polarization simultaneously and less sensitivity to optical and mechanical tolerances than the Michelson interferometer.

While a large number of different variations of the basic Michelson concept have been proposed, (see e.g. Steel, 1971) only two main designs have seen wide application: the original flat mirror design of Michelson and the cat's eye retroreflector which offers first order compensation against tilt. Other designs such as corner reflectors or the more elaborate compensating scheme of Schindler (1970) have also been used but remain exceptions rather than the rule. It is also pertinent to discuss the relative merits of the step-by-step advancement of the Michelson mirror versus a continuous motion of the mirror at a constant velocity. A third design worth examining utilizes internal modulation. All of the design considerations implied above apply to all spectral ranges and will therefore be discussed before the summaries of instrumentation which are grouped according to spectral range. Most of the other points to be made in this review apply mainly to one instrument or to one spectral region and will thus be discussed in the chapter

devoted to the appropriate spectral region.

a) Cat's Eyes versus Flat Mirrors:

The cat's eye, which incidentally is already depicted in Michelson's original papers (see Michelson, 1927), makes the interferometer less sensitive to small misalignment of the optical reflectors than is an instrument utilizing flat mirrors. To our knowledge, the concept was first used in practice by Connes and Connes (1966). The arm of the Michelson interferometer containing the moving reflector requires precision mechanical elements to translate the mirror with negligible tilt over distances up to tens of centimeters. To overcome this severe requirement, corner reflectors (e.g. Felgett, 1958) have been used in the past, but cat's eyes should be preferred for several reasons: less polarization; use of the small mirror as a field mirror; and even use of the small mirror as a modulator for internal modulation, as discussed below. The choice between flat mirrors or cat's eyes depends on the maximum permissible tilt, which must be small compared to the ratio of wavelength to beam diameter. If a sufficiently precise drive mechanism is available then a flat mirror is a simple and efficient solution. For low and medium spectral resolution requiring mirror displacements of centimeters, such drive mechanisms have been constructed, and some are commercially available. In the far-infrared necessary tolerances can, in general, be maintained without elaborate designs.

For high spectral resolution, that is for pathlengths above 10 cm, it becomes increasingly difficult to hold the tolerances, particularly in the near-infrared; the cat's eye is then often recommended. The choices available to the designer (use of a flat mirror or a cat's eye)

may also be strongly influenced by cost considerations. It must be determined whether it is more effective to place the effort in the design of a self compensating system such as cat's eyes, or in the design of an adequate drive mechanism. Generally, however, no single recommendation can be made; the solution depends on the overall systems concept, on shop capabilities, and often on personal preferences.

b) Step-by-Step vs Continuous Motion:

In the continuous sweep mode, the path difference between both arms of the interferometer increases linearly with time, while in the step-by-step mode of operation the reflector carriage is advanced in discrete steps from one sampling point to the next. At each point the signal is averaged (integrated) before being digitized. The main motivation for the step-by-step mode is to use the minimum number of samples for a certain spectral resolution, that is for a certain mirror displacement. The step-by-step mode permits sampling intervals very close to the theoretical limit set by the Shannon sampling theorem. In the continuous mode a certain degree of oversampling is necessary because electronic filters cannot be designed with infinitely sharp cut-off frequencies; however, satisfactory operation has been achieved with sampling margins as low as 15%. Considerations of the sampling efficiency were important at the time when computational techniques to transform the interferograms into spectra were barely capable of following the rapid advances in instrumentation. Now the Cooley-Tukey method (Cooley and Tukey, 1965) permits fast and efficient Fourier transformation and the difference in the number of sample points between both methods is not as critical except for cases with very high spectral resolution, corresponding to 10^6 samples and more. The step-by-step and the continuous recording

techniques are in theory equally efficient, if one neglects the time lost by the first method while moving the mirror to a new position and re-setting the integrator (Hanel, et al., 1969). The choice between both techniques should again depend on systems and cost considerations.

c) Internal Modulation:

The idea of internal modulation was originally proposed by Mertz (1965) but first successfully implemented by Connes and Connes (1966). Internal modulation superimposes an oscillatory motion on the step-by-step or continuous displacement of the Michelson mirror. The amplitude of this superimposed oscillation must be kept smaller than one-half of the shortest wavelengths of interest and the frequency high compared to the stepping frequency or to the highest signal frequency in the case of continuous mirror motion. Internal modulation is therefore most efficient for cases where a small spectral interval is to be covered and it becomes less efficient where a wide interval is to be used. The recovered signal, after synchronous rectification, is proportional to the slope of the original interferogram. The process corresponds to differentiation. The resulting interferogram of a well balanced instrument shows point symmetry with respect to the origin and is the sinus rather the cosinus transform of the spectrum. The method suppresses the DC value of the interferogram and low frequency fluctuations and, therefore, has been particularly successful in suppressing the effect of atmospheric scintillations, a very important consideration for observations of faint astronomical sources from the ground. The method of internal modulation has been analyzed the detail by Chamberlain (1971) who finds an increase in signal to noise ratio of two by internal modulation (called phase modulation) over the more conventional recording of the interferogram (called

amplitude modulation). However, Chamberlain compares an instrument with internal modulation to one which records the amplitude but uses an external chopper. The chopper reflects half the energy away before it enters the interferometer. It is quite possible that the merit which Chamberlain assigns to the internal modulation scheme is, at least in part, a consequence of the chopper mechanism chosen for the comparison. Nevertheless experimental results obtained with internal modulation are very impressive but possibly for reasons not fully appreciated today.

3.2 Far-Infrared Instruments

Fourier spectroscopy has played the dominant role in the far-infrared. Almost all observations have been made with Michelson interferometers. The laminar grating interferometer of Strong (1954) has been used primarily far laboratory investigations (e.g. Dowling, 1967), and only recently by Stettler et al., (1974) for solar research. In a discussion of instrumentation for the far-infrared, it is convenient to group individual reports by institutions, as the results presented in papers are often obtained with the same or similar instrumentation.

The "Groupe Infrarouge Spatial" of the Meudon Observatory (see Table 1) has been quite active in the far-infrared. The solar brightness, as well as earth atmospheric emission and absorption, has been studied from the ground, aircraft and balloons. In all cases, a Michelson interferometer was used with a diaphragm-type beamsplitter. The balloon measurements and the earlier groundbased observations used an ONERA pneumatic detector (Chatanier and Gauffre, 1972) with an NEP of 2×10^{-10} $WHz^{-1/2}$ while the more recent Caravelle measurements were carried out with a gallium-doped germanium bolometer with an NEP of $3X10^{-13}WHz^{-1/2}$ The balloon instrument of the Meudon group (Gay, 1970) mechanically chopped

the telescope beam before the cassegrain focus against a beam from the same general area in the sky but which bypassed the telescope. The reference beam had the same solid angle (f/5) as the telescope exit and both beams were reflected twice by similar surfaces. Instrument calibration is well discussed including the effect of saturation in the signal channel.

The group at the National Physical Laboratory in England has a long and well established record in far-infrared spectroscopy. From the early groundbased observations by Gebbie, et al. (1968),through aircraft measurements on a Comet 2E and a Concorde, up to balloon-borne measurements, the group has explored the transmission and emission properties of the Earth's atmosphere with good spectral resolution. The basic instrument used by this group is the National Physics Laboratory modular interferometer (Chantry, et al. 1969), sometimes modified to take full advantage of both output beams. In early measurements and in the balloon-borne case, the detector was a Golay cell while in the more recent versions, a Rollin detector (InSb) cooled to liquid Helium temperatures served as the infrared receiver. The NPL group prefers Melinex (polyethylene terephthalate) over Mylar as a beam splitter material. Some of the observations (Harries, et al. 1973; Burroughs and Harries, 1970) have been made with internal modulation by oscillating the fixed interferometer mirror. The moving mirror is activated by a micrometer either in a stepping mode or by moving at constant speed; a reference interferometer is not used. The spectra, particularly those recorded with the Rollins detector, are of good quality but results are given in

terms of relative intensity only.

A research group at the University of Oregon (Nolt, et al.,1971; Nolt, et al., 1972) also used the modular NPL interferometer on a mountain top (Mauna Kea, Hawaii) and on an airplane (NASA CV-990). The interferometer was operated in the stepping mode with a thick mylar beamsplitter. An indium antimonide doped germanium detector was cooled to 0.3 to 0.4K by pumping on liquid He^3.

Another group active in far infrared spectroscopy by means of FTS is at the High Altitude Observatory of NCAR in Boulder, Colorado. Solar spectra have been recorded from Pikes Peak, Colorado, and from the NASA CV-990 aircraft (Eddy et al., 1969a; Eddy et al., 1969b; Mankin et al., 1973). The instrument used by this group is a Michelson interferometer with metal mesh beamsplitters. These beamsplitters were found to be affected less than mylar beamsplitters by acoustical vibration present in aircraft. The gold coated flat interferometer mirror was advanced in steps by a micrometer rod. Two gallium-doped germanium detectors mounted in the same dewar served as receivers, each detector was optimized for part of the spectral range. A capacitive pneumatic detector monitors the total energy. Chopping against a reference blackbody and calibration with respect to a liquid nitrogen source provides absolute calibration. Unfortunately, results are given only in arbitrary units.

Jennings and Moorwood (1971) from the University College, London made balloon measurements in the 100 - 1000 cm^{-1} range. The instrument uses a Mylar beamsplitter at an unusually high angle of 65^{o} between incoming ray and normal to reduce the effect of multiple interference in

the beamsplitter, ("channel spectrum"). A reference interferometer with the 0.5461 μm mercury line is mechanically coupled to the infrared interferometer. The infrared detector is a thermocouple tuned to the chopper frequency of 16 Hz. Attention was given to absolute calibration by chopping against a liquid nitrogen open dewar. Good spectra have been obtained, unfortunately, at rather low spectral resolution.

J. Beckman, Queen Mary College, London, measured chromospheric emission in the 5-40 cm^{-1} range with a conventional Michelson interferometer using InSb detectors, cooled to liquid He temperature (Beckman, et al., 1973). The measurements were obtained during the June 30, 1973 solar eclipse over North Africa from the Concorde 001 aircraft.

3.3 Intermediate-Infrared Instruments

In the last few years the intermediate-infrared region (200-2000 cm^{-1}) has also seen advances in instrumentation and observing techniques. In this spectral region and in the far-infrared, thermal emission by the instrument and telescope is a dominating factor compared to the near-infrared and visible part of the spectrum where thermal emission can often be neglected.

In the intermediate-infrared, Michelson interferometers have recorded planetary spectra from the ground, from aircraft, from balloon and even from space vehicles. Most data have been taken with thermal detectors, either thermister bolometers (NEP$\sim 10^{-8}$ W $Hz^{-1/2}$) operating at ambient temperatures or gallium-doped germanium bolometers (NEP$\sim 10^{-13}$ W$Hz^{-1/2}$) operating at 2K. In some cases mercury and copper-doped germanium photoconductors (NEP$\sim 10^{-10}$ to 10^{-12} W $Hz^{-1/2}$) have been operated at 4K.

Recently pyroelectric bolometers (NEP $\sim 10^{-9}$ to 10^{-10} W $Hz^{-1/2}$) have tended to replace thermistor bolometers for operation at ambient temperatures.

The instrument which has so far yielded the highest spectral resolution in the intermediate-infrared is a dual beam interferometer (Hanel et al., 1969). This interferometer uses the same area of the beamsplitter for both beams but separates them by dividing the solid angle. In contrast, the Connes type instruments, to be discussed in the chapter on near-infrared instruments, uses the full solid angle for each beam but different areas on the beamsplitter to recombine the reflected beams. Thus, the techniques exhibit duality with respect to each other.

The dual input-dual output capability permits operation in several modes. One input may be allowed to see planetary radiation, the other adjacent sky, or one input the planet and the other an internal blackbody. The sky radiation must then be recorded sequentially. In principle, the temperature of the internal reference blackbody may be chosen so that the net flux from the reference input equals the flux from the observing input; the flux difference is then zero and consequently also the central peak in the interferogram. The latter fact can be used to reduce the dynamic range in the recording system which often is of great concern. The dual input-output technique permits also a first order correction to intensity fluctuations of the source, by ratio recording. Techniques for absolute calibration of the telescope transmission have been discussed (Hanel et al., 1968).

The degree of balance between both input beams which can be obtained with this instrument is adequate in first order. For the recording of

very weak sources which are orders of magnitude below the sky emission, it is advantageous to oscillate the secondary mirror in the telescope as suggested first by F. Low (1966). This technique has proven to be effective in the suppression of sky noise for broad band radiometry and there is no reason why it should not be equally effective for spectroscopy. Such an arrangement is under preparation by Aumann (private communication 1973).

Most recently Ridgeway and Capps (1974) have been able to obtain good quality emission spectra of Jupiter in the 10 μm window from the Kitt Peak solar telescope. Their instrument has two inputs and two detectors. The beams occupy different portions of the permissible solid angle. Data are recorded in the continuous mode of operation. Good balance between both beams was obtained by adjusting the aperture of the reference beam.

Combs, et al., (1974) measured the spectrum of Jupiter in the 10-13 μm region from the Cassegrain focus of the 224 cm telescope at Mauna Kea Observatory with a Michelson interferometer. The interferometer operated with flat mirrors in the stepping mode and a gold coated potassium chloride beamsplitter. The field of view was 36 sec of arc. An interferogram of Jupiter required ~90 minutes of integration time for adequate signal to noise.

The instrumentation used by Thekaekara et al., (1969) to measure the solar constant from the NASA CV-990 aircraft included a commercially available interferometer with a thermistor bolometer for the 667 to 4000 cm^{-1} range. A spectral resolution of about 25 cm^{-1} has been achieved.

A group at the Lebedev Physical Institute of the Academy of Science, USSR has been developing an interferometer for space use. A paper describing the initial instrument (BIFS-1) by Markov, et al., (1970) has

been translated into English (ARCRL-70-0716, 20 Nov. 1970 Translation No. 87). The instrument operates in the 250 to 1000 cm^{-1} range with a spectral resolution of up to 1 cm^{-1}. A stretched film of 6 μm Terylane serves as a beamsplitter with good response near 300 and 700 cm^{-1} but with a gap near 500 cm^{-1}. The moving mirror is stepped in 2 μm increments. Calibration by a standard lamp during the "fly-back" period of the mirror and chopping against space are characteristic features of this instrument. A more recent version of this interferometer, called BIFS-2, has been flown on a balloon by Ivanov et al., (1973). Spectra obtained cover thermal emission from Earth between approximately 200 and 700 cm^{-1} with a spectral resolution of 10-15 cm^{-1}. A noise equivalent radiance of $1\text{-}2 \times 10^{-7}$ W cm^{-2} sr^{-1}/cm^{-1} has been quoted.

The thermal emission spectra of Earth and Mars have been observed with Michelson interferometers flown on Nimbus 3, 4, and Mariner 9 (Hanel, et al., 1970; 1971a; 1972a). These instruments are similar to each other with later models exhibiting progressively better performance. Apodized spectral resolution and noise-equivalent-radiance have been improved from 5 cm^{-1} to 2.4 cm^{-1} and from approximately $(0.6\text{-}2) \times 10^{-7}$ to 0.5×10^{-7} W cm^{-2} sr^{-1}/cm^{-1}, respectively. All these interferometers, known by the acronym IRIS, use flat mirrors and sweep continuously under control of a phase locked loop. Thermister bolometers serve as infrared detectors. A monochromatic line from a neon discharge lamp provides the signal for a reference interferometer mounted concentric to the main interferometer.

All IRIS's made use of space and a built-in blackbody as references to obtain absolute calibration (Hanel, et al., 1972b). The Earth orbiting instruments compensated the motion of the field of view due to the high speed of the satellite by using a counter-rotating mirror. Beamsplitters were constructed on potassium bromide and cesium iodide substrates, for the Earth- and Mars-orbiting instruments respectively, by vacuum deposition of many layers of dielectric materials. Good efficiency has been obtained over a spectral range as high as ten to one (200-2000 cm^{-1}).

The IRIS flown to Mars on Mariner 9 has an additional, somewhat unusual, feature. The instrument digitizes the interferogram at a higher rate (3x) than required but sums then three quantized words before transmission to the ground. This improves the dynamic range and provides a numerical filter to reject frequencies which may otherwise be aliased into the spectrum. The digital filter operates after the analog to digital converter, and therefore does not contribute phase shift between infrared signal and the quantization command. A more sophisticated numerical filter is planned for an IRIS to be flown on a future spacecraft (Mariner Jupiter Saturn 1977). First a running average of four digital words is taken and then an average of three. The resulting filter function is shown in Figure 3 along with the filter function applicable to straight averaging over three words.

3.4 Near Infrared and Visible Region Instruments

Undoubtedly the most successful instrument in the near-infrared has

been the double beam interferometer designed by Connes and Connes (1966). The spectra recorded by this instrument were indeed orders of magnitude superior to then available data. The Connes observed first from Table Mountain and the Steward Observatory (Connes and Connes, 1966) and later from the Observatoire de Saint Michel (Connes et, al., 1969). The same instrument is now at the Lunar and Planetary Laboratory of the University of Arizona. Shortly after the Connes constructed their first instrument a second model was built by R. Beer et al., (1971a) at JPL. The second instrument is now installed permanently at the Coude focus of the 2.7 m telescope at the McDonald Observatory, Univ. of Texas. The French group has developed second (Pinard, 1967) and third generation instruments (Guelachvili and Maillard, 1971; Connes, et al., 1970) of the Connes types, but primarily for laboratory use. A 50 cm drive version of these later instruments has been adapted to planetary and stellar infrared observations, the most recent observations being made at the coude focus of the 5 meter telescope at Palomar Observatory (Connes and Michel, 1974). Spectra of Venus and Mars were obtained with the best resolution being .016 cm^{-1}.

The Connes interferometer is a double beam instrument designed for two inputs and two detectors. The beams recombine at different areas of the beamsplitter but use the full solid angle in each beam. This design permits the beamsplitter coating to be deposited at opposite sides of the substrate. No additional compensating substrate is required. Cat's eyes retroreflectors and an internal modulation scheme by oscillating the small secondary mirror of the cat's eye retroreflector are distinctive features of this interferometer. The Connes instruments have been

operated in the step-by-step mode with electronic integrators performing the signal averaging process. Advancement from one step to the next is servo controlled.

Another interesting version of the step-by-step double beam interferometer was developed by Schindler (1970): The cat's eye approach has been carried a step further to make the interferometer not only independent of tilt but also independent of lateral displacement of the reflectors. The price payed for this independence is attenuation by seven reflections in each arm, compared to one reflection in the flat mirror design. The resulting relatively compact instrument is intended for space application.

In addition to the Connes type instruments several smaller interferometers have gathered planetary data in the near-infrared. These instruments have often been adaptations of commercially available interferometers or have used elements such as complete commercial drive systems for the Michelson mirror. Most of these interferometers are of the continuous sweep type and many have been operated with small telescopes mounted on the NASA Convair 990 or Lear-Jet. Operation on aircraft requires rather careful designs to overcome vibration effects. Further details are shown for the near infrared in Table 3 and for the visible in Table 4. One particular observation may be mentioned: the observation of the unexpected sodium D lines on Io by Brown (1973). It must be somewhat disheartening to the purists of Fourier spectroscopy that Brown used a conventional grating instrument to verify his discovery, originally recorded with a Michelson interferometer.

Although most observers use the Michelson interferometer, two applications of polarization interferometers can be reported. Thekaekara,

et al., (1969) installed a commercially available polarization interferometer in the NASA CV-990 to analyze the spectral radiance of the sun and to reevaluate the solar constant. The other polarization interferometer has been designed by F.S. Ahern as part of his thesis at the University of Maryland (private communication, 1973). The instrument is capable of recording simultaneously spectra in both planes of polarization between 0.33 and 2.5 μm up to a resolution of 10 cm^{-1}. Preliminary spectra of stellar sources as well as Venus, Mars, Saturn, Uranus, Neptune and the moon have been obtained between .36 and .7 μm at resolution of approximately 200 cm^{-1} but have not yet been published.

4. SCIENTIFIC RESULTS

The application of Fourier spectroscopy to studies of the planets has yielded significant results so far and promises further insight into conditions and processes active in the solar system. From the viewpoint of planetary research, the infrared is a very significant spectral region because it contains the vibration and rotation frequencies of most molecules, as well as pressure induced resonances of molecules and atomic constituents such as hydrogen and helium. Pressure induced effects play an important role in the physics of the atmospheres of the outer planets.

For convenience, the results obtained by Fourier spectroscopy are summarized below for the Sun and for each individual planet.

4.1 Sun

The Sun is an extremely strong source of radiation at all wavelengths. Therefore, good spectra have been obtained with conventional grating spectrometers, and the need for applying the advantages of Fourier spectroscopy

for the purpose of solar research has not been as strong as for weak objects. Furthermore, many of the physically interesting phenomena in the Sun concern atomic species which have their electronic transitions in the ultraviolet. For these reasons relatively few investigators have applied Fourier techniques to study the infrared emission of the Sun. However, the Sun has been used as a reference in the study of other planets, to remove the effect of Fraunhofer lines and of absorption in the Earth's atmosphere. Such comparison spectra have in general not been used to gain knowledge on the Sun and will, therefore, not be discussed.

Measurements of the solar spectrum have been obtained with seven spectral instruments, including two interferometers, from the NASA Convair CV-990 flying at 11.58 km (Thekaekara, et al., 1969). One of the interferometers covered the .3 - 2.6 μm spectral range, the other 2.5 -15 μm. The measured spectral irradiances from this series of instruments currently represents the best definition of the solar spectrum. The data indicate that the solar effective blackbody temperature decreases with increasing wavelength; 5360K at 5 μm, 5000K at 15 μm and 4950K at 20 μm. The solar constant was found to be 1352 W/ m^2 (1.934 cal/min cm^2) or about 3.3% lower than the previously accepted value.

Gay, et al., (1968) have presented the first spectra of the sun in the 33 - 200 cm^{-1} range ($\Delta\nu$ = .5 cm^{-1}) from a balloon-borne interferometer. The temperatures inferred for the photosphere-chromosphere transition zone from the 50-100 cm^{-1} range were approximately 4600 K which lies between the values predicted by the Bilderberg Continuum Atmosphere (BCA) and Harvard-Smithsonian Reference Atmosphere (HSRA) models. In the 150-200 cm^{-1} region,

the observed temperatures are between 5000 and 5500 K, considerably higher than model predictions. A temperature of 4370 K for the mean solar disc was determined from Convair CV-990 measurements in the 32-42 cm^{-1} range (Eddy, et al., 1969b). Stettler, et al. (1974) have used a balloon-borne lamellar-grating interferometer to measure the solar spectrum in the 20-90 cm^{-1} range with 5 cm^{-1} resolution. The measured solar brightness temperatures, along with measurements of other workers are compared to the HSRA model in Figure 2 of Stettler, et al. (1974).

The solar spectrum has been measured in the near-infrared (1800 - 9200 cm^{-1} with $\Delta\nu$ =0.5 cm^{-1}) by Johnson, et al., (1973) from a Lear Jet at 14 km. This spectrum is shown in Figure 4; the solar and terrestrial spectral features are noted.

The upper chromosphere of the Sun was investigated, using its far infrared emission, with a Michelson interferometer on the Concorde 001 during the June 30, 1973, solar eclipse. The spectral range covered was 5 - 40 cm^{-1}. Only a brief description of the experiment and the indication of successful data acquisition have been announced to date (Beckman, et al., 1973).

4.2 Mercury

The planet closest to the Sun is difficult to observe because of the small angular separation from the Sun. Mercury could support a tenuous atmosphere and spectroscopic observations are desirable to detect possible constituents or set upper limits. Furthermore, near-infrared reflectivity and possible emission features at longer wavelength could yield information on the mineral composition of the surface.

The only FTS observations reported in the literature are the high resolution spectra obtained by Fink, et al. (1974) in the 3700-5300 cm^{-1} range. Based on these spectra, upper limits have been established on the CO_2 and CO abundances. With statistical correlation techniques and comparisons between synthetic and observed spectra, upper limits of .12 and .05 cm atm were set for CO_2 and CO, respectively.

4.3 Venus

Venus, our closest neighbor in space, has been explored by Fourier spectroscopy from the ground and from aircraft. Spectra of high resolution (0.08 cm^{-1}) have been obtained by Connes from the 1.9 m telescope of the Steward Observatory in June and July, 1966. The numerous spectral traces in the 4000-8500 cm^{-1} region are now published in atlas form (Connes et al. 1969) and the results on CO, the discoveries of HCl and HF have been published by Connes et al. (1967b), Connes, et al. (1968), and Young (1971). New data on Venus and Mars have been acquired recently by Connes and Michel (1974) with a 50 cm drive interferometer at the coude focus of the 5 m telescope at Mt. Palomar. Preliminary results are shown in Figures 5 and 6 for Venus over a 10 cm^{-1} spectral range displayed with a spectral resolution of 0.016 cm^{-1}.

Two of the outstanding problems concerning the atmosphere of Venus are the abundance of water vapor and the composition of the visible clouds. Several investigations have made an attempt to resolve these questions, thereby increasing our understanding of Venus.

Fink, et al. (1972) obtained spectra of Venus during five observation periods in January and February, 1969 with an interferometer flown

aboard the NASA CV-990 aircraft at an altitude of approximately 12.2 km. A spectral resolution of 5 cm^{-1} was obtained in the 3700-7800 cm^{-1} region (see Figure 7). The total water vapor content in the Earth stratosphere was less than 10μm with the water vapor in the optical path inside the aircraft estimated at 1-2 μm. Synthetic Venus spectra, including the water vapor contributions from the Earth's stratosphere and the atmosphere inside the airplane, were computed and compared to the observed spectra. In these calculations, the Venus atmosphere was represented both with a discrete reflecting layer model and with a homogenous, isotropic scattering model. By comparisons in the 1.4, 1.9, and 2.7 μm water vapor bands, H_2O to CO_2 mixing ratios of 0.6×10^{-6} and 1.0×10^{-6} were determined for the reflecting and the scattering models respectively. The good agreement between both numbers suggests that the derived mixing ratio is not very dependent on the particular atmospheric model. As summarized by Fink et al. (1972) these values of water vapor amounts are one to two orders of magnitude below previous determinations. Internal consistency on the absolute amount of water vapor, as determined spectroscopically, for the upper atmosphere of Venus remains a problem. Inadequate atmospheric models for interpretation, systematic errors in instrumental calibration or in definition of the background continuum, or a secular change on Venus are all possible explanations for the inconsistencies in the derived Venus water vapor amounts.

A large number of spectra of Venus in the intermediate-infrared have been obtained by Hanel, et al. (1971b), from the coude focus of the 2.7 m telescope at McDonald Observatory. The observations, taken during

three time periods in Spring 1969, Fall 1970, and Fall 1973, cover the 400-1600 cm^{-1} region with resolutions varying from .2 to .7 cm^{-1} in the apodized mode. Lunar spectra, taken at approximately the same air mass, were used to correct the Venus spectrum for absorption due to the telescope and the terrestrial atmosphere.

The spectra of Venus obtained in the Fall 1970 observing session had a spectral resolution of 0.25 cm^{-1} with the instrumental field of view being 31 sec of arc, the Venus angular diameter being 41 sec of arc (see Figure 8). The molecular line structure is associated with the rotational lines of upper state CO_2 bands. The appearance of the line structure indicates that the emission originates in a region of the Venus atmosphere with a negative temperature gradient. A broad diffuse absorption feature, currently associated with sulphuric acid clouds (Young, 1973) is evident in the 870-930 cm^{-1} region. With the exception of the rotational lines of the 927 cm^{-1} CO_2 band, the 870-930 cm^{-1} feature appears as a continuum thus supporting the assumption that the feature is due to particles and not due to a so far unidentified gas. The data in the 20 μm window represent the first spectroscopic observations of Venus in this region. The theoretical spectrum shown also indicates that the fine structure in the Venus spectrum can be explained fairly well by molecular CO_2.

A volume extinction coefficient for the cloud particles has been derived from the 1969 observations assuming knowledge of the temperature profile from the Mariner 5 and Venera data and a carbon dioxide atmosphere (Samuelson, et al., 1974). The derived cloud opacity (see Figure 9) indicates a general increase by a factor of 2 in the volume extinction coefficient

from 700 to 1400 cm^{-1}. The absolute value of the extinction coefficient suggests a tenuous haze of particles rather than dense cloud. A mass mixing ratio for the cloud particles of $5x10^{-6}$ was inferred. Good agreement was found between the measured extinction coefficients and calculated values determined for clouds of small droplets with a refractive index of a 75% aqueous H_2SO_4 solution. Due to the large absorption cross-section of H_2SO_4, the effect of scattering was found to be very small. This analysis of Fourier transform spectra strongly supports the hypothesis of H_2SO_4 solutions for the Venus clouds (Sill, 1972; Young, 1973).

Beer, et al. (1971b) measured the reflectance spectrum of Venus in the 3-4μm range at a .54cm^{-1} resolution. Comparison with a solar spectrum shows strong broad absorption features in the continuum near 2850 and 3050 cm^{-1}. Venus spectra were also obtained by the Lunar and Planetary Laboratory group with the original Connes interferometer at the Steward Observatory 2.3 m telescope (Dierenfeldt, et al., 1973). Analysis of the molecular bands of CO_2 and CO in the 1 - 3 μm region yielded a temperature of 250 ±10K and a pressure of 75 mb. The authors infer a relatively sharp boundary for the visible cloud deck.

4.4 Earth

The infrared group at the Observatoire de Meudon has measured atmospheric transmission from a balloon and from the high altitude Gornergrat Observatory. Analysis of nine water-vapor lines in the measured 33-200 cm^{-1} range yielded a mean stratospheric water-vapor mixing ratio of $4x10^{-7}$ g/g above the balloon float altitude of 25 km (Gay, et al., 1968: Gay, 1970). Evident in the ground-based measurements, from 5-35 cm^{-1}, are atmospheric absorption lines of O_2,O_3, and N_2O (Biraud, et al., 1969). Stratospheric emission spectra in the 25-200 cm^{-1} range (see Figure 10), taken during daytime and nighttime flights from a Caravelle 116 aircraft contained absorption lines due to H_2O, O_2 and O_3 (Baluteau, et al., 1972a; Baluteau, et al., 1972b; Baluteau and Bussoletti, 1973;

Baluteau, et al., 1973). An unexpected feature in the 8 cm^{-1} region of the daytime spectra is attributed to quasiperiodic time and amplitude fluctuations in the solar chromosphere (Baluteau, et al., 1973). The authors point out that if this interpretation is correct, these fluctuations should also influence other regions of the far-infrared spectrum.

Gebbie, et al. (1971) recorded spectra in the 5-35 cm^{-1} range ($\Delta\nu$ = 0.5 cm^{-1}) over a 150 m horizontal path to determine if the anomalous features reported by Baluteau et al. (1973) are present. The results closely correlate with the slant path observations, showing anomalous features at 7-11, 22 and 28 cm^{-1}; this indicates a terrestrial rather than solar origin of the anomalies.

The NPL group has made numerous observations of atmospheric transmission and stratospheric emission with a far-infrared Fourier spectrometer from the Jungfraujoch Observatory (Gebbie, et al., 1968; Burroughs and Chamberlain, 1971), from a Comet 2E aircraft (Burroughs and Harries, 1970; Harries and Burroughs, 1971a, 1971b; Harries, et al. 1972), from a balloon (Harries, et al., 1973) and from the Concorde 002 aircraft (Harries, 1973). The lines of H_2O, O_2 and O_3, as well as HNO_3, NO_2, N_2O and SO_2 have been identified in these spectra (see Figure 11). From the ratios of H_2O/O_2 and O_3/O_2 lines volume mixing ratios for H_2O and O_3 have been derived. The inferred stratospheric water concentrations of $2x10^{-6}$ g/g are in general agreement with a dry stratosphere model. The Concorde measurements were made during a tour of the Far East, approximately 30 spectra being obtained over a latitude range 40S to 40N

(Harris, 1973). Individual volume mixing ratios for HNO_3, H_2O, N_2O and O_3 have been derived for these spectra.

Observations from the NASA CV-990 by Eddy, et al. (1969a) of the sky radiation in the 20-125 cm^{-1} range showed the presence of absorption lines due to stratospheric H_2O, O_2 and O_3. Estimates of the H_2O and O_3 content present above the aircraft were 0.5-5 pr μm and 0.25 cm atm, respectively. Three spectral features at 21.2, 35-36, and 49.5 cm^{-1} are attributed to absorption by the H_2O dimer for levels with the rotational quantum number K=1,2 and 3, respectively. Mankin, et al. (1973) have measured the solar spectrum and sky brightness from Pikes Peak, Colorado (altitude, 4301m) for conditions with an overhead water content of .02 precipitable cm. Two previously unreported atmospheric windows are evident in the solar spectra in the 42-46 cm^{-1} and 48-52 cm^{-1} ranges with the average transmission for each window being in the order of 25%.

A balloon-borne Michelson interferometer was used by Jennings and Moorwood (1971) to measure the downward sky emission in the 100-1000 cm^{-1} range with a resolution of 34 cm^{-1}. At the float altitude of 38 km the only sky emission detected was from the 667 cm^{-1} band of CO_2.

The far infrared absorption of the atmosphere above 4.2 km has been measured from Mauna Kea Observatory by Nolt, et al. (1971) with an NPL modular interferometer. Solar spectra with a resolution of .2 cm^{-1} in the 5-40 cm^{-1} range indicated structure due to atmospheric constituents, including five molecular oxygen rotational transitions. The same interferometer was used to measure the sky emission spectrum in the 5-20 cm^{-1} range ($\Delta\nu$=0.1 cm^{-1}) from the NASA CV-990 aircraft

(Nolt, et al., 1972).

The infrared interferometer spectrometers (IRIS) carried on the Nimbus 3 and 4 meteorological satellite measured the thermal emission spectrum of the Earth and its atmosphere between 400 and 1600 cm^{-1}. The apodized spectral resolution was 5 cm^{-1} for Nimbus 3, and 2.8 cm^{-1} for Nimbus 4. The Nimbus 3 IRIS operated for three months while the Nimbus 4 IRIS was still operating after two years in orbit, although data were recorded for only one year. During the orbital operation approximately 10^6 calibrated spectra were obtained from Nimbus 4 covering a variety of geophysical and meteorological conditions. A typical mid-latitude spectrum for a cloudless atmosphere is illustrated in Figure 12. The spectrum shows the molecular features of H_2O, CO_2, O_3 and CH_4. Numerous research investigations including the retrieval of temperature, water vapor and ozone profiles and the determination of surface temperatures and aerosol effects have been pursued with the IRIS spectra (Conrath, et al., 1970; Hanel, et al., 1972b; Kunde, et al., 1974a; Prabhakara, et al., 1974). Estimates of temperature and humidity profiles obtained from a spectrum taken over the Mediterranean (Hanel and Conrath, 1970) are shown in Figure 13.

Balloon-borne FTS observations of the Earth's upward radiance have been obtained in the 170-710 cm^{-1} range (Ivanov, et al., 1973). Two apodized spectra have been published for winter and summer conditions at spectral resolutions of 15 and 10 cm^{-1}, respectively, exhibiting atmospheric absorption by H_2O and CO_2, Figure 14.

Spectra of the atmospheric transmission were measured over the 400-1400 cm^{-1} range with a spectral resolution of 0.25 cm^{-1} from the McDonald Observatory (2200 m elevation) (this group) and over the 700-8500 cm^{-1} range ($\Delta\nu$= 1.3 cm^{-1}) from Kitt Peak (2064 meter elevation) (Ridgway and Capps, 1974). These spectra, shown in Figures 15 and 16, exhibit features of H_2O, CO_2, O_3, CH_4 and N_2O.

One of the first spectroscopic identifications of NO in the lower stratosphere was made with a Fourier spectrometer viewing the sun in the 1350-3333 cm^{-1} range ($\Delta\nu$ = .25 cm^{-1}) from an NC 135 aircraft (Toth, et al. 1973). The identification has been made from 2 R-branch lines and the Q-branch of the 1-0 band of NO (Figure 17) with the derived volume mixing ratio being 1 ppb.

4.5 Mars

Mars has been explored by Fourier techniques from the ground and from an orbiting spacecraft. Beer, et al. (1971c) obtained high resolution spectra ($\Delta\nu$ = .58 cm^{-1}) of the full disk of Mars during the 1969 opposition in the 2500-3500 cm^{-1} range. No features attributable to the Martian atmosphere were evident in the spectrum. It has been suggested that the dip in the spectrum in the 3300 cm^{-1} region is associated with water of hydration in the Martian regolith. Beer et al. do not find features in their spectrum which can be attributed to the only remaining "Sinton Band" still in question, the band at 2900 cm^{-1}. Upper limits were also derived for a number of molecular species on Mars.

The infrared spectroscopy experiment on the Mariner 9 orbiter provided information on atmospheric and surface properties of Mars from

observation of the thermal emission spectrum in the 200-2000 cm^{-1} range. Over 20,000 spectra are included in the final data set. The majority of the spectra were taken in the southern hemisphere during the summer season. Typical spectra, illustrating the differences between spectra from the north polar hood, south polar region and mid-latitudes on Mars, are shown in Figure 18.

All the features in the Martian spectra have been identified with gaseous H_2O and CO_2, entrained dust, and ice crystal clouds in the Martian atmosphere. These features, except for the ice crystals, are evident in the spectrum in Figure 19, and average of 1747 individual IRIS spectra. Absorption by water vapor occurs in the 200-500 and 1400-1800 cm^{-1} regions with CO_2 absorption most evident in between 600 and 750 cm^{-1}. Weak CO_2 bands can be recognized at 961, 1064, 1260, 1366, and 1932 cm^{-1}. The broad features in the 400-550 and 900-1200 cm^{-1} regions are due to silicate dust entrained in the Martian atmosphere. The averaging of such a large number of spectra improves the signal to noise ratio by about 40, yielding an effective noise-equivalent-radiance of approximately 10^{-9} W cm^{-2} sr^{-1}/cm^{-1} in the displayed spectrum. The averaging process is very effective in reducing random noise but does not reduce systematic errors. An effect of a systematic error caused by small non linearities in the analog to digital converter of the instrument, may be seen as weak spurious features at multiple frequencies of the strong CO_2 bands, for example at 1440 cm^{-1}. Synthetic radiances, considering only the effect of atmospheric CO_2 and H_2O, are included for comparison.

Although it has been suspected that the Martian white clouds were composed of water ice, the IRIS spectra offer the first direct spectroscopic evidence (Curran, et al., 1973). Water ice clouds have been identified in the north polar hood and in the region of the shield

volcanos of the Tharsis Ridge from broad absorption features in the 225-350 and 550-950 cm^{-1} spectral regions (see Figure 20). Comparison of a spectrum calculated for clouds of particles with the optical constants for water ice with an observed spectrum from the Tharsis Ridge region indicates water ice clouds composed of particles with mean radius 2.0 μm and integrated cloud mass 10^{-4} g cm^{-2}.

Surface pressures have been derived from the IRIS spectra for the latitude region +20° to -60°. The observed pressure variations correspond to a topographic variation over the planet of at least two atmospheric scale heights (~20km). These results represent the first inference of surface pressures from thermal emission spectra. Information on the atmospheric temperature fields, the surface temperature, atmospheric water vapor and entrained dust have also been inferred from the IRIS spectra (Hanel, et al., 1972c; Hanel, et al., 1972d; Conrath, et al., 1973).

Larson, et al. (1973) derived a Martian atmosphere water vapor abundance of 20 μm from a comparison of a model atmosphere synthetic spectrum and the observed spectrum for the 1.4 μm H_2O band. The observation refers to the entire disk of Mars and were obtained at L_s=232°, late spring in the southern hemisphere, just prior to the planet-wide dust storm.

Fourier transform observations ($\Delta\nu$~10 cm^{-1}) of the south polar cap of Mars, obtained midway through spring during the 1971 opposition, show eleven narrow features associated with the polar cap (Larson and Fink, 1972). All eleven features have been identified with solid CO_2 from comparison with laboratory CO_2 frost spectra (see Figure 21). No evidence of H_2O frost is seen in the observed spectra and Larson and

Fink conclude CO_2 frost is the major constituent of the south polar cap during that portion of the season when the measurements were obtained.

4.6 Jupiter

The first interferometric observations of Jupiter were taken in the near-infrared in January, 1966 by Connes et al. (1969) with a resolution of 0.4 cm^{-1}, however, results have not yet been published from these spectral traces.

Johnson (1970) observed Jupiter in the 2400-8300 cm^{-1} region with 8 cm^{-1} resolution during April 1968 and April 1969. The reflection spectrum indicated several regions of zero reflectance due to strong absorption by H_2, CH_4 and NH_3 in the Jovian atmosphere.

Deuterated methane, CH_3D, has been identified from observations in the 4-5 μm window region of Jupiter by Beer et al. (1972), as shown in Figure 22. Lines of the P-branch (p2-p11) of the ν_2 band of CH_3D were identified from full disk observations in the 1800-2200 cm^{-1} region ($\Delta\nu$ = .55 cm^{-1}). The total abundance above the main cloud deck was found to be in the range of 2.3-2.9 cm atm. A large depression of the continuum is noted in the 2080-2130 cm^{-1} region; Beer and Taylor (1973a) suggest this feature is due to bond absorption by a solid species in the Jovian clouds. Several unidentified narrow lines remain in the spectrum. An isotopic D/H ratio of 4.8 X 10^{-5} was inferred for Jupiter from the CH_3D abundance, a value somewhat lower than the terrestrial ratio of 1.57 X 10^{-4} (Beer and Taylor, 1973a). Further comments concerning Jovian D/H ratio from the measurements of CH_3D may be found in the paper of Beer and Taylor (1973b).

Other parameters for the Jovian atmosphere have been estimated from high resolution spectra ($\Delta\nu$ = .22 cm^{-1}) of the $3\nu_3$ CH_4 band in the

9050 cm^{-1} region (Maillard et al. 1973). The spectrum is shown in Figure 23. The dominant source responsible for broadening of the lines is the rotation of Jupiter ($\Delta\nu$=.4 cm^{-1}). Using a reflecting layer model, synthetic line profiles were computed, convolved with rotational broadening and the instrumental profile and compared to the observational data to derive the atmospheric parameters. The Lorentz half-width of 0.10 cm^{-1} yields a pressure of 2 atm at the base of the reflecting layer. The derived rotational temperature and CH_4 abundance was 150±15K and 38±8m-atm, respectively.

Measurements of the central third of the Jovian disk were made by Potter (1974) in the range 6000-11000 cm^{-1} ($\Delta\nu$=.5 cm^{-1}). Only the spectral traces, but no interpretation, have been published so far.

The first measurements of Jupiter by Fourier spectroscopy in the 10 μm region were obtained by Ridgway and Capps (1974) and Ridgway (1974a) with the 150-cm McMath solar telescope in June 1973. A 7.5 arc second aperture was centered on the disk with time integrations of 2-3 hours necessary to obtain an adequate signal to noise ratio at the 1.3 cm^{-1} spectral resolution. Numerous lines of the ν_2 NH_3 band are evident in absorption in the 750-870 cm^{-1} region. Both acetylene (C_2H_2) and ethane (C_2H_6) have been identified in the 800 cm^{-1} region with the lines occurring in emission (Figure 24). Preliminary analysis yielded an ethane to acetylene ratio of two whereas photochemical investigations predict a ratio of 200. The estimates are strongly dependent on the atmospheric model. A more refined spectral analysis is necessary to verify the above conclusion. The detection of acetylene and ethane has independently

been confirmed by Combes, et al. (1974) with FTS spectra in the same spectral region obtained at Mauna Kea Observatory. Further data analysis by Ridgway (1974b) has lead to the tentative identification of PH_3 in the Jovian atmosphere (Figure 25).

4.7 Galilean Satellites

During the June 1972 opposition of Jupiter Fourier observations were extended to the Galilean satellites by Fink et al. (1973) and Pilcher et al. (1972), both groups obtaining spectra in the 2500-8000 cm^{-1} range. Fink et al. (1973) found the spectrum of Io quite similar to that of the Sun, with no additional spectral features present (see Figure 26). Strong absorptions in the Europa and Ganymede reflection spectra compared well only with absorption in water ice, indicating large amounts of ice present on the surfaces of both satellites. In contrast the Callisto spectrum showed only weak water ice features. Fink et al. (1973) also set an upper limit of .5 cm atm. for both methane and ammonia on the satellites.

The reflectance spectra of the Galilean satellites by Pilcher et al. (1972) are shown in Figure 27. The effective observing time for a spectrum is approximately 1 hour. From the strength of the water frost absorption features the percentage of frost-covered surface was estimated to be 50-100 percent for Europa, 20-65 percent for Ganymede, and 5-25 percent for Callisto. Io was found to be anomalous in having a high surface reflectivity without the spectral signature of water ice. Pilcher et al. (1972) have found 20 percent more frost cover on the leading side of Ganymede than on the trailing side and they inferred silicates for the material underlying the water frost.

An unexpected discovery on Io, made by Brown (1973) with a Fourier spectrometer operating in the visible region, was the time-varying emission by sodium atoms. A sodium columnar abundance of 1.8×10^{12} atoms/cm^2 for Io was derived from the measurements of the sodium D lines at 0.589 μm.

4.8 Saturn

The first interferometric observation of Saturn were taken in August, 1966 with a resolution of 1.7 cm^{-1} (Connes, et al. 1969) in the 4000-9000 cm^{-1} range. More recently, Potter (1974) made measurements of Saturn in the 6000-11000 cm^{-1} range ($\Delta\nu$=.5 cm^{-1}). No interpretation of these spectra have yet been published.

Atmospheric parameters for Saturn have been derived from spectra obtained between 4000 and 12000 cm^{-1} with the 193 cm telescope of St. Michel Observatory by de Bergh, et al. (1973). The instrumentation was the same as used to obtain Jupiter spectra (Maillard, et al. 1973). Three spectra of Saturn were recorded, each requiring about four hours of observing time. All three spectra were averaged to obtain a signal to noise ratio adequate for further data analysis. The resolution in the apodized average spectrum was 0.26 cm^{-1} with Doppler broadening due to planetary rotation reducing the effective spectral resolution to 0.45 cm^{-1}. Comparable spectral resolutions can be attained with photographic or photoelectric means only over a limited spectral range. The FTS spectra not only cover a larger spectral range, but also allow the continuum to be better defined. Synthetic line profiles were compared with observations in the R-branch of the $3\nu_3$ CH_4 band for a reflecting

layer model. The resultant atmospheric parameters were 134K for the rotational temperature, 0.15 cm^{-1} for the mean collisional half-width of the CH_4 lines, and 42 m-atm for the methane abundance with an effective pressure of 1.4 atm.

4.9 Saturn Rings

Water ice has been identified as a constituent of the rings of Saturn from FTS spectra in the 2000-8500 cm^{-1} range (Kuiper, et al. 1970a & 1970b; Pilcher et al. 1970). Using the temperature dependence of the ice feature at 6056 cm^{-1}, the temperature of the rings was determined to be 80K (Fink and Larson, 1973).

4.10 Neptune

The only Fourier transform measurements on Neptune are those of A'Hearn et al. (1974) obtained with a polarization interferometer in the 4000-6000 Å range. The spectra indicate methane absorption features in the atmosphere of Neptune. No analysis of these data has been published.

5. THE FUTURE OF FTS

The last half decade has seen wide application of Fourier spectroscopy to planetary research. Extraordinary results have been obtained. Will this trend of development continue or has the technique reached perfection? This question is, of course, difficult to answer. Perhaps the question should be recast as; what are the limitations of F.T.S.? The limitations have been discussed by Martin (1972) for infrared astronomy. We will follow the concept of Martin's paper but concentrate on the limits and prospects of FTS with respect to planetary research.

5.1 The AΩ or etendue Advantage

The first property which makes Fourier spectroscopy so valuable is the large AΩ product (etendue or throughput advantage). It was first fully recognized by Jaquinot and Dufour (1948) and Jaquinot (1960). The AΩ advantage of the interferometers over the conventional grating spectrometers is not restricted to Fourier Transform Spectrometers. The Fabry-Perot interferometer, for example, also shows a large AΩ product. Has this desirable property been fully used in the exploration of the planets?

From Earth and its immediate vicinity the planets appear as small objects in the sky with angular diameters of less than a minute of arc and in the case of Pluto of only 0.2 second of arc. With the exception of our moon the natural satellites of the planets have rather small apparent sizes. Ganymede, with 1.67 second of arc, appears as the largest satellite, followed by the other Gallilean satellites, then by Titan and Triton.

The angular size and the corresponding solid angle of the planets and some of their satellites are shown in Figure 28 versus diameter and collecting area of typical telescopes. This often used diagram is convenient to discuss the limitations of telescopes and interferometers; of course, observations are often limited by other factors, such as seeing conditions or detector noise. The diagonal lines are marked at the right and lower side by the corresponding AΩ product (telescope throughput). On the left and upper side the wavelength corresponding to the diffraction limit is given in micrometers. The wavelength diffraction limit and the AΩ product are related by

$$A\,\Omega_{diff} \approx \lambda^2_{diff}.$$

The Michelson interferometer may be operated without severe degradation due to off-axis rays if the $A\Omega$ product of the interferometer satisfies the criterion

$$A_i \Omega_i \leq \frac{2\pi A_i}{R}$$

where R is the resolving power. Because $A\Omega$ is invariant in an optical system, either the telescope or the interferometer may contain the limiting aperture. If the system is limited by the interferometer the observer might have chosen a smaller telescope or a smaller field of view without affecting the signal-to-noise ratio in the recorded spectrum. Conversly, if the system is limited by the telescope the use of the larger telescope would be clearly advantageous. In the ideal case telescope and interferometer are matched, $A_t\Omega_t = A_i\Omega_i$. The maximum theoretical resolving power R is then:

$$R = 2\pi A_i / A_t \Omega_t .$$

The diameter of interferometer mirrors which determine A_i is limited by practical considerations to a few cm in the near and intermediate-infrared and to perhaps slightly larger values in the far infrared. For convenience of the display we assume a diameter of 4.5 cm and calculate the maximum resolving power. The result is also shown in Figure 28 by the numbers in the center of the diagonal lines.

It is apparent that virtually all FTS observations of the planets from groundbased telescopes have been limited in $A\Omega$ by the telescope rather than by the interferometer. Only the most recent near-infrared

measurements of Venus by Connes and Michel (1974) with a 10 sec of arc field of view have achieved a resolution of 3×10^5 indicated by a cross mark in Figure 28. In this case the Hale telescope and the Connes interferometer have been well matched. In all other cases other limitations, mostly detector noise, have prevented groundbased observers from fully exploiting the $A\Omega$ advantage of interferometers. Until a large infrared telescope becomes available to groundbased observers the $A\Omega$ capacity of interferometers will not be fully exploited. Mertz (1965) and Connes, et al. (1967) have strongly advocated such a large telescope devoted to the infrared.

In contrast to this, interferometers in close proximity to a planet can take full advantage of the large $A\Omega$ product of the instrument without being limited by the telescope. The interferometers in Earth orbit and on Mariner 9 were limited in throughput only by the interferometer. The interferometer now under construction for the Mariner Jupiter Saturn mission in 1977 will have a 50 cm telescope. The field of view of the telescope (0.25^0) will be matched to the maximum $A\Omega$ of the interferometer.

At the present time then, for most cases the $A\Omega$ advantage of interferometers used in FTS will be limited for Earth based observers, at least in the foreseeable future, by the sizes of available telescopes, although in some cases matching of telescope and interferometer has all ready been achieved. Observations of the planets from relatively close range will allow full exploitation of the high $A\Omega$ product of interferometers.

5.2 The Multiplex Advantage

The multiplex advantage of Fourier spectroscopy exists only as long as detector noise is independent of the incident flux. Detector technology is advancing steadily; within the not too distant future, detectors will become available which will be limited more and more by the incident background radiation. A discussion of the state of the art of infrared detectors in 1971 is given by Lena (1972). Under truly background-noise limited conditions the multiplex advantage of FTS disappears; the FTS and the conventional grating spectrometer then become equally efficient in this respect. Reduction of the background noise beyond this point requires cooling of the interferometer and even the telescope to cryogenic levels, say to about 20K. This will be advantageous for certain astronomical applications. For planetary research, however, cooling of the interferometer or telescope to temperatures below the brightness temperature of the planets will not yield significant improvement, since the background seen by the detector will then be determined by the flux from the source to be studied, the planet itself.

For groundbased operation cooling of the telescope is not practical. It is also probable that atmospheric emission and its fluctuation (sky noise) will set limits to the observational capabilities of the ground-based observer long before the telescope emission becomes significant, particularly for telescopes specifically designed with low emissivity in the infrared.

Operation of space borne interferometers will gain from the multiplex advantage for considerable time to come. Not until it becomes practical to fly background-noise limited detectors, cooled to temperatures of the order of a degree K on a spacecraft towards the planets will the multiplex advantage of the Michelson interferometer become insignificant.

In summary, at the present and probably for the next decade the multiplex advantage of Fourier spectroscopy will be a significant and important consideration. Eventually, however, with the availability of truly background limited detectors the multiplex advantage will disappear.

5.3 Other Advantages

Several other advantages of FTS can gainfully be applied to planetary research. First, Fourier Transform instruments are capable of covering a very wide spectral range. Ratios of maximum to minimum wavenumber of 10:1 are not uncommon. Wide spectral range at simultaneously high spectral resolution is particularly important for the exploratory aspect of planetary research. The unexpected discovery of the HF and HCl lines in the Venus spectra or the information obtained on the particulates in the Martian atmosphere from the Mariner 9 IRIS are good examples of serendipity made possible due to wide spectral coverage. Without the wide spectral range or with only a few radiometric channels available, the interpretation of data must be based in large part on preconceived assumptions and models. For the less explored planets in particular, such models are often inaccurate and possibly even incorrect. The wide spectral range, and high spectral resolution are,therefore, properties of FTS which

make it attractive for exploratory missions.

A further important property of FTS is excellent wavenumber precision. Many instruments discussed in chapter 3 use the monochromatic line of a laser or of a gas discharge source as a wavenumber reference. An absolute wavenumber precision of 1.2×10^{-4} cm^{-1} rms error has been achieved by Pinard (1970). Wavenumber precision is important in ratioing high resolution spectra to solar or lunar spectra or to each other, as required, for example, to eliminate the effect of Fraunhofer lines or telluric absorption lines.

A final significant property of FTS is the precision and absolute accuracy of intensity calibration. Fourier spectrometers are at least as precise and can be as well calibrated in intensity as conventional grating instruments and radiometers. This point is stressed because it is not yet commonly accepted. Ten years ago great doubt existed that Michelson interferometers could be used in a radiometric sense. Several examples shown in chapters 3 and 4 (e.g. the stability of calibration of the Mariner 9 interferometer) clearly demonstrate that FTS can be used where radiometric precision is of importance.

6. CONCLUSIONS

In the mid-sixties Pierre and Janine Connes made the first recordings of planetary spectra by means of Fourier spectroscopic techniques (Connes and Connes, 1966). Since the Connes' pioneering efforts in the 1 - 3 μm range, large fractions of the reflection and emission spectra of many objects in the solar system have been recorded by means of FTS. Except for Uranus and Pluto, all planets, the Galilean satellites and the rings of Saturn have been observed over fractions of their spectra with varying spectral and spatial resolutions. Interferometers mounted on ground-based telescopes or carried on various types of aircraft, balloons, Earth satellites and space probes have operated over different parts of the spectrum from the far infrared to the visible with spectral resolutions as high as 0.016 cm^{-1}. Despite this effort large fractions of the electromagnetic spectrum reflected or emitted by the planets are unexplored. Even in regions where preliminary spectra exist higher precision, spectral resolution, and in some cases better spatial resolution are of great importance.

The next decade will show further application of FTS on a much broader scale. The use of larger telescopes and improved detectors will allow corresponding improvements over existing spectra in terms of signal-to-noise and spectral resolution, and furthermore, will permit fainter objects to be observed. FTS investigations from aircraft, especially the NASA C-141, promise to open up spectral regions inaccessible so far to ground observers. Investigations from space craft promise full exploitation of all advantages of FTS; more over, spacecraft observations also promise spatial resolution and spectral coverage not possible from ground based or aircraft observatories.

Based on the results of the FTS investigations summarized in this review, exciting new discoveries and subsequent advances in the knowledge of the solar system can be expected from FTS observations in the forthcoming years.

Acknowledgments

It is a pleasure to thank Dr. J. Pearl for his help and valuable comments.

References

A'Hearn, M. F., Ahern, F. J., and Zipoy, D. M.: 1974, Appl. Opt., 13, 1147.

Baluteau, J. P., and Bussoletti, E.: 1973, Nature, 241, 113.

Baluteau, J. P., Bussoletti, E., Lena, P., and Marten, A.: 1972a, A. J. Broderick (ed), Proceedings of the Second Conference on the Climatic Impact Assessment Program, DOT-TSC-OST-73-4, P. 99.

Baluteau, J. P., Bussoletti, E., Langlet, A., and Roucher, J.: 1972b, Eldo-Cecles/Esro-Cers Scient. and Tech. Rev., 4, 353.

Baluteau, J. P., Bussoletti, E., and Epchtein, N.: 1973, Nature, 244, 562.

Becker, E. D. and Farrar, T. C.: 1972, Science, 178, 361.

Beckman, J., Begot, J., Charvin, P., Hall, D., Lena, P., Soufflot, A., Liebenberg, D., and Wraight, P.: 1973, Nature, 246, 72.

Beer, R., and Taylor, F. W. : 1973a, Ap.J., 179, 309.

Beer, R., and Taylor, F. W.: 1973b, Ap. J. Letters, 182, L131.

Beer, R., Norton, R. H., and Seaman, C. H.: 1971a, The Rev. of Sci. Instr., 42, 1393.

Beer, R., Norton, R. H., and Martonchik, J. V.: 1971b, Ap. J. Letters, 168, L121.

Beer, R., Norton, R. H., and Martonchik, J. V.: 1971c, Icarus, 15, 1.

Beer, R., Farmer, C. B., Norton, R. H., Martonchik, J. V., and Barnes, T. G.: 1972, Science, 172, 1360.

Bell, R. J.: 1972, Introductory Fourier Transform Spectroscopy, Academic Press, New York.

Biraud, Y., Gay, J., Verdet, J. P., and Zeau, Y.: 1969, Astron. & Astrophys., 2, 413.

Brigham, E. O.: 1974, The Fast Fourier Transform, Prentice-Hall, Inc., New Jersey.

Brown, R. A.: 1973, Presentation at IAU Symposium No. 65, Torun, Poland.

Burroughs, W. J., and Harries, J. E.: 1970, Nature, 227, 824.

Burroughs, W. J., and Chamberlain, J.: 1971, Infrared Physics, 11, 1.

Chamberlain, J.: 1971, Infrared Physics, 11, 25.

Chantry, G. W., Evans, H. M., Chamberlain, J., and Gebbie, H. A.: 1969, Infrared Physics, 9, 85.

Chantanier, M., and Gauffre, G.: 1972, in V. Manno and J. Ring (eds.), Infrared Detection Techniques for Space Research, D. Reidel Publishing Company, Dordrecht - Holland, P. 141.

Combes, M., Encrenaz, Th., Vapillon, L., Zeau, Y., and Lesqueren, C.: 1974, preprint.

Connes, J.: 1961, Rev. Opt., 40: 45, 115, 171, 185, 231.

Connes, P.: 1970, in L. Goldberg, D. Layzer and J. G. Phillips (eds.), Annual Review of Astronomy and Astrophysics, Vol. 8, Annual Reviews Inc., Palo Alto, California.

Connes, J., and Connes, P.: 1966, J. Opt. Soc. Am., 56, 896.

Connes, P., and Michel, G.: 1974, Ap. J. Letters, 190, L29.

Connes, P., Connes, J., Kaplan, L. D., and Benedict, W. S.: 1968, Ap. J., 152, 731.

Connes, J., Connes, P., and Maillard, J. P.: 1969, Atlas des Spectres Planetaires Infrarouge, Editions du C.N.R.S., Paris.

Connes, P., Fellgett, P., and Ring, J.: 1967a, Science Journal, April, 66.

Connes, P., Connes, J., Benedict, W. S., and Kaplan, L. D.: 1967b, AP. J., 147,1230.

Connes, J., Delouis, H., Connes, P., Guelachvili, G., Maillard, J. P., and Michel, G.: 1970, Nouv. Rev. Opt. Appl., 1, 3.

Conrath, B. J., Hanel, R. A., Kunde, V. G., and Prabhakara, C.: 1970, JGR, 75, 5831.

Conrath, B., Curran, R., Hanel, R., Kunde, V., Maguire, W., Pearl, J., Pirraglia, J., Welker, J., and Burke, T.: 1973, JGR, 78, 4267.

Cooley, J. W., and Tukey, J. W.: 1965, Math, Comput., 19, 297.

Curran, R. J., Conrath, B. J., Hanel, R. A., Kunde, V. G., and Pearl, J. C.: 1973, Science, 182, 381.

de Bergh, C., Vion, M., Combes, M., and Lecacheaux, J.: 1973, Astron & Astrophys., 28, 457.

Dierenfeldt, K. E., Fink, U., and Larson, H. P.: 1973, BAAS, 5, 17, abstract.

Dowling, J. M.: 1967, Appl. Opt., 6, 1580.

Dowling, J. M.: 1971, in G. A. Vanasse, A. T. Stair, Jr., and D. J. Baker (eds.), Aspen International Conference on Fourier Spectroscopy, 1970, AFCRL-71-0019, P. 55.

Eddy, J. A., Lena, P. J., and MacQueen, R. M.: 1969a, JAS, 26, 1318.

Eddy, J. A., Lena, P. J., and MacQueen, R. M.: 1969b, Solar Physics, 10, 330.

Felgett, P. B.: 1958, J. Phys. Radium, 19, 187, 237.

Fink, U., and Larson, H. P.: 1973, BAAS, 5, 25, abstract.

Fink, U., Dekkers, N. H., and Larson, H. P.: 1973, Ap. J. Letters, 179, L155.

Fink, U., Larson, H. P., Kuiper, G. P., and Poppen, R. F.: 1972, Icarus, 17, 617.

Fink, U., Larson, H.P., and Poppen, R.F.: 1974, AP. J., 407.

Fox, K.: 1972, in K. N. Rao and C. W. Mathews (eds), Molecular Spectroscopy: Modern Research, Academic Press, Inc., New York, Chapter 3.

Gay, J.: 1970, Astron. & Astrophys., 6, 327.

Gay, J., Lequeux, J., Verdet, J. P., Turon-Lacarrieu, P., Bardet, M., Roucher, J., and Zeau, Y.: 1968, Astrophysical Letters, 2, 169.

Gebbie, H. A., Chamberlain, J., and Burroughs, W. J.: 1968, Nature, 220, 893.

Gebbie, H. A., Bohlander, R. A., and Pardoe, G. W. F.: 1971, Nature, 230, 521.

Griffiths, P. R., Foskett, C. T. and Curbelo, R.: 1972, Applied Spectroscopy Reviews, 6, 31.

Guelachvili, G., and Maillard, J. P.: 1971 in G. A. Vanasse, A. T. Stair, Jr., and D. J. Baker (eds), Aspen International Conference on Fourier Spectroscopy, 1970, AFCRL-71-0019, P. 151.

Hanel, R. A., and Conrath, B. J.: 1970, Nature, 228, 143.

Hanel, R. A., Forman, M., Stambach, G., and Meilleur, T.: 1968, J. Atmos. Sci., 25, 586.

Hanel, R., Forman, M., Meilleur, T., Westcott, R., and Pritchard, J.: 1969, Appl. Opt., 8, 2059.

Hanel, R. A., Schlachman, B., Clark, F. D., Prokesh, C. H., Taylor, J. B., Wilson, W. M., and Chaney, L.: 1970, Appl. Opt., 9, 1767.

Hanel, R. A., Schlachman, B., Rogers, D., and Vanous, D.: 1971a, Appl. Opt., 10, 1376.

Hanel, R. A., Kunde, V. G., Meilleur, T., and Stambach, G.: 1971b, in C. Sagan, T. C. Owen, and H. J. Smith (eds), Planetary Atmospheres, D. Reidel Publishing Company, Dordvecht-Holland, P. 44.

Hanel, R., Schlachman, B., Breihan, E., Bywaters, R., Chapman, F., Rhodes, M., Rodgers, D., and Vanous, D.: 1972a, Appl. Opt., 11, 2625.

Hanel, R. A., Conrath, B. J., Kunde, V. G., Prabhakara, C., Revah, I., Salomonson, V. V., and Wolford, G.: 1972b, JGR, 77, 2629.

Hanel, R. A., Conrath, B. J., Hovis, W. A., Kunde, V. G., Lowman, P. D., Pearl, J. C., Prabhakara, C., and Levin, G. V.: 1972c, Science, 175, 305.

Hanel, R., Conrath, B., Hovis, W., Kunde, V., Lowman, P., Maguire, W., Pearl, J., Pirraglia, J., Prabhakara, C., Schlachman, B., Levin, G., Straat, P., and Burke, T.: 1972d, Icarus, 17, 423.

Harries, J. E.: 1973, Nature, 241, 515.

Harries, J. E., and Burroughs, W. J.: 1971a, Quart. J. R. Met. Soc., 97, 519.

Harries, J. E., and Burroughs, W. J.: 1971b, DES Report No. 7, National Physical Laboratory, Teddington, Middlesex, England.

Harries, J. E., Swann, N. R. W., Beckman, J. E., and Ade, P. A. R.: 1972, Nature, 159, 1972.

Harries, J. E., Swann, N. R. W., Carruthers, G. P., and Robinson, G. A.: 1973, Infrared Physics, 13, 149.

Houghton, J. T., and Taylor, F. W.: 1973, Rep. Prog. Phys., 36, 827.

Hunten, D. M.: 1968, Science, 162, 313.

Hunten, D. M.: 1971, Space Science Reviews, 12, 539.

Ivanov, V. V., Kartashov, A. V., Kukin, S. G., and Markov, M. N.: 1973, Short Contributions in Physics. Transactions of the P. N. Lebedev Physical Institute of the Academy of Sciences of the U.S.S.R., 5, 1. Translation by John Pearl, GSFC.

Jacquinot, P.: 1960, Rep. Prog. Phys., 13, 267.

Jacquinot, P., and Dufour, C. J.: 1948, J. Rech. C.N.R.S., 6, 91.

Jennings, R. E. and Moorwood, A. F. M.: 1971, Appl. Opt., 10, 2311.

Johnson, H. L.: 1970, Ap. J. Letters, 159, L1.

Johnson, H. L., Forbes, F. F., Thompson, R. I., Steinmetz, D. L., and Harris, O.: 1973, Pub. Astron. Soc. Pacific, 85, 458.

Johnson, T.V., and McCord, T.B.: 1971, Ap. J., 169, 589.

Jones, A.V.: 1973, Space Science Reviews, 15, 355.

Kuiper, G. P., Cruikshank, D. P., and Fink, U.: 1970a, as reported in Sky and Telescope, 39, 14.

Kuiper, G. P., Cruikshank, D. P., and Fink, U.: 1970b, Sky and Telescope, Feb., 80.

Kunde, V. G., Conrath, B. J., Hanel, R. A., Maguire, W. C., Prabhakara, C. and Salomonson, V.V.: 1974a,JGR, 79, 777.

Kunde, V. G., Hanel, R. A., Crosby, D., Maguire, W. C., and Meilleur, T.: 1974b,Presentation at Division of Planetary Sciences, AAS Meeting at Palo Alto, California.

Larson, H. P., and Fink, U.: 1972, Ap. J. Letters, 171, L91.

Larson, H. P. Fink, U., and Michel, G.: 1973, BAAS, 5, 13, abstract.

Lee, R. H., MacQueen, R. M., and Mankin, W. G.: 1970, Appl. Opt., 9, 2653.

Lena, P.: 1972, in V. Manno and J. Ring (eds), Infrared Detection Techniques for Space Research, D. Reidel Publishing Company, Dordrecht-Holland, P. 103.

Low, F. J.,: 1961, J. Opt. Soc. Amer., 51, 1300.

Low F. J.: 1966, Proceedings of the IEEE, 54, 477.

Maillard, J. P., Combes, M., Encrenaz, Th., and Lecacheux, J.: 1973, Astron. & Astrophys., 25, 219.

Mankin, W. G., Eddy, J. A., MacQueen, R. M., Lee, R. H., and Querfeld, C. W.: 1973, Nature, 245, 8.

Markov, M. N., Vedernikov, V. I., Ivanob (sic), V. V., Kartacheb (sic), A. V., and Petrov, V. S.: 1970, AFCRL-70-0716.

Marov, M. Y.: 1972, Icarus, 16, 415.

Martin, D. H.: 1972, in V. Manno and J. Ring (eds), Infrared Detection Techniques for Space Research, D. Reidel Publishing Company, Dordvecht-Holland, P. 267.

Mertz, L.: 1958, J. Phys. Rad., 19, 233.

Mertz, L.: 1965, Transformations in Optics, Wiley, New York.

Michelson, A. A.: 1927, Studies in Optics, University of Chicago Press, Chicago.

Newburn, R. L. and Gulkis, S.: 1973, Space Science Reviews, 3, 179.

Nolt, I. G., Radostitz, J. V., and Donnelly, R. J.: 1972, Nature, 236, 444.

Nolt, I. G., Martin, T. Z., Wood, C. W., and Sinton, W. M.: 1971, J. Atm. Sci., 28, 238.

Pilcher, C. B.: 1973, Interferometric Observations of Jupiter and the Galilean Satellites, Ph.D. Thesis, Massachusetts Institute of Technology.

Pilcher, C. B., Ridgway, S. T., and McCord, T. B.: 1972, Science, 178, 1087.

Pilcher, C. B., Chapman, C. R., Lebofsky, L. A., and Kieffer, H. H.: 1970, Science, 167, 1372.

Pinard, J.: 1967, J. Phys., 28, C2, 136.

Pinard, J.: 1970, Ann. Phys., 2.

Potter, A. E.: 1974, Preprint of NASA Special Publication.

Prabhakara, C., Dalu, G., and Kunde, V. G.: 1974, JGR, to be published.

Richards, P. L.: 1964, J. Opt. Soc. Am., 54, 1474.

Ridgway, S. T.: 1974a, Ap. J. Letters, 187, L41.

Ridgway, S. T.: 1974b, Presentation at DPS, AAS Annual Meeting, Palo Alto, California.

Ridgway, S. T., and Capps, R. W.: 1974, Rev. Sci. Instrum., 45, 676.

Sagan, C., Owen, T. C., and Smith, H. J. (eds.): 1971, Planetary Atmospheres, IAU Symp. 40, Springer-Verlag, New York.

Samuelson, R. E., Hanel, R. A., Kunde, V. G., Maguire, W. C., and Herath, L. W.: 1974, Icarus, submitted for publication.

Schindler, R. A.: 1970, Appl. Opt., 9; 301.

Sill, G. T.: 1972, Comm. Lunar Planet. Lab., 9, 191.

Stair, Jr., A. T.: 1971, in G. A. Vanasse, A. T. Stair, Jr., and D. J. Baker (eds), Aspen International Conference on Fourier Spectroscopy, 1970, AFCRL-71-0019, P. 127.

Steel, W. H.: 1967, Interferometry, Cambridge University Press, New York.

Steel, W. H.: 1971, in G. A. Vanasse, A. T. Stair, Jr., and D. J. Baker (eds), Aspen International Conference on Fourier Spectroscopy, 1970, AFCRL-71-0019, P. 43.

Stettler, P., Kneubühl, F. K., and Müller, E. A.: 1974, submitted to J. Astron. & Astrophy. for publication.

Strong, J.: 1954, J. Opt. Soc. Am., 44, 352.

Strong, J. D., and Vanasse, G. A.: 1960, J. Opt. Soc. Amer., 50, 113.

Thekaekara, M. P., Kruger, R., and Duncan, C. H.: 1969, Applied Optics, 8, 1713.

Toth, R. A., Farmer, C. B., and Schindler, R. A., Raper, O. F., and Schaper, P. W.: 1973, Nature, 244, 7.

Vanasse, G. A. and Sakai, H.: 1967, Progress in Optics, Vol. VI, 260.

Vanasse, G. A., Stair, A. T., and Baker, D. J. (editors): 1971, AFCRL-71-0019.

Young, A. T.: 1973, Icarus, 18, 546.

Young, L. D. G.: 1971, J. Quant. Spectrosc. Radiat. Transfer, 11, 385.

TABLE 1. FTS INVESTIGATIONS IN THE FAR-INFRARED SPECTRAL REGION

	Investigators	Institution	Vehicle	Observation Date	Spectral Range(cm^{-1})	Spectral Resolution(cm^{-1})	Detector (T)/Beamsplitter	NEP ($WHz^{-1/2}$)	FOV	Results
1	Gay, et al.,1968	Obs. de Meudon	Balloon	Jan., 1968	33-200	.50(A)	ONERA pneumatic Golay type/Mylar	$2x10^{-10}$		Atm trans. Solar T_{bb}
2	Biraud, et al., 1969	"	Ground-based	Feb-March 1968	5-35	.50(A)	ONERA pneumatic Golay type/Mylar	"		Atm trans.
3	Baluteau, et. al., 1972b	"	Caravelle 116 Aircraft	May, July, 1972	25-200	.07-.2(u)	Ga-Ge bol. (2)/Mylar	$3x10^{-13}$	14^{o}	Strat. emission
4	Gebbie et al., 1971	NBS	Ground-based	Nov., 1970-Feb., 1971	5-35	.5	Golay cell/			Atm trans.
5	Gebbie et al., 1968	NPL	Ground-based	April, 1968	5-53	.5	Golay cell/Melinex			Atm trans.
6	Burroughs and Chamberlin, 1971	"	"	Mar-April, 1969	5-35	.125-.5 (A)	Golay cell/Melinex			Atm trans.
7	Harries and Burroughs, 1971a	"	Comet 2E Aircraft	Nov., 1969	20-65	.5	Golay cell /			Strat. emission
8	" 1971b	"	"	April, 1970	18-98	.25(u)	Golay cell/			" "

	Investigators	Institution	Vehicle	Observation Date	Spectral Range(cm^{-1})	Spectral Resolution(cm^{-1})	Detector (T)/Beamsplitter	NEP ($WHz^{-1/2}$)	FOV	Results
9	Harries, et al., 1972	NPL	Comet 2E	Nov., 1971	10-36	.065(u)	Rollin In Sb electron bol. (2-4)/			Strat. emission
10	Harries, et al., 1973	"	Balloon	Oct., 1971	20-65	.5(u)	Golay cell/ Melinex			" "
11	Harries, 1973	"	Concorde 002 Aircraft	June, 1972	10-30	.067(u)	Rollin In Sb electron bol.(2-4)/		5^{0}	" "
12	Eddy, et al., 1969a	HAO	Convair 990 Aircraft	Aug.,1968	20-125	.26(A)	Ga-Ge bol. (2.2)/ electro formed nickel mesh	$9x10^{-14}$		Atm trans.
13	Eddy, et al., 1969b	"	"	" "	20-75	.25	"			Solar T_{bb}
14	Mankin, et al., 1973	"	Ground-based	April, 1971	40-54	.065	Ga-Ge bol. (2-4)/metal mesh			Atm trans.
15	Jennings and Moorwood, 1971	Univ. College London	Balloon	Aug, 1969	100-1000	34(A)	Ga-Ge bol. (2-4)/ Mylar	10^{-13}	3°	Downward atm emission
16	Nolt, et al., 1971	Univ. of Oregon	Ground-based	March,1969	5-40	.25(A)	Ge:In Sb bol. (.3)/			Atm trans.

	Investigators	Institution	Vehicle	Observation Date	Spectral Range(cm^{-1})	Spectral Resolution(cm^{-1})	Detector (T)/Beamsplitter	NEP ($WHz^{-1/2}$)	FOV	Results
17	Nolt, et al., 1972	Univ. of Oregon	Convair 990 Aircraft	Aug., 1971	2-20	.1(A)	Ge:In Sb bol. (.3)/		10^{o}	Strat. emission
18	Stettler, et al., 1974	Swiss Fed. Inst. of Tech.	Balloon	April, 1971	20-90	5.			28'	Solar T_{bb}
19	Beckman, et al., 1973	Queen Mary College, London	Concorde 001 Aircraft	June 30, 1973	5-40	.5(A)	InSb bol.(4)/			Solar Chromosphere

NPL - National Physical Laboratory

HAO - High Altitude Observatory, National Center for Atmospheric Research

NBS - National Bureau of Standards

TABLE 2. FTS INVESTIGATIONS IN THE INTERMEDIATE-INFRARED SPECTRAL REGIONS

	Investigators	Institution	Vehicle	Observation Date	Spectral Range(cm^{-1})	Spectral Resolution(cm^{-1})	Detector (T)/Beamsplitter	NEP ($WHz^{-1/2}$)	FOV	Results
20	Thekaekara, et al., 1969	GSFC	Convair 990 Aircraft	Aug., 1967	667-4000		Thermistor bol.(310)/		12^{o}	Solar constant
21	Lee, et al., 1970	HAO	Ground-based		770-1430	5	Ga-Ge bol. (2)/Germanium	$1x10^{-13}$	5'	Atm trans.
22	Hanel, et al., 1970	GSFC	Nimbus 3	April-July 1969	400-1600	5(A)	Thermistor bol.(250)/ KBr		8^{o}	Terrestrial thermal emission
23	Hanel, et al., 1971a	"	Nimbus 4	April,1970-April,1971	"	2.8(A)	"		5^{o}	Terrestrial thermal emission
24	Hanel, et al., 1972a	"	Mariner 9	Nov., 1971-Aug., 1972	200-2000	2.4(A)	Thermistor bol.(250)/ CSI		4.5^{o}	Mars thermal emission
25	Hanel, et al., 1969	"	Ground-based	Spring, 1969 Fall, 1970	400-1400	.25-.67(A)	Ga-Ge bol. (2)/KBr	$1x10^{-12}$ $-5x10^{-13}$	30"	Venus T_{bb} Atm trans. Atm emission
26	Ridgway, and Capps, 1974	KPNO	Ground-based		700-8500	1.3	Ge bol. (1.7)	$1x10^{-13}$	7"	Atm trans., JupiterNH_3
27	Ridgway, 1974a	"	"	June, 1973	750-1300	1.3	"	"	"	Jupiter thermal emission
28	Ivanov, et al., 1973	USSR	Balloon	Jan., June, 1972	170-710	2.5-15				Terrestrial thermal emission

	Investigators	Institution	Vehicle	Observation Date	Spectral Range(cm^{-1})	Spectral Resolution(cm^{-1})	Detector (T)/Beamsplitter	NEP ($WHz^{-1/2}$)	FOV	Results
29	Combes, et al., 1974	Obs. de Meudon	Ground-based	August,1973	740-1000	1.3	Ge. bol. (a)/KCl		36"	Jupiter thermal emission

GSFC - Goddard Space Flight Center

HAO - High Altitude Observatory, National Center for Atmospheric Research

KPNO - Kitt Peak National Observatory

TABLE 3. FTS INVESTIGATIONS IN THE NEAR-INFRARED

	Investigators	Institution	Vehicle	Observation Date	Spectral Range(cm^{-1})	Spectral Resolution(cm^{-1})	Detector (T)/Beamsplitter	NEP ($WHz^{-1/2}$)	FOV	Results
30	Thekaekara et al., 1969	GSFC	Convair 990 Aircraft	Aug., 1967	4000-33,333		Pbs/		$+5^{o}$	Solar constant
31	Johnson, 1970	U. of Arizona	Ground-based	Apr., 1968, 1969, Nov., 1968	2400-8300	8				Jupiter, Saturn reflectance
32	Johnson, et al., 1973	"	NASA Lear jet		1800-9200	.5(A)	InSb(77)/			Solar
33	Beer, et al., 1971c	JPL	Ground-based	May-June, 1969	2500-3500	.58(A)	Pbs Photocond.(77)/			Mars reflectance
34	Beer, et al., 1971b	"	"	October, 1970	2400-3200	.54	"			Venus reflectance
35	Beer, et al., 1972	"	"	May, 1971	1800-2200	.55	"			Jupiter CH_3D
36	Fink, et al., 1972	LPA	Convair 990 Aircraft	Jan-Feb, 1969	3700-7800	5				Venus H_2O
37	Kuiper, et al., 1970a & b	"	Ground-based	Nov. 1969	2000-8500					Saturn rings reflectance
38	Larson et al., 1973	"	Convair 990 Aircraft	1971	2860-9100	1.3				Mars H_2O

	Investigators	Institution	Vehicle	Observation Date	Spectral Range(cm^{-1})	Spectral Resolution(cm^{-1})	Detector (T)/Beamsplitter	NEP ($WHz^{-1/2}$)	FOV	Results
39	Larson & Fink, 1972	LPL	Ground-based	July, 1971	4000-9000	10(A)				Mars polar cap
40	Dierenfeldt et al., 1973	"	"							Venus CO_2, CO
41	Fink et al., 1974	"	"	Nov., 1971	3700-5300	.134				Mercury CO_2 CO upper limit
42	Fink, et al., 1973	"	"	June-July 1972	2500-10000	25(u)				Galilean llites-reflectance
43	Maillard, et al., 1973	Obs. de Meudon	"	May, 1972	4000-12000	.22(A)	PbS/		- 25"	Jupiter reflectance
44	de Bergh, et al., 1973	"	"	Dec.,1972	4000-12000	.26			15"	Saturn reflectance
45	Potter, 1974	JSC	"	Nov.,1972	6000-11000	.5(u)	Ge Photovoltaic(77) /			Jupiter, Saturn reflectance atlas
46	Pilcher, et al., 1972	MIT	"	June-July 1972	2500-8000	33				Galilean satellites, reflectance
47	Toth, et al., 1973	JPL	NC135 Aircraft	Mar., 1973	1350-3333	.25				Terrestrial NO

Investigators	Institution	Vehicle	Observation Date	Spectral Range(cm^{-1})	Spectral Resolution(cm^{-1})	Detector (T)/Beam-splitter	NEP ($WHz^{-1/2}$)	FOV	Results
Connes & Michel, 1974	Lab. Aime' Cotton, C.N.R.S.	Ground-based	Oct.-Nov. 1974	4000-10000	.016	PbS /		10"	Venus, Mars reflectance

GSFC - Goddard Space Flight Center

JPL - Jet Propulsion Laboratory

LPL - Lunar and Planetary Laboratory

JSC - Johnson Space Center

MIT - Massachusetts Institute of Technology

TABLE 4 FTS INVESTIGATIONS IN THE VISIBLE SPECTRAL REGIONS

	Investigators	Institution	Vehicle	Observation Date	Spectral Range(cm^{-1})	Spectral Resolution(cm^{-1})	Detector (T)/Beamsplitter	NEP ($WHz^{-1/2}$)	FOV	Results
49	Brown, 1973	Harvard Univ.	Ground-based	May, 1972	14300-23800					Io sodium
50	A'Hearn, et al., 1974	Univ. of Maryland	"		16000-25000	410				Neptune

FIGURE CAPTIONS

Figure 1 - Planetary radiance due to emitted and reflected solar radiation. The thermal emission has been computed assuming blackbody behavior of the planets at the representative temperatures indicated. The curves of the reflected solar radiation consider the change in the solar constant for the mean orbital distance of the planet from the Sun and the corresponding bolometric albedo shown in parentheses. Reflected and scattered solar radiation dominates above approximately 2000 cm^{-1}, for the terrestrial and above 1000 cm^{-1} for the outer planets. Thermal radiation emitted by the planet itself is the most important source of radiation below these wavenumbers.

Figure 2 - Summary of FTS observations of the Sun and planets from 1968 to early 1974. The observations have been made from aircraft, balloons, spacecraft, and from ground-based telescopes, as indicated. The numbers refer to the listings of observations in Tables 1 to 4. The transmittance of the Earth's atmosphere is schematically shown in the uppermost trace.

Figure 3 - Attenuation of numerical filters applied in the IRIS instrument to the amplitudes in the interferogram after quantization by analog to digital converter.

Figure 4 a, b, c - The solar spectrum obtained with a FTS with 0.5 cm^{-1} resolution from 1800 to 9200 cm^{-1}. The observation was made from a Lear Jet flying at 14 km by Johnson, et al. (1973).

Figure 5 - Spectra of Venus. The top spectra represent observations by Connes, et al. (1969) at 0.1 cm^{-1} resolution. The lower spectrum is a high resolution (0.016 cm^{-1}) measurement in the region of strong CO_2 absorption made by Connes and Michel (1974) with the 5m telescope at Mt. Palomar. The rotational line structure of the CO_2 band is well developed at the higher resolution.

Figure 6 - Same as Figure 5, except for a different interval containing isotopic lines of HCl.

Figure 7 - Infrared spectra of Venus from a FTS aboard the NASA CV-990 aircraft covering the 1.4 μm water vapor band (Fink, et al., 1972). The spectral resolution is 5 cm^{-1}. Comparison with synthetic Venus spectra yields 1.6 μm of precipitable water vapor in the two-way transmission of the Venus atmosphere for a reflecting layer model or .25 μm of precipitable water vapor per scattering mean free path for a scattering model.

Figure 8 a, b, c - Thermal emission spectrum of Venus in the 450-1250 cm^{-1} range at 0.25 cm^{-1} resolution. The observed spectrum was taken at the coude focus of the 2.7 m telescope at McDonald Observatory (Kunde, et al., 1974). CO_2 bands in the atmosphere of Venus are at 791, 828, 865, 961 and 1064 cm^{-1} with a broad diffuse absorption feature evident in the 890 cm^{-1} region. The synthetic spectrum was computed with the Mariner 5 temperature profile, including CO_2 molecular absorption and an

absorbing aerosol with the spectral characteristics shown in Figure 9 (Samuelson, et al., 1974). For clarity, the synthetic spectrum has been displaced 20K vertically downward as indicated by the vertical arrows.

Figure 9 - The volume extinction coefficient for the Venus clouds at R=6110 km (Samuelson, et al. 1974). The volume extinction coefficient, denoted by the solid line, was calculated for cloud particles of a 75% aqueous sulfuric acid solution with a size distribution as determined from polarization data on Venus. The good agreement between theoretical and empirical coefficients strengthens the argument for clouds of Venus composed of aqueous sulfuric acid droplets.

Figure 10 a, b, c, d - Stratospheric thermal emission spectra obtained from Caravelle 116 aircraft in 30-190 cm^{-1} range with 0.18 cm^{-1} resolution (Baluteau and Bussoletti, 1973). Examples of two spectra, vertically displaced, exhibit numerous atmospheric H_2O, O_3 and O_2 lines. The line assignments at the bottom of the Figures are:
H_2O (————) and O_3 (------), the height of the line being proportional to the logarithm of the line strength. Only the line positions are given for O_2 (– – – – – –).

Figure 11 - Sub-millimetre far-infrared stratospheric emission obtained by Harries (1973) from the Concorde 002 at 0.067 cm^{-1} resolution. The molecular lines evident in the spectrum have been identified

for the species HNO_3, N_2O, NO, NO_2, SO_2, H_2O, O_2 and O_3. Volume mixing ratios have been inferred for most of the species from the observed spectra.

Figure 12 - Thermal emission spectrum of the Earth measured by the FTS on the Nimbus 4 spacecraft; the spectral resolution is 2.8 cm^{-1} (Kunde, et al., 1974). The spectrum is the average of eight spectra over the Atlantic Ocean near Wallops Island in June-July, 1970. Under cloud free conditions, strong bands of CO_2, O_3 and H_2O are marked; features due to N_2O and CH_4 may also be seen in the spectrum.

Figure 13 a, b - Vertical profiles of atmospheric temperatures and water vapor inferred from a Nimbus 4 IRIS spectrum over the Mediterranean (Hanel and Conrath, 1970). Measurements of temperature and humidity obtained from a nearby radiosonde are shown for comparison.

Figure 14 - Balloon-borne FTS spectra of the Earth obtained during the winter (upper, $\Delta\nu$=15 cm^{-1}) and summer (lower, $\Delta\nu$ =10 cm^{-1}) by Ivanov, et al. (1973). Absorption features due to pure rotational lines of water vapor occur in the 170 - 420 cm^{-1} region and due to CO_2 in the 570 - 710 cm^{-1} region. The vertical scale is in Watt cm^{-2} $ster^{-1}$ cm; the horizontal scale in wavenumbers (cm^{-1}) and wavelength (μm).

Figure 15 - Transmission spectrum ($\Delta\nu$ = .25 cm^{-1}) for Earth's atmosphere from McDonald Observatory, 2200 meter elevation (this group). The air mass is approximately 1.4. The transmission was derived from observations of the Moon. Secondary effects due to non-blackbody emissivity of the Moon, possibly dust

in the Earth's atmosphere and the effect of the overcoating on the telescope mirrors are still present in the spectrum. The absorption features are due to H_2O, CO_2, O_3, N_2O, and CH_4.

Figure 16 - Transmission spectrum ($\Delta\nu$ = 1.3cm^{-1}) for Earth's atmosphere from Kitt Peak, 2064 meter elevation (Ridgway and Capps, 1974). The air mass is approximately 1.6. The spectrum was recorded in two sections with two beamsplitters.

Figure 17 - Identification of NO in the lower atmosphere (11-26km) from FTS aircraft spectra in the 1872-1892 cm^{-1} range (Toth, et al., 1973) looking at the solar spectrum through the atmosphere. A mean mixing ratio of 1 ppb was derived from three NO features. A Q branch and 2 R branch lines are visible in the observed spectra. The three solar spectra with a resolution of .25 cm^{-1}, shown are for solar zenith angles: A, 82°, B, 86° and C, 91°.

Figure 18 - Thermal emission spectra obtained from the infrared interferometers on the Mariner 9 ($\Delta\nu$ = 2.4 cm^{-1}) and Nimbus 4 ($\Delta\nu$ = 2.8 cm^{-1}) spacecraft. (a) Martian north polar hood (revolution 102); (b) Martian south polar region (revolution 30); (c) Martian midlatitude (revolution 92); (d) fractured quartz (laboratory spectrum); (e) Sahara desert (recorded in 1970 from Nimbus 4 (Hanel, et al., 1972d). The Martian spectra of the north polar (a) and south polar (b) regions indicate strong temperature inversions in the lower Martian atmosphere from the shape of the CO_2 band in the 600 - 700 cm^{-1} region. Measured over a similar spectral range and with nearly the same spectral and spatial resolution, these spectra provide the opportunity for a comparative analysis between Mars and Earth.

Figure 19 - Average thermal emission spectrum of Mars obtained with Mariner 9 IRIS. Over 1700 spectra have been averaged to reduce the random noise. Spectral features have been identified with CO_2, H_2O, entrained silicate dust and ice crystal clouds. A synthetic spectrum, vertically displaced by 25K, including molecular absorption by CO_2 and H_2O is shown for comparison. The insert shows a magnified portion of the same spectrum.

Figure 20 - Mariner 9 IRIS measurements of the lower Arcadia region under clear conditions and of the Tharsis Ridge region under conditions of partial cloudiness. The Tharsis Ridge spectrum shows broad absorption features from 550-950 cm^{-1} and 225-350 cm^{-1}, similar to the theoretical ice cloud spectrum shown in the upper portion of the Figure. Comparison of the observed and calculated spectra indicate the water ice clouds are composed of particles with mean radius 2 μm and an integrated cloud mass of 10^{-4} g cm^{-2} (Curran, et al. 1973).

Figure 21 - A spectrum of the south polar cap of Mars taken with the original Connes interferometer from Steward Observatory (Larson and Fink, 1972), the resolution being 10 cm^{-1}. The upper portion of the Figure shows the spectrum of the center of the disk, the spectrum of the south polar cap and the cap/center ratio spectrum. Eleven narrow features show in the ratio spectrum and are attributed to the composition of the polar cap. Comparison with laboratory spectra of CO_2 and H_2O frost, lower portion, suggests CO_2 frost as a major constituent of the polar cap.

Figure 22 - The spectrum of the entire disk of Jupiter obtained by Beer, et al (1972) at the coude focus of the 2.7 m telescope at McDonald Observatory is shown in part (a). The spectral resolution is .55 cm^{-1}. The middle spectrum is of the Sun with the lower spectrum the Jupiter/Sun ratio. Singly deuterated methane, CH_3D, has been identified in the ratio spectrum, the J-manifolds of the P branch of the ν_2 band are indicated at the base of (c). This represents the first observation of deuterium in the Solar System with the inferred D/H ration being $(2.8 \text{ to } 7.5) \times 10^{-5}$.

Figure 23 - The spectrum of Jupiter (lower line) in the wavelength range 9000-9700 cm^{-1} with .22 cm^{-1} resolution (Maillard, et al. 1973). The solar comparison spectrum is given by the upper line. The inset denotes a portion of the R branch of the $3\nu_3$ CH_4 band which has been used to derive some of the parameters for the Jovian atmosphere.

Figure 24 - Thermal emission spectrum of Jupiter ($\Delta\nu = 1.3$ cm^{-1}) in the 12μm terrestrial atmospheric window region (Ridgway, 1974a) is shown in lower portion. Approximately 3 hours of integration time were required for the observed spectrum, the spatial resolution being 7.5 sec of arc. Strong absorption features of the ν_2 band of NH_3 are evident throughout the above spectrum. The dashed line is the predicted H_2 continuum. Strong emission lines, identified with C_2H_2 and C_2H_6, are evident in the 800 cm^{-1} region. The upper spectrum represents the telluric transmission at Kitt Peak at the time of the Jupiter observations.

Figure 25 - Thermal emission spectrum of Jupiter ($\Delta\nu = 1.3$ cm^{-1}) in the 12μm terrestrial atmospheric window region (Ridgway, 1974a) is shown in lowest spectrum. The synthetic NH_3 spectrum is shown by middle curve. A tentative identification of PH_3 results from comparison of upper synthetic PH_3 spectrum with the observations (Ridgway, 1974b).

Figure 26 - FTS spectra of the four Galilean satellites ($\Delta\nu = 25$ cm^{-1}) obtained by Fink, et al. (1973). Moon and stellar comparisons (η Boo, dashed line) are shown for narrow features and general albedo characteristics, respectively. Large amounts of water ice are indicated on the surface of Europa and Ganymede with Callisto showing faint ice absorptions. No ice absorption is evident on Io.

Figure 27 - Reflectivities of Galilean satellites from 2500-8000 cm^{-1} ($\Delta\nu$ = 33 cm^{-1}) and water frost (Pilcher, et al., 1972). The strongest water frost absorptions are for JII (Europa) with weaker absorptions for JIII (Ganymede). Absorptions are not evident for JI (Io) and JIV (Callisto).

Figure 28 - Angular resolving power versus mirror diameter is shown for a number of large telescopes used in planetary research. The diagonal lines are marked at the right and lower side by the telescope throughput ($A_t \Omega_t$) and at the left and upper side by the diffraction limited wavelength in micrometers. R is the maximum resolving power which may be attained for a given planetary object and telescope with a Michelson or Fabry Perot interferometer using a 4.5 cm dia aperture. Only in the Connes and Michel (1974) measurement of Venus (indicated by +) have the interferometer and telescope been well matched. All other FTS observations of planets from ground based telescopes have been limited in $A\Omega$ by the telescope, not the interferometer.

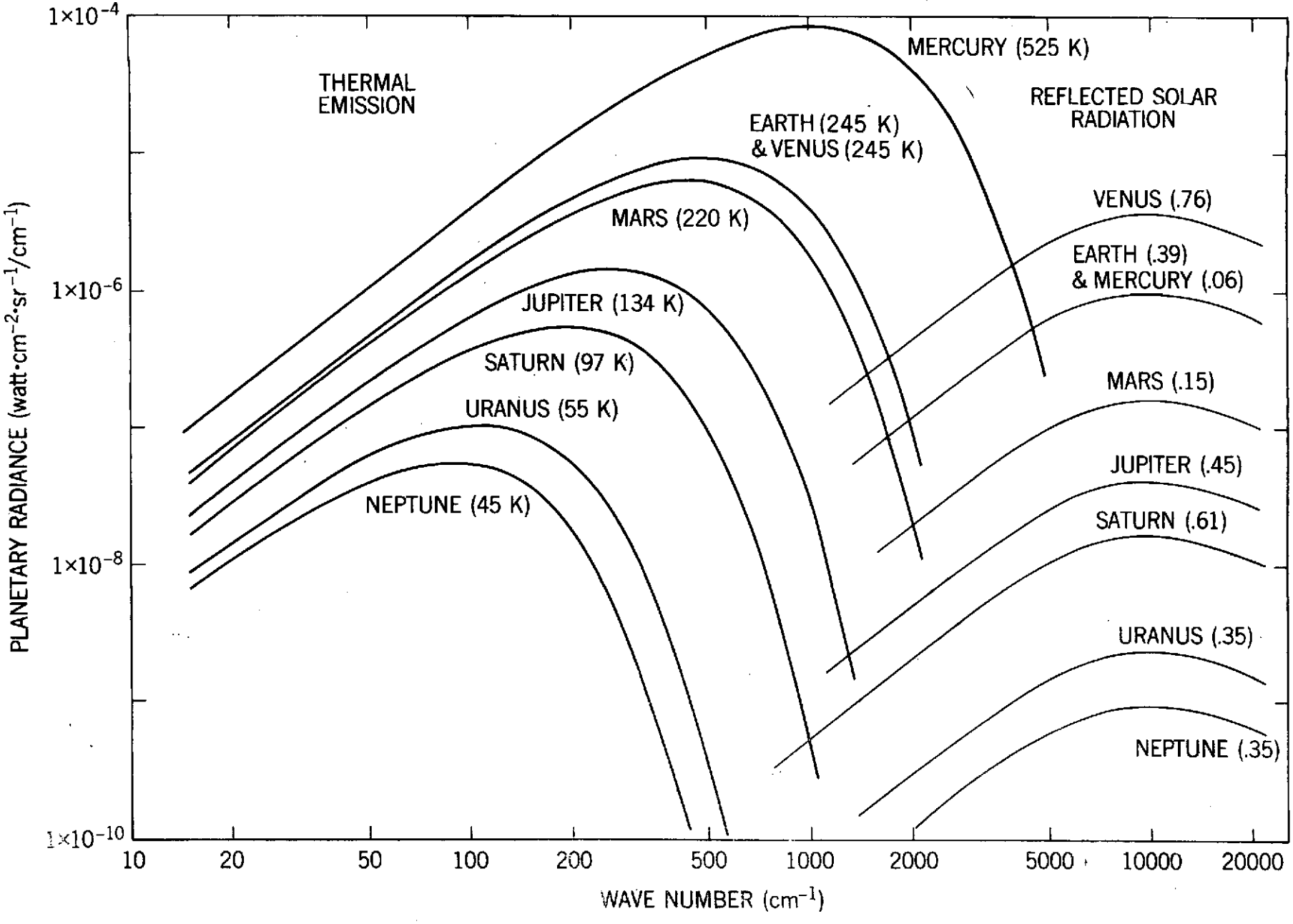
THERMAL EMISSION
REFLECTED SOLAR RADIATION
MERCURY (525 K)
EARTH (245 K) & VENUS (245 K)
MARS (220 K)
JUPITER (134 K)
SATURN (97 K)
URANUS (55 K)
NEPTUNE (45 K)
VENUS (.76)
EARTH (.39) & MERCURY (.06)
MARS (.15)
JUPITER (.45)
SATURN (.61)
URANUS (.35)
NEPTUNE (.35)
PLANETARY RADIANCE (watt·cm⁻²·sr⁻¹/cm⁻¹)
1×10⁻⁴
1×10⁻⁶
1×10⁻⁸
1×10⁻¹⁰
10
20
50
100
200
500
1000
2000
5000
10000
20000
WAVE NUMBER (cm⁻¹)

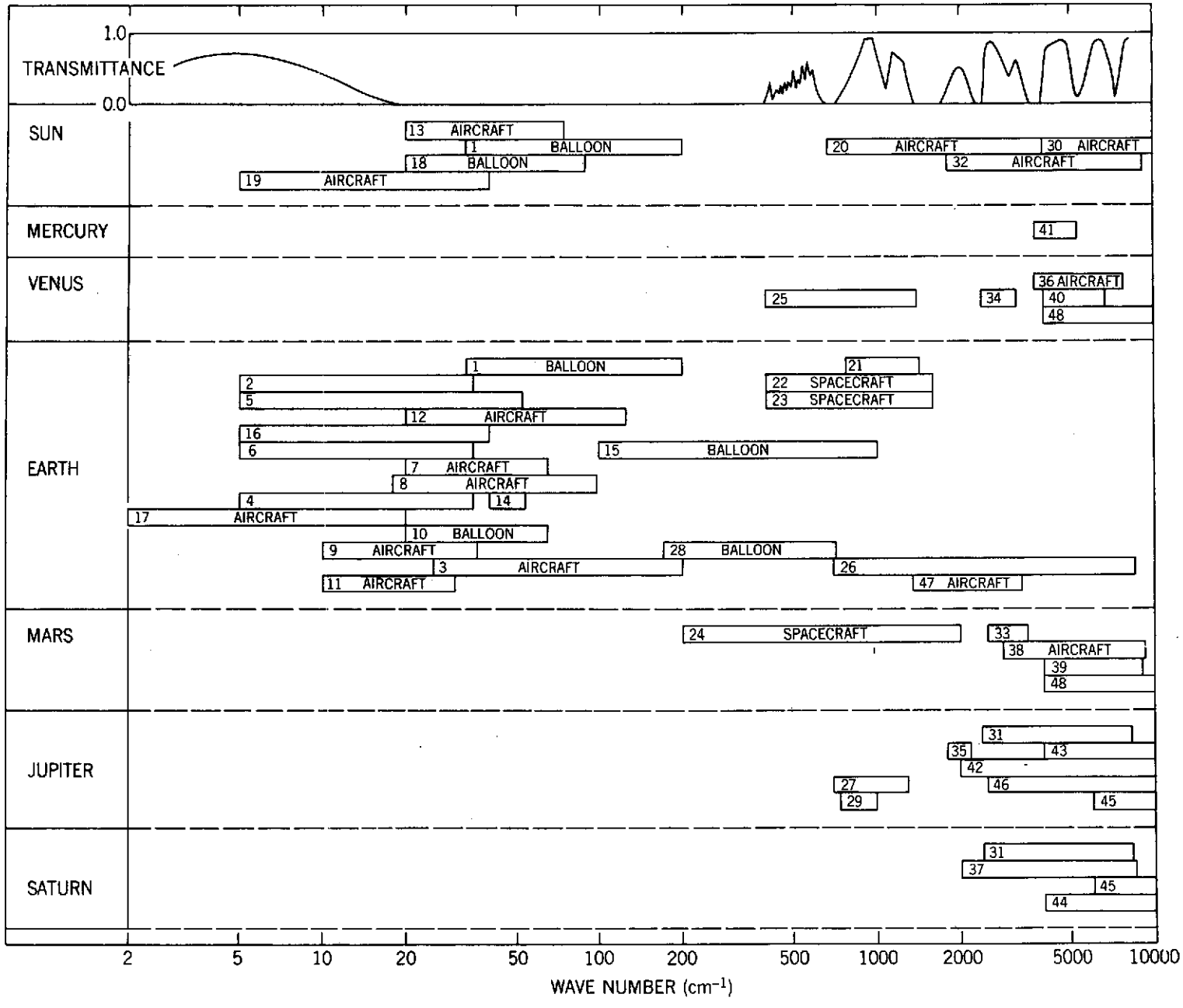
1.0
TRANSMITTANCE
0.0
SUN
13 AIRCRAFT
1 BALLOON
18 BALLOON
19 AIRCRAFT
20 AIRCRAFT
30 AIRCRAFT
32 AIRCRAFT
MERCURY
41
VENUS
36 AIRCRAFT
25
34
40
48
EARTH
1 BALLOON
21
2
22 SPACECRAFT
5
23 SPACECRAFT
12 AIRCRAFT
16
6
15 BALLOON
7 AIRCRAFT
8 AIRCRAFT
4
14
17 AIRCRAFT
10 BALLOON
9 AIRCRAFT
28 BALLOON
3 AIRCRAFT
26
11 AIRCRAFT
47 AIRCRAFT
MARS
24 SPACECRAFT
33
38 AIRCRAFT
39
48
JUPITER
31
35
43
42
27
46
29
45
SATURN
31
37
45
44
2
5
10
20
50
100
200
500
1000
2000
5000
10000
WAVE NUMBER (cm⁻¹)

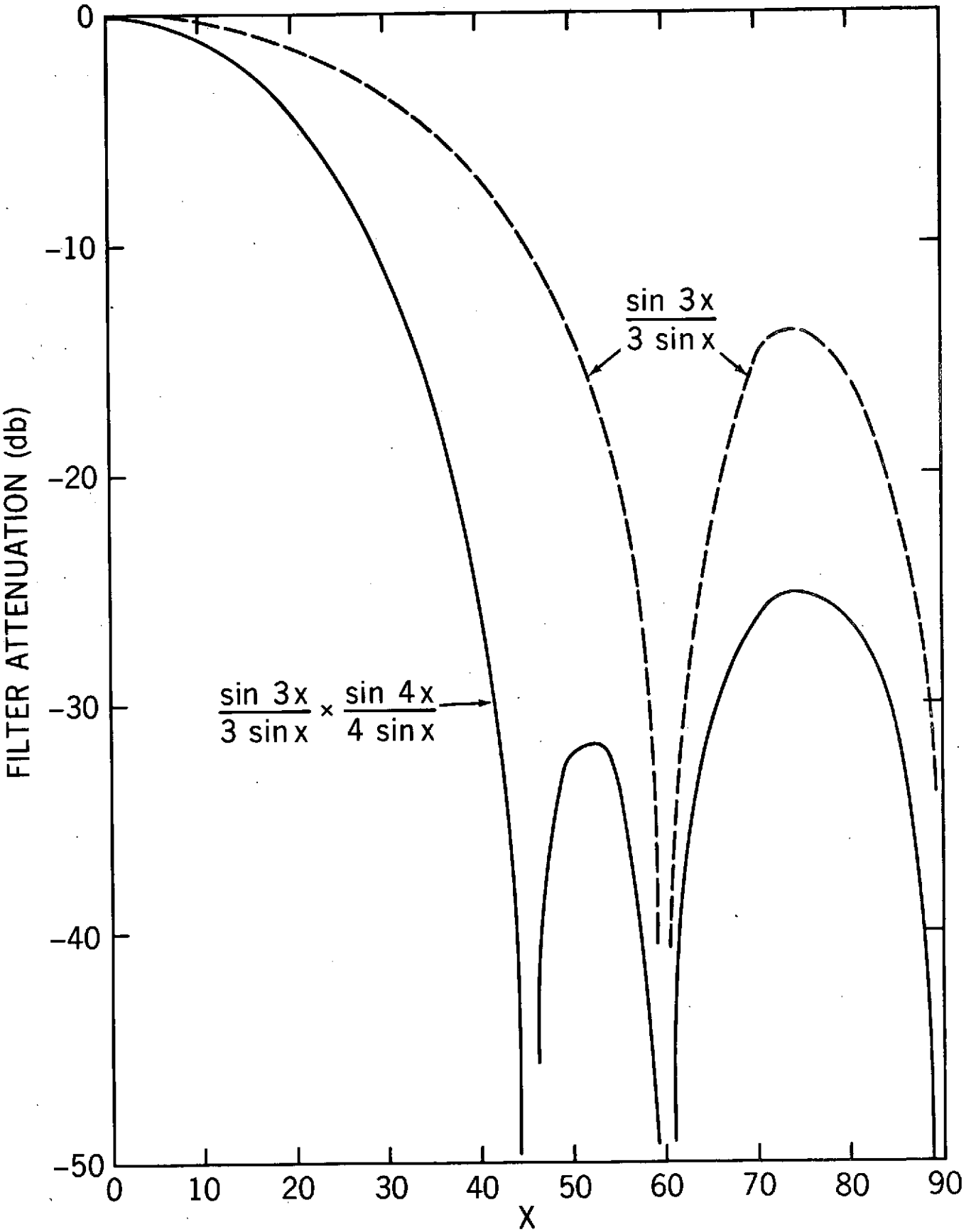
0
-10
-20
-30
-40
-50
FILTER ATTENUATION (db)
0
10
20
30
40
50
60
70
80
90
X
sin 3x / 3 sin x
sin 3x / 3 sin x × sin 4x / 4 sin x

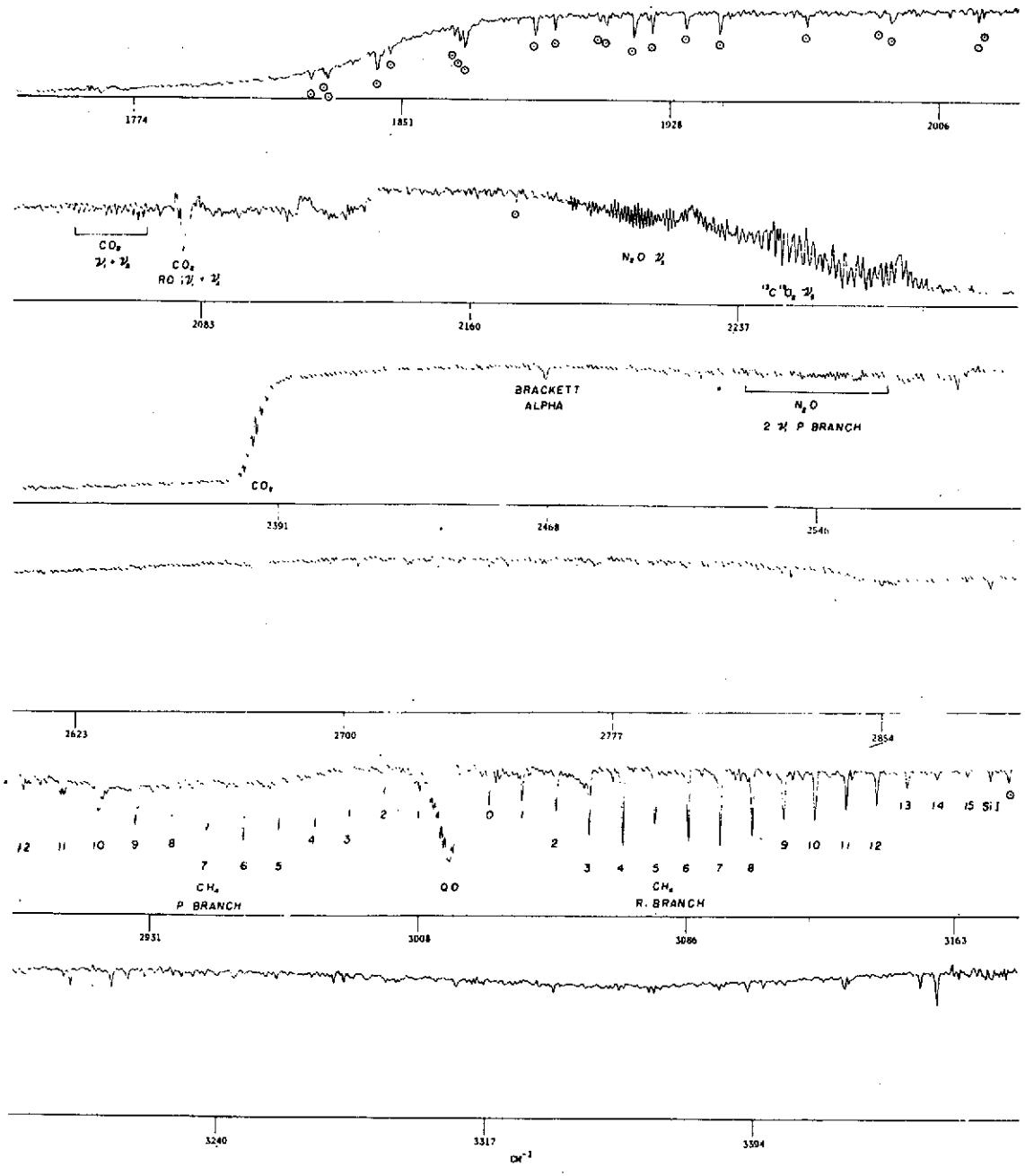
1774
1851
1928
2006
CO2
ν1 + ν3
CO2
RO ν1 + ν3
N2O ν1
13C16O2 ν1
2083
2160
2237
BRACKETT
ALPHA
N2O
2 ν1 P BRANCH
CO2
2391
2468
2546
2623
2700
2777
2854
12 11 10 9 8 7 6 5 4 3 2 1
CH4
P BRANCH
QQ
0 1 2 3 4 5 6 7 8 9 10 11 12 13 14 15 SII
CH4
R. BRANCH
2931
3008
3086
3163
3240
3317
3394
cm-1

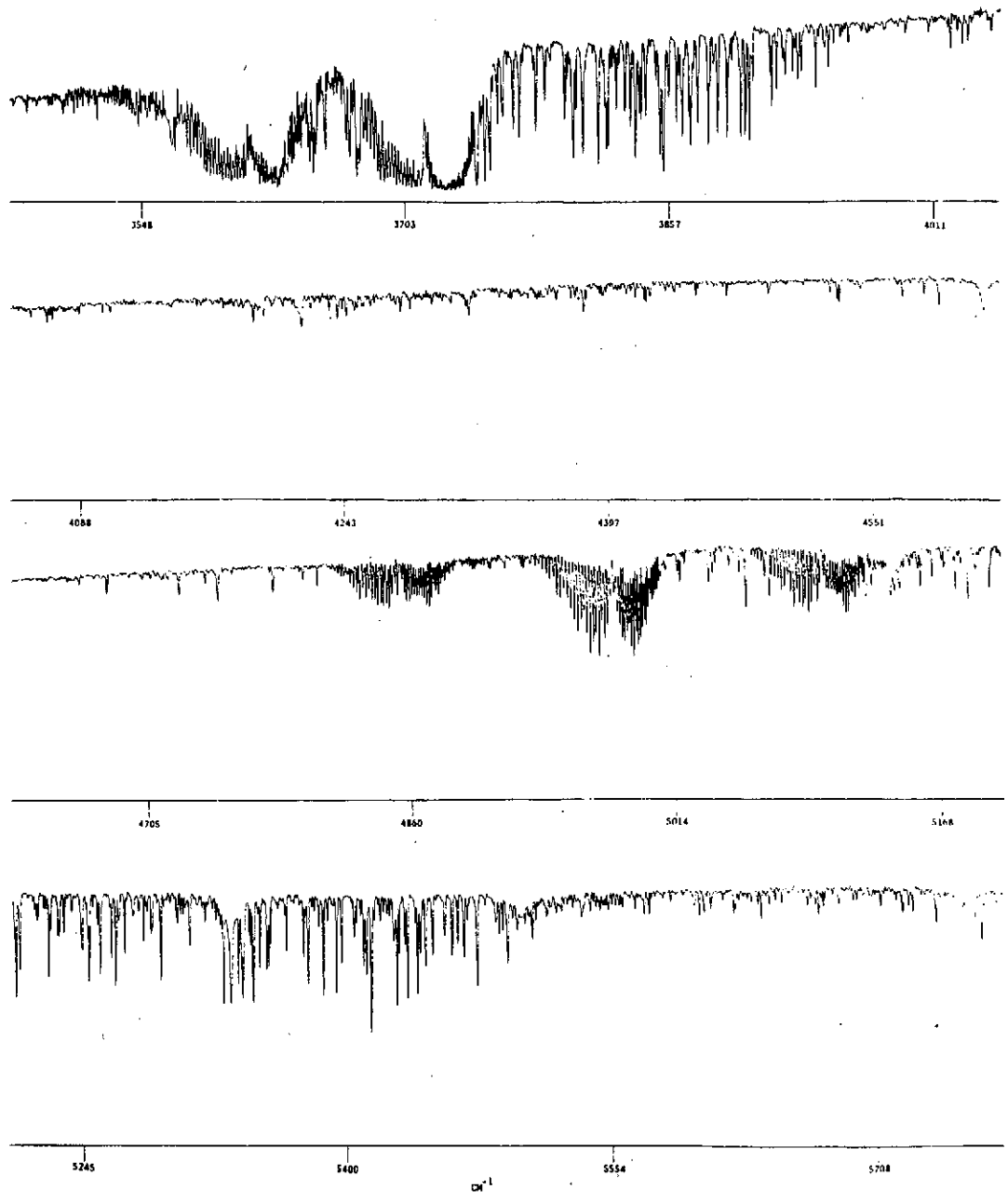
3548
3703
3857
4011
4088
4243
4397
4551
4705
4860
5014
5168
5245
5400
5554
5708
cm-1

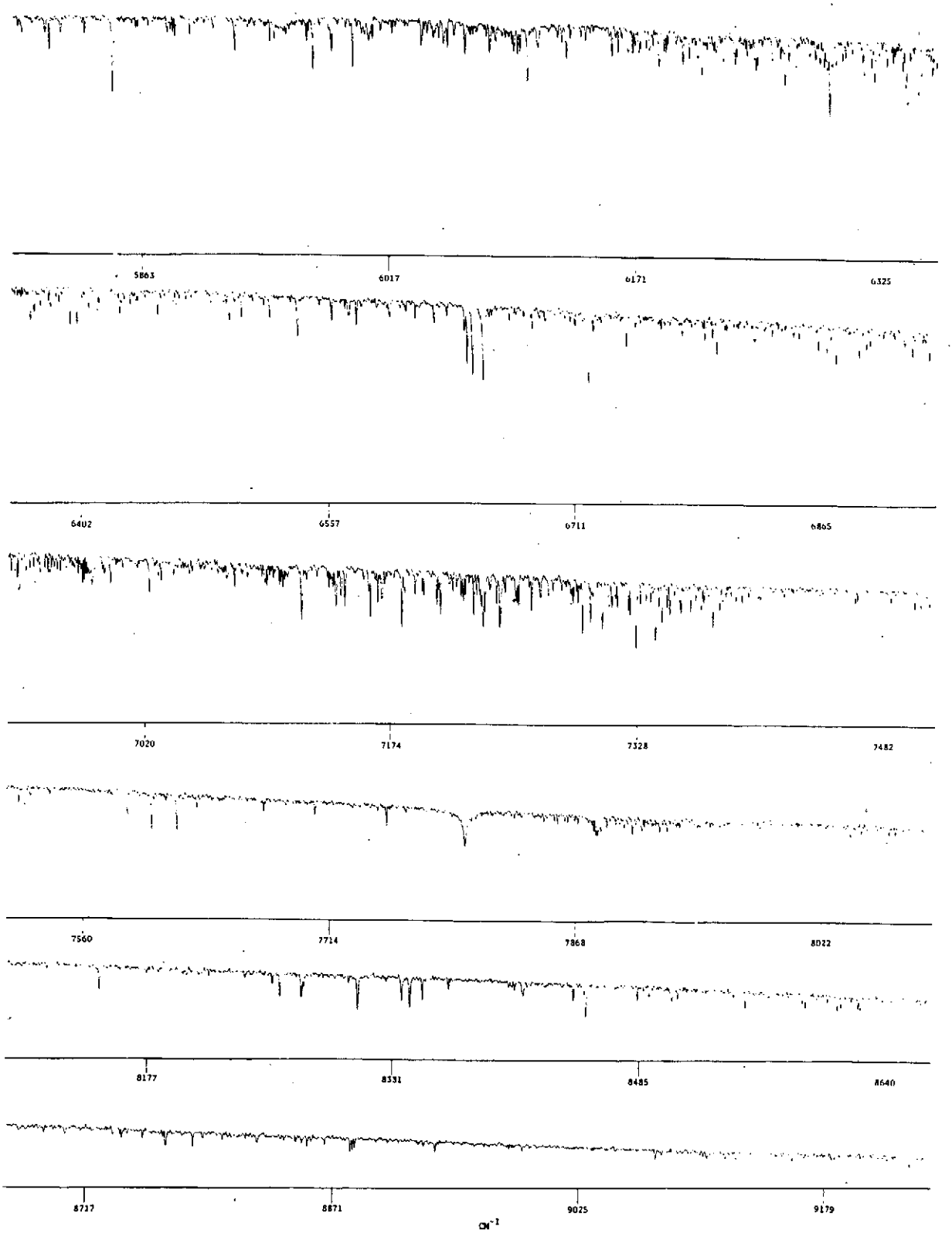
5863
6017
6171
6325
6402
6557
6711
6865
7020
7174
7328
7482
7560
7714
7868
8022
8177
8331
8485
8640
8717
8871
9025
9179
cm⁻¹

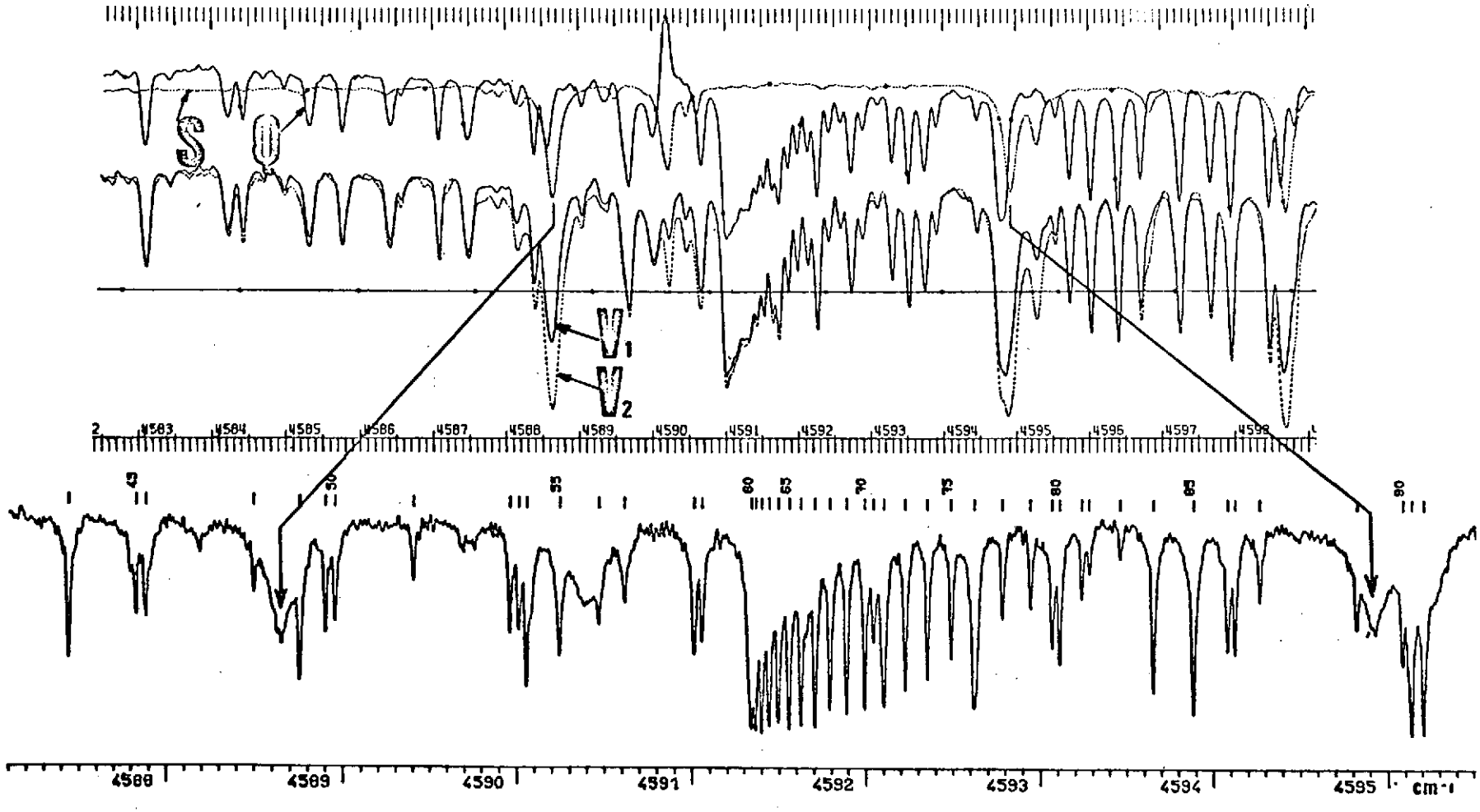
S
0
ν_1
ν_2
4583
4584
4585
4586
4587
4588
4589
4590
4591
4592
4593
4594
4595
4596
4597
4598
4588
4589
4590
4591
4592
4593
4594
4595
cm-1

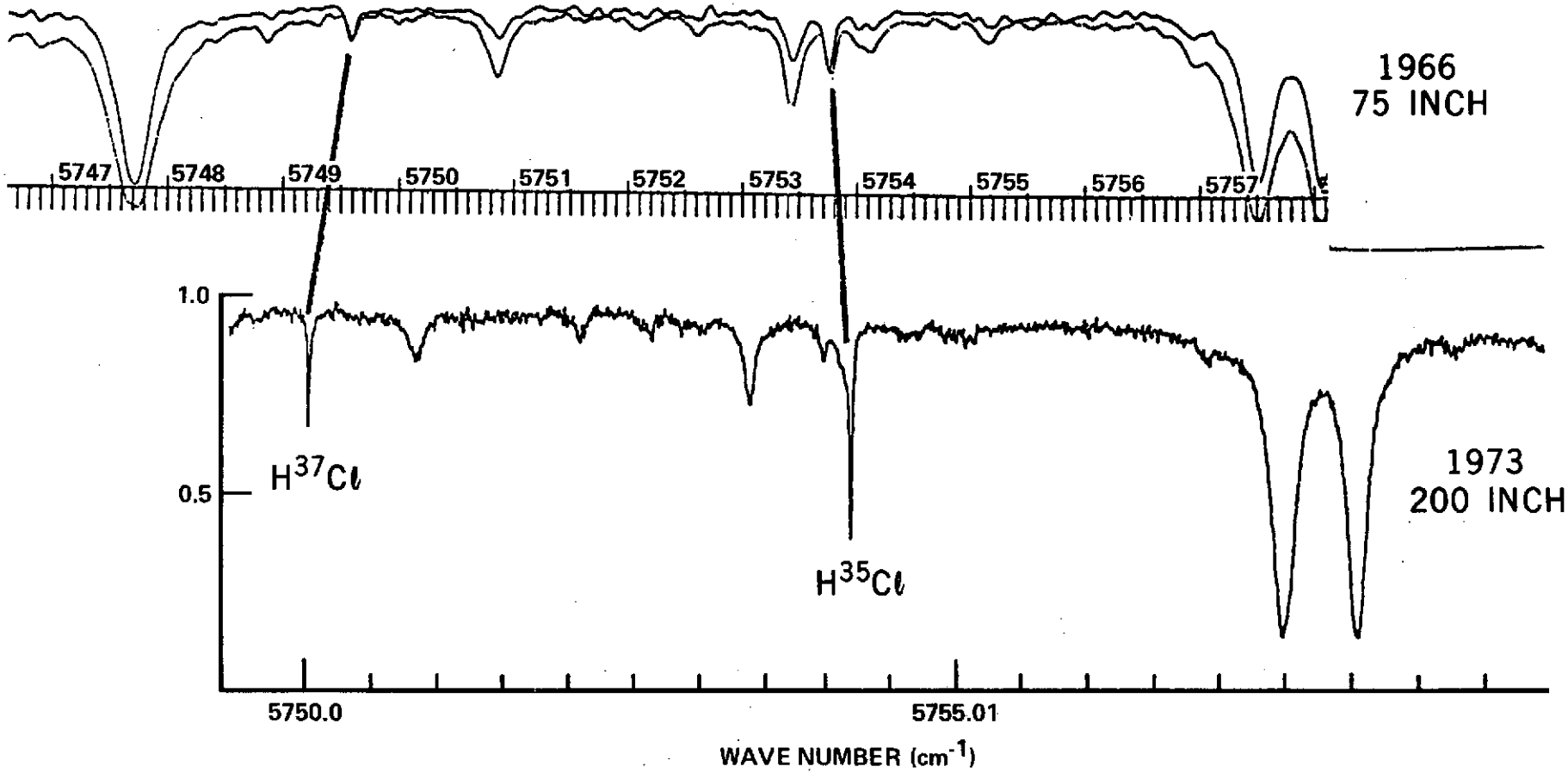
1966
75 INCH
5747
5748
5749
5750
5751
5752
5753
5754
5755
5756
5757
1.0
0.5
H37Cl
H35Cl
1973
200 INCH
5750.0
5755.01
WAVE NUMBER (cm-1)

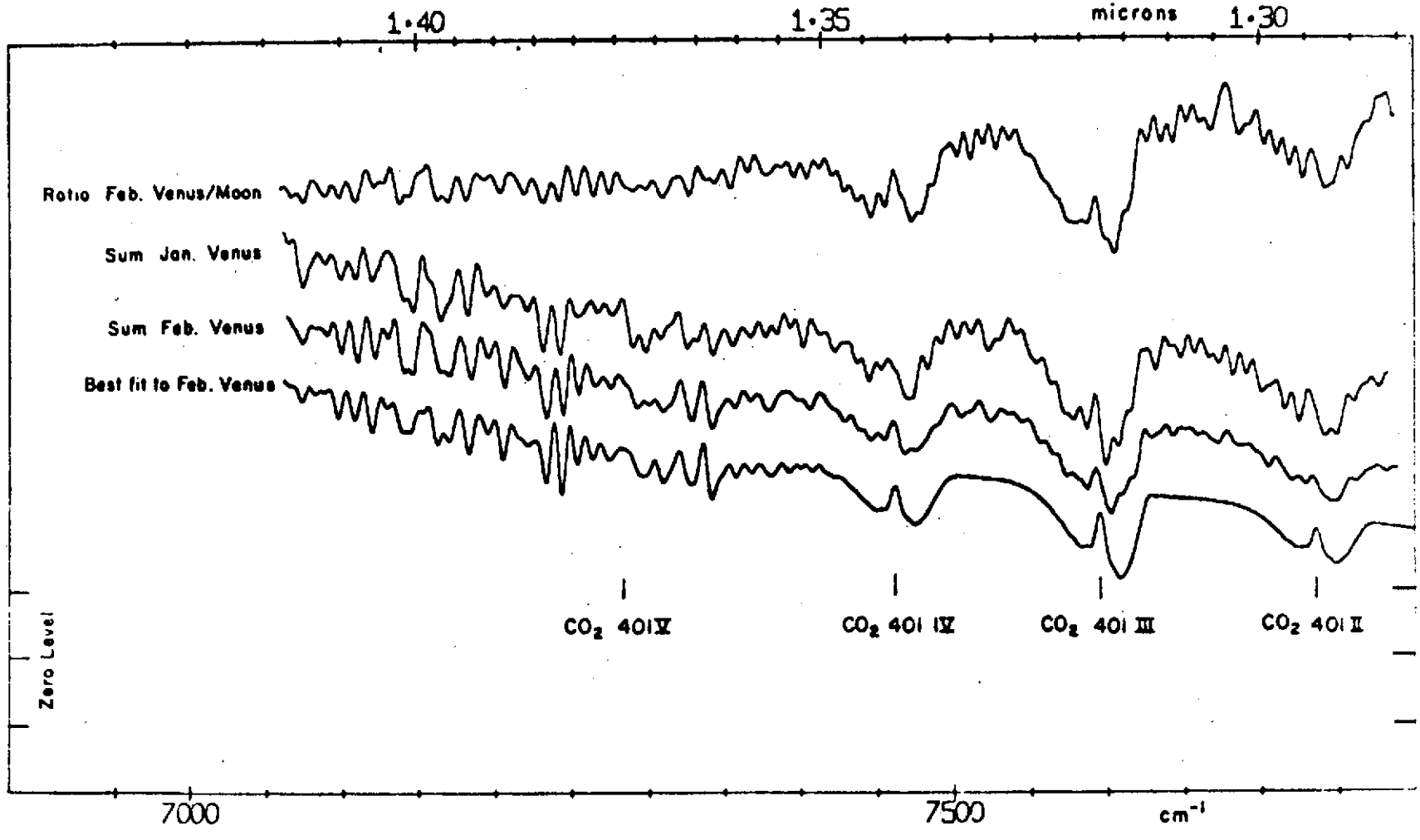
1·40
1·35
microns
1·30
Ratio Feb. Venus/Moon
Sum Jan. Venus
Sum Feb. Venus
Best fit to Feb. Venus
CO_2 401 IV
CO_2 401 III
CO_2 401 II
Zero Level
7000
7500
cm^{-1}

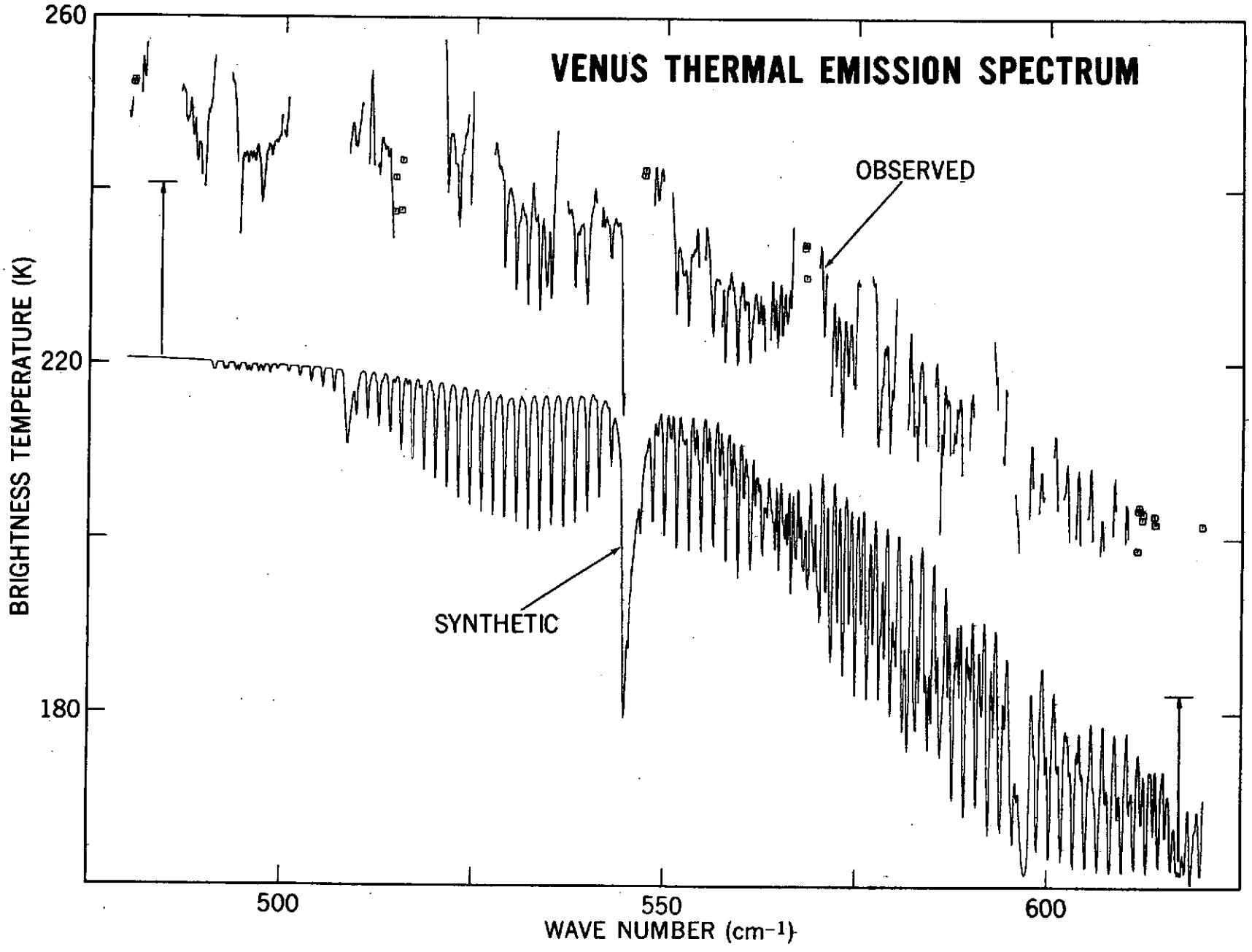
VENUS THERMAL EMISSION SPECTRUM
OBSERVED
SYNTHETIC
BRIGHTNESS TEMPERATURE (K)
260
220
180
500
550
600
WAVE NUMBER (cm⁻¹)

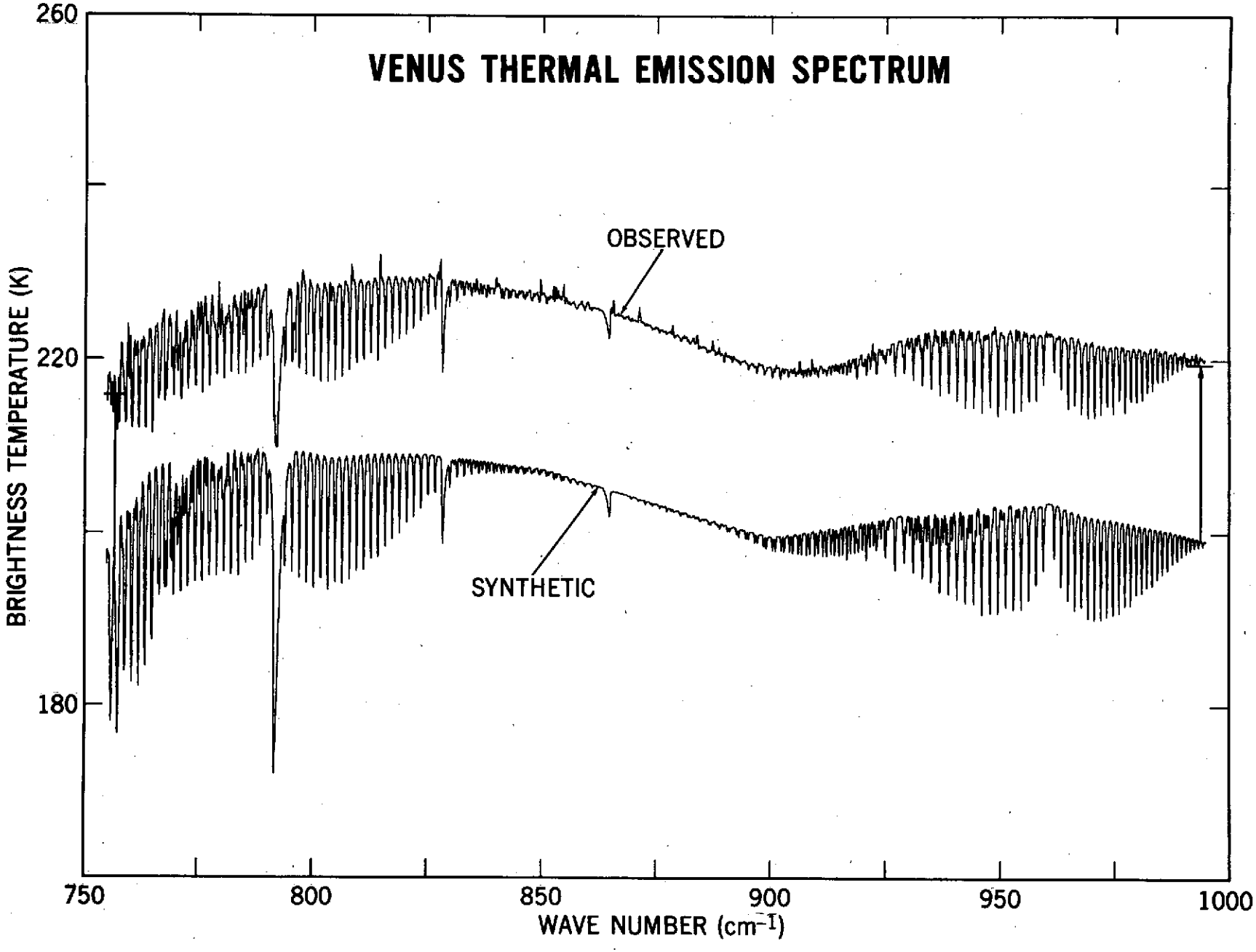
VENUS THERMAL EMISSION SPECTRUM
OBSERVED
SYNTHETIC
BRIGHTNESS TEMPERATURE (K)
260
220
180
750
800
850
900
950
1000
WAVE NUMBER (cm⁻¹)

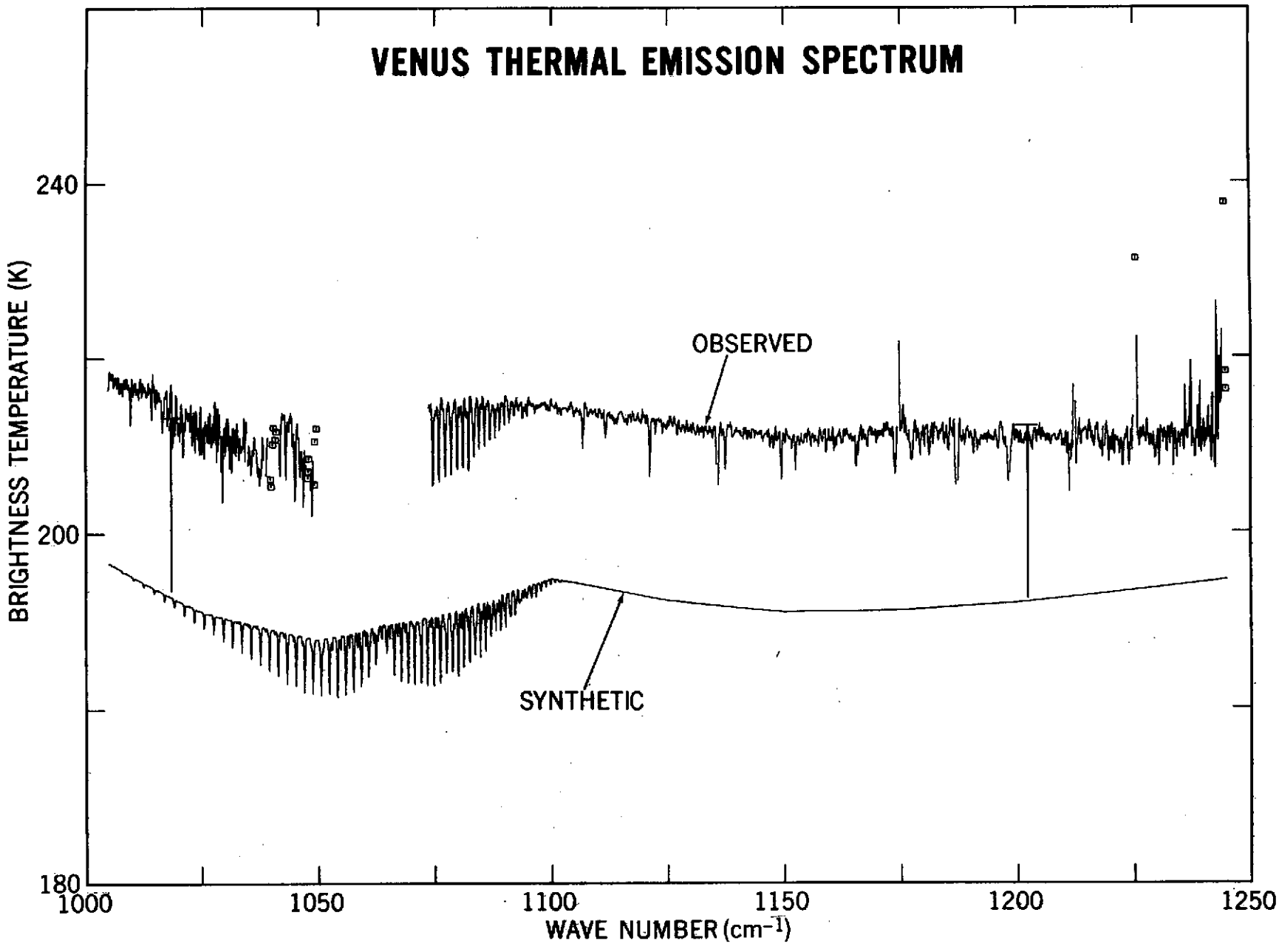
VENUS THERMAL EMISSION SPECTRUM
BRIGHTNESS TEMPERATURE (K)
240
200
180
OBSERVED
SYNTHETIC
1000
1050
1100
1150
1200
1250
WAVE NUMBER (cm⁻¹)

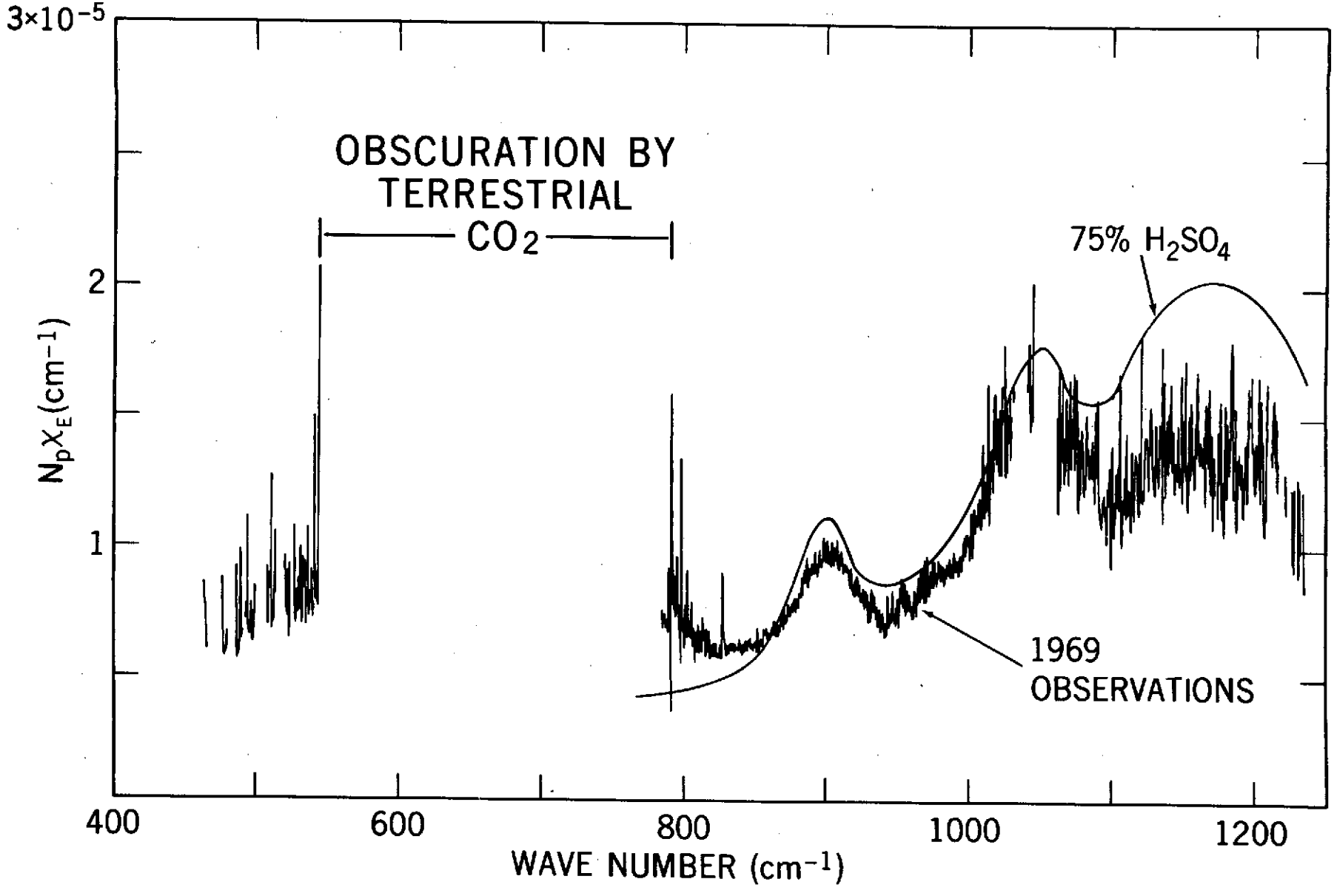
3×10⁻⁵
2
1
$N_p\chi_E(cm^{-1})$
OBSCURATION BY
TERRESTRIAL
CO_2
75% H_2SO_4
1969
OBSERVATIONS
400
600
800
1000
1200
WAVE NUMBER (cm^{-1})

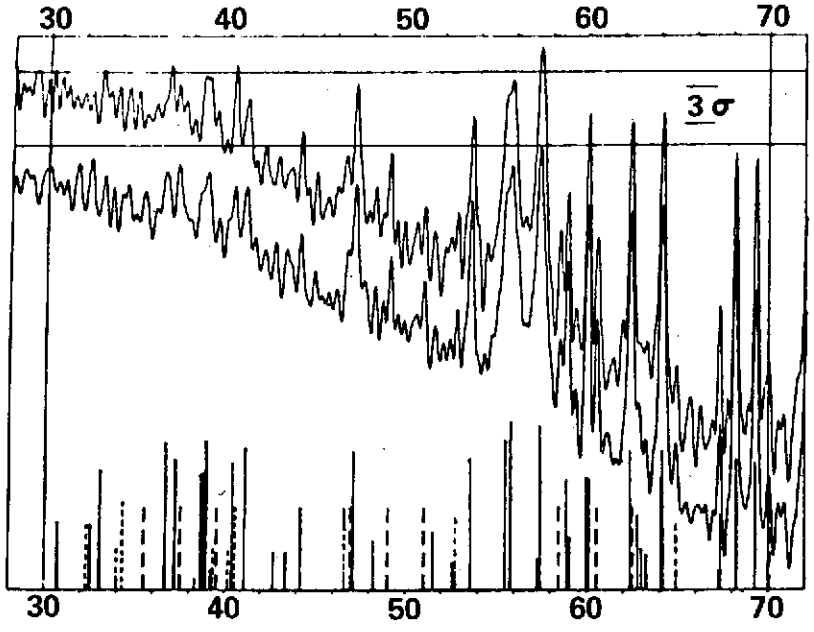
30
40
50
60
70
3σ

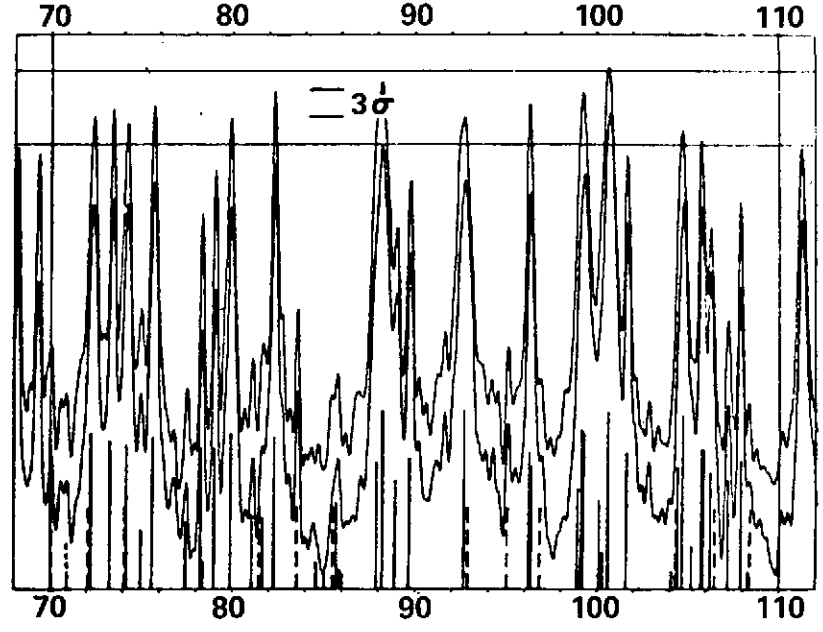
70
80
90
100
110
3σ

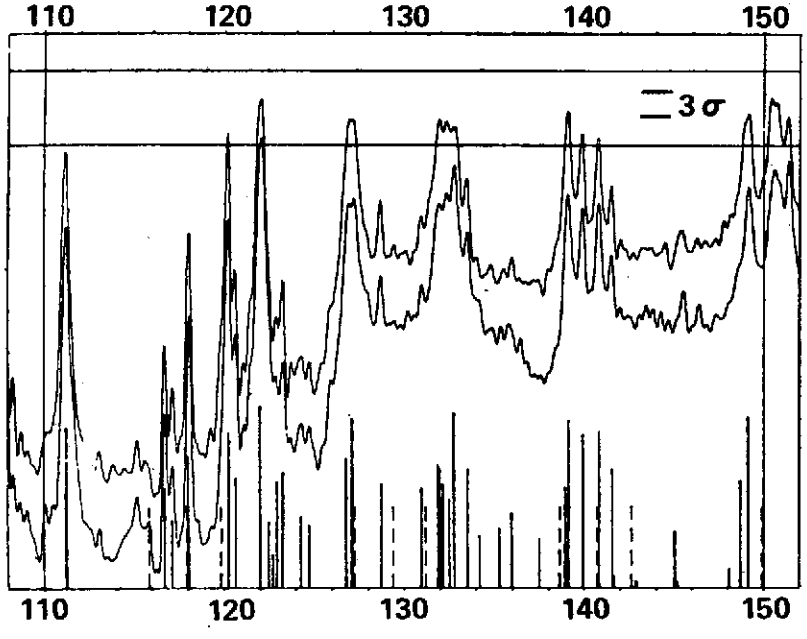
110
120
130
140
150
3σ

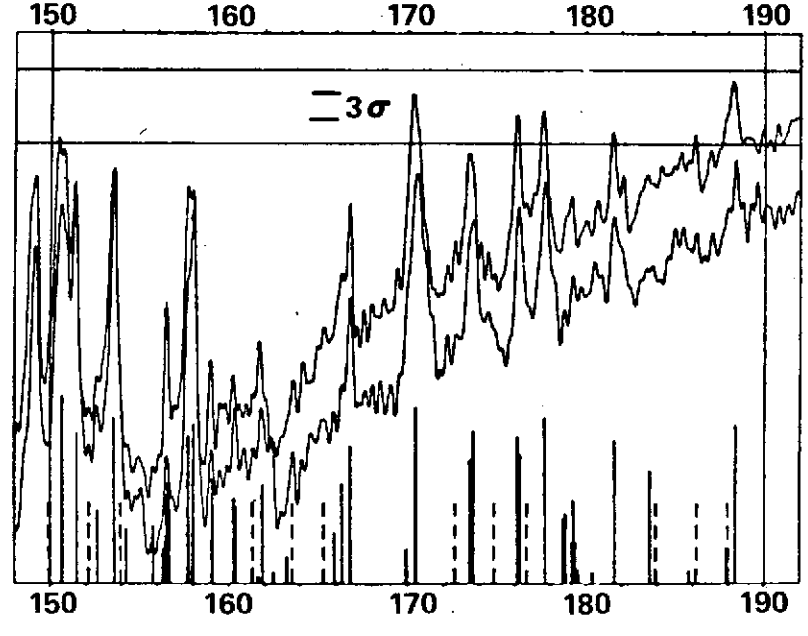
150
160
170
180
190
3σ

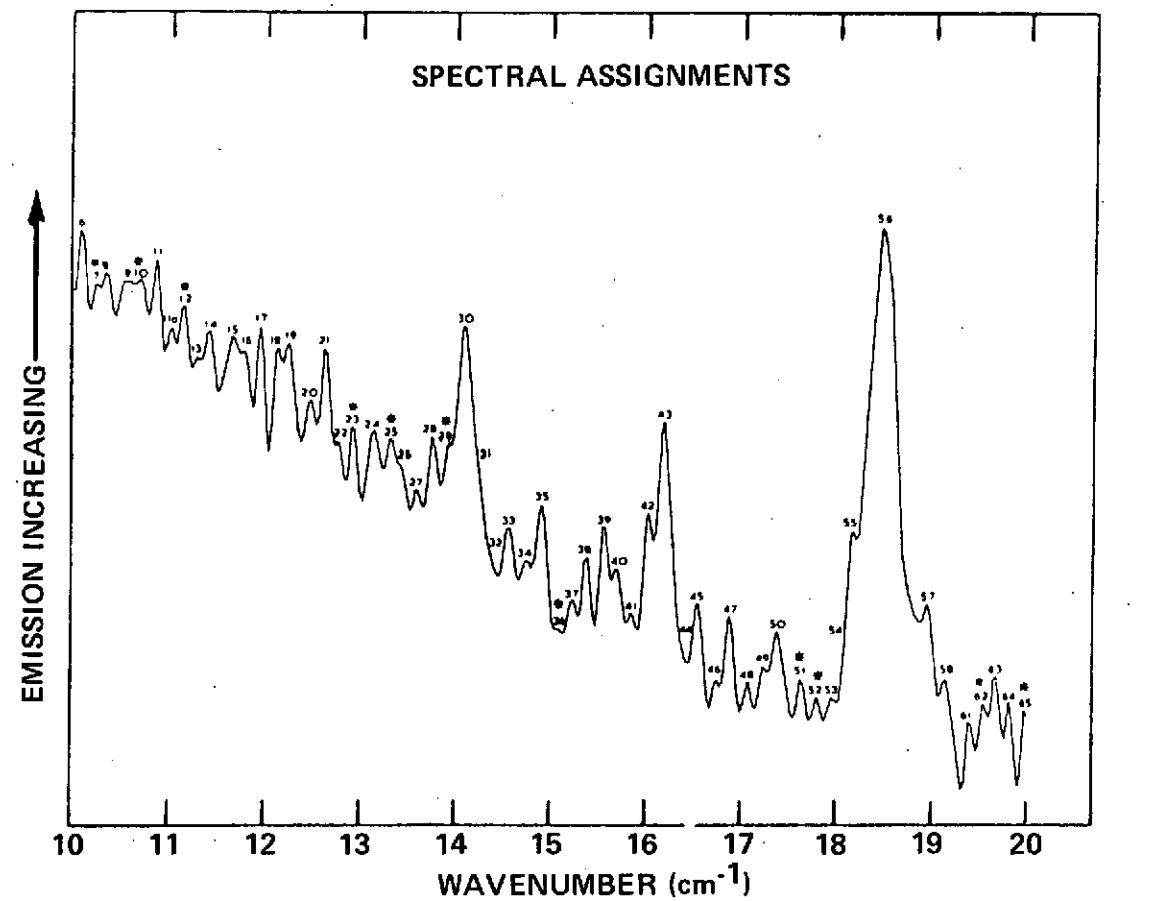
SPECTRAL ASSIGNMENTS
EMISSION INCREASING
10
11
12
13
14
15
16
17
18
19
20
WAVENUMBER (cm-1)

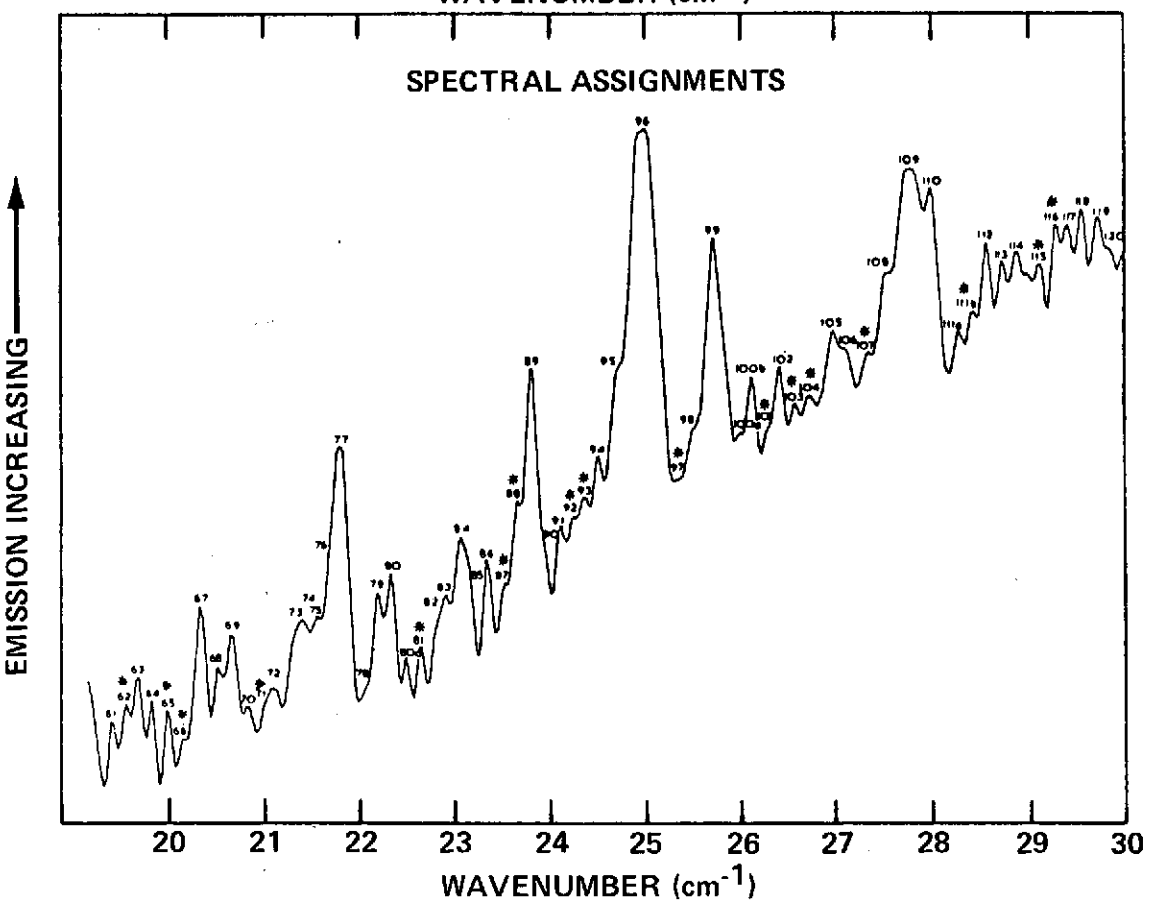
SPECTRAL ASSIGNMENTS
EMISSION INCREASING
20
21
22
23
24
25
26
27
28
29
30
WAVENUMBER (cm-1)

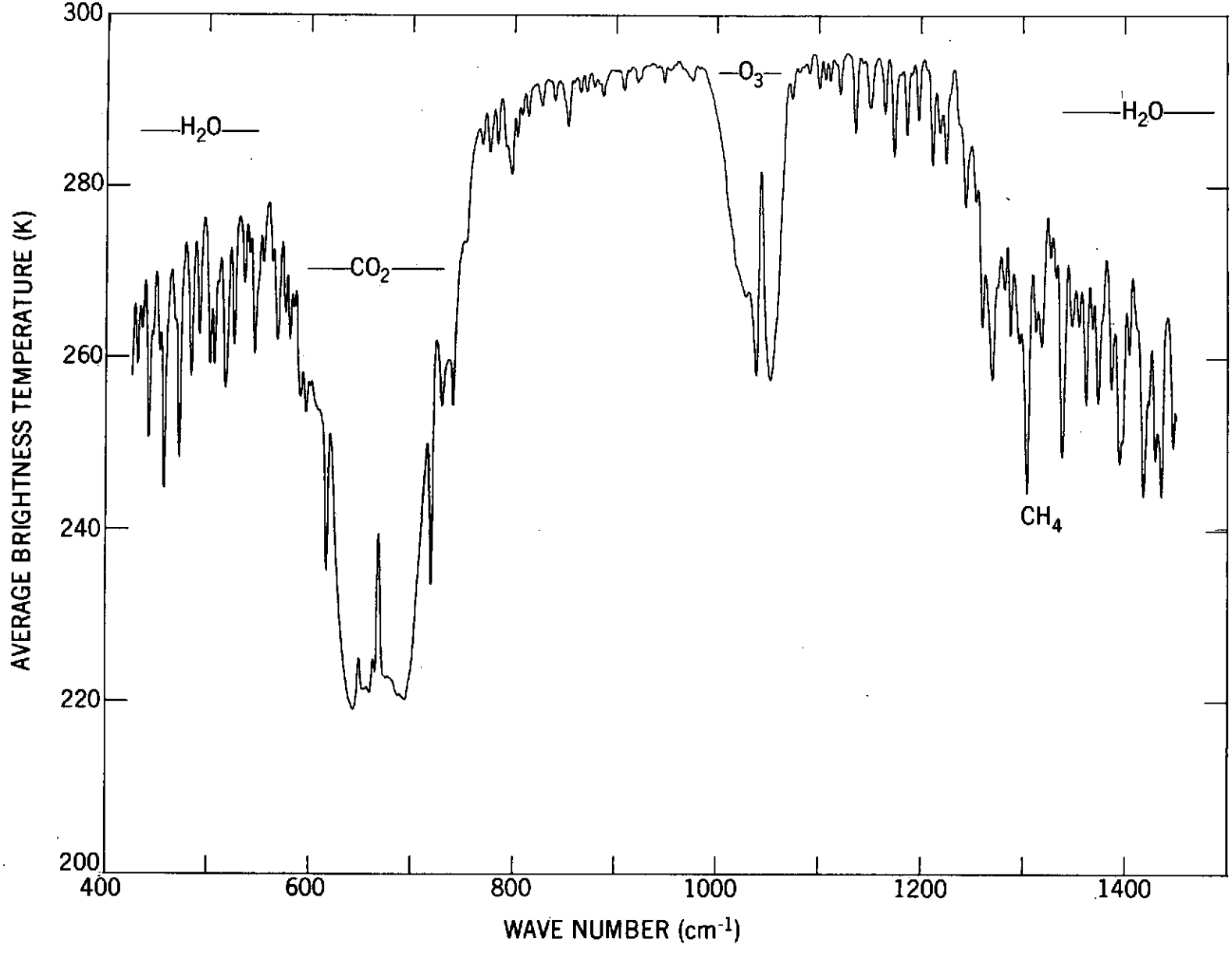
300
280
260
240
220
200
400
600
800
1000
1200
1400
AVERAGE BRIGHTNESS TEMPERATURE (K)
WAVE NUMBER (cm-1)
H2O
CO2
O3
H2O
CH4

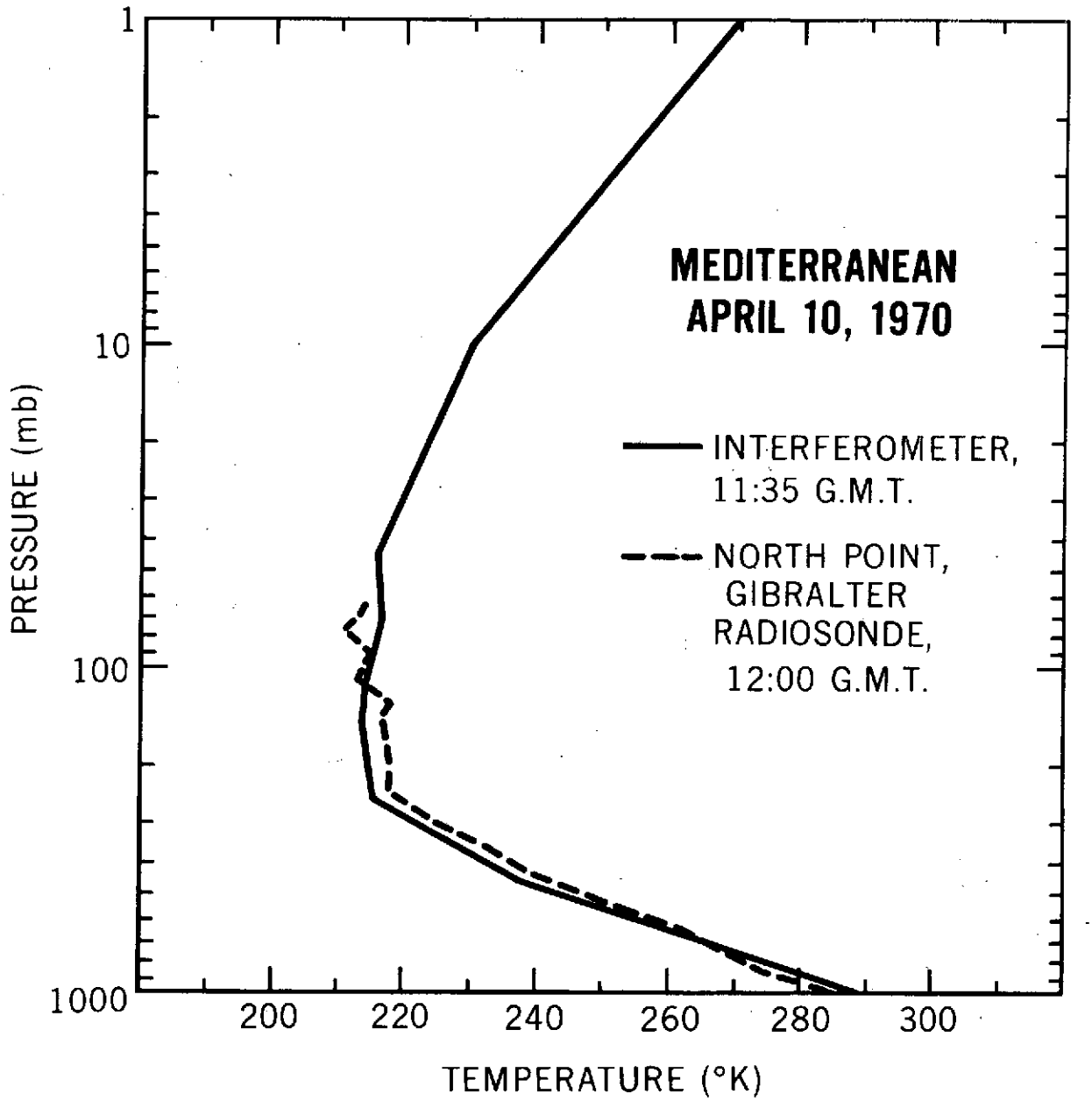
MEDITERRANEAN
APRIL 10, 1970
INTERFEROMETER, 11:35 G.M.T.
NORTH POINT, GIBRALTER RADIOSONDE, 12:00 G.M.T.
PRESSURE (mb)
1
10
100
1000
200
220
240
260
280
300
TEMPERATURE (°K)

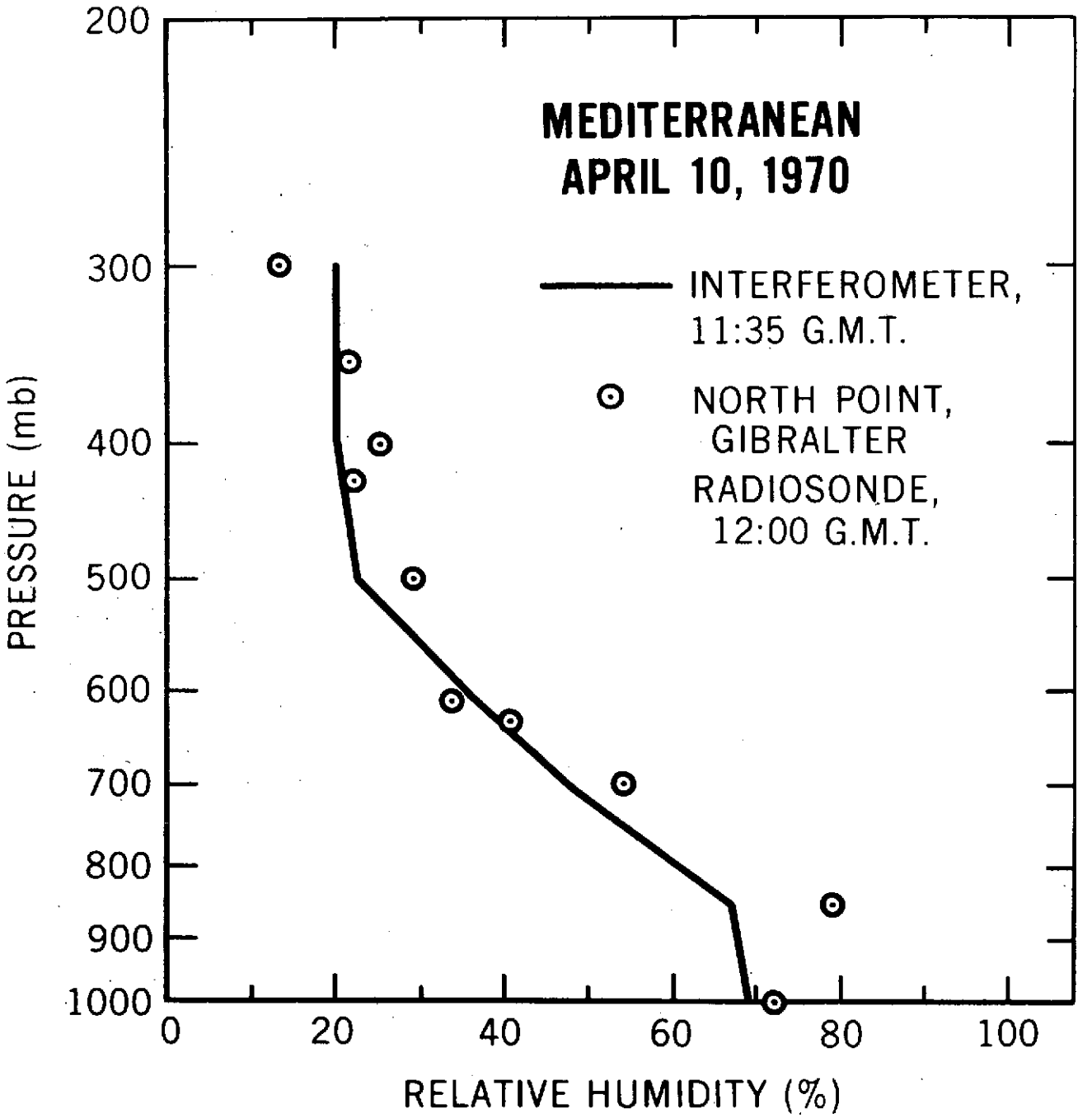
MEDITERRANEAN
APRIL 10, 1970
INTERFEROMETER, 11:35 G.M.T.
NORTH POINT, GIBRALTER RADIOSONDE, 12:00 G.M.T.
PRESSURE (mb)
200
300
400
500
600
700
800
900
1000
0
20
40
60
80
100
RELATIVE HUMIDITY (%)

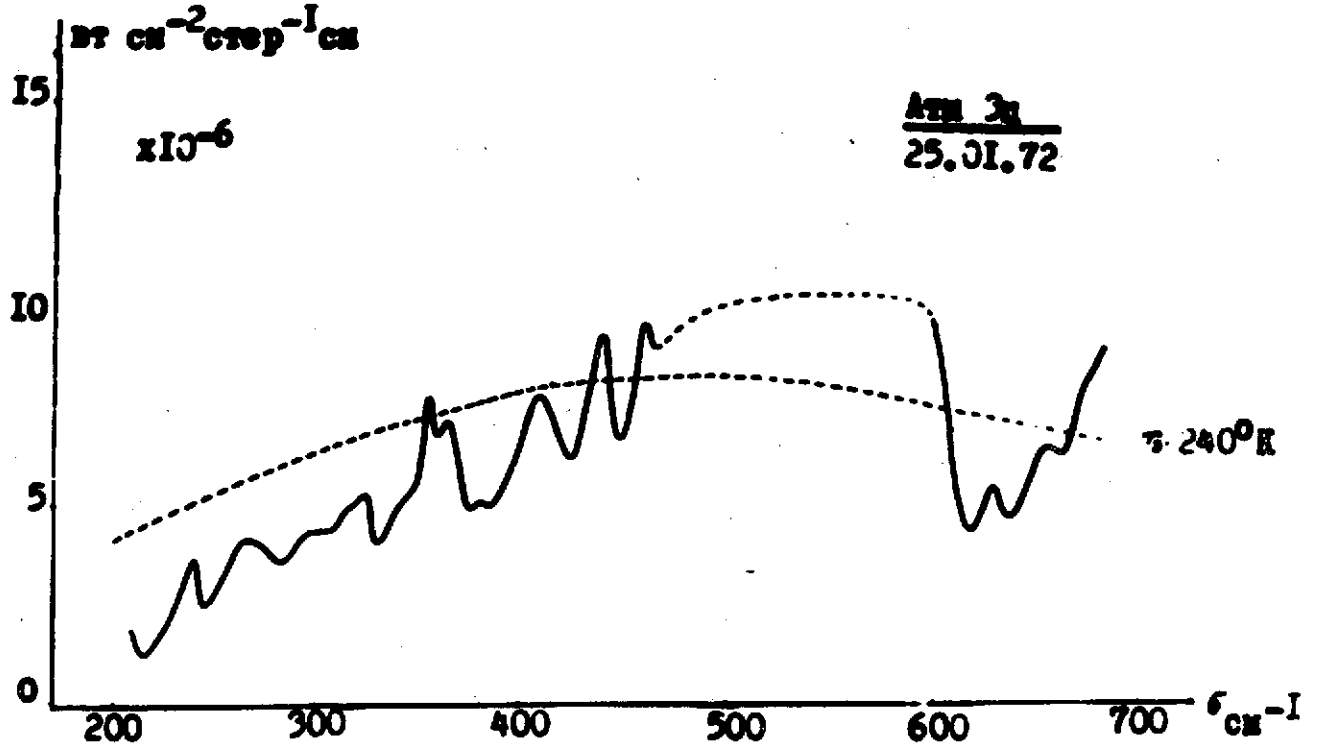
вт см⁻²стер⁻¹см
I5
xI0⁻⁶
Атм Зн
25.0I.72
I0
5
0
T≈240°K
200
300
400
500
600
700
σ см⁻¹

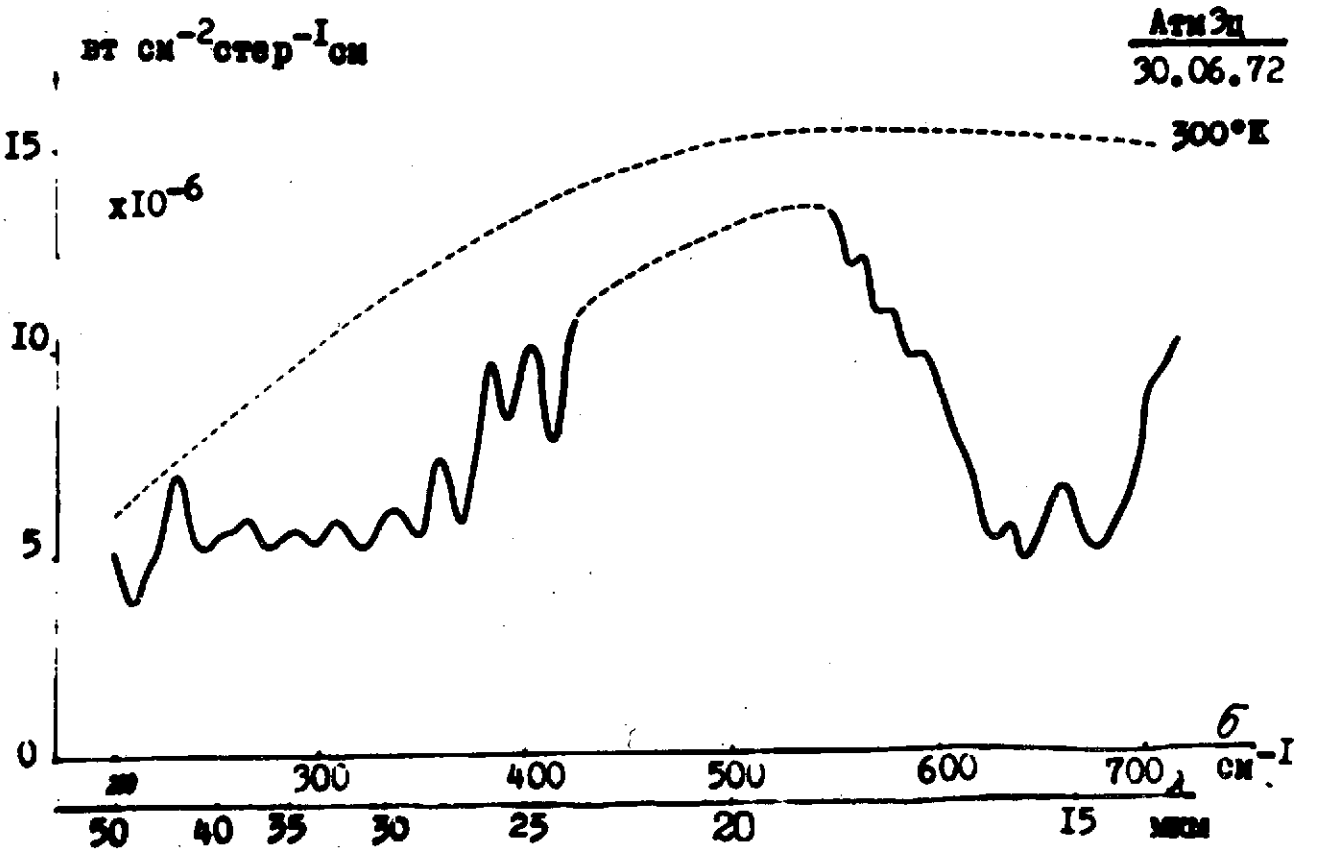
вт см⁻²стер⁻¹см
Атм Зн
30.06.72
300°K
I5
xI0⁻⁶
I0
5
0
σ
см⁻¹
300
400
500
600
700
50
40
35
30
25
20
I5
мкм

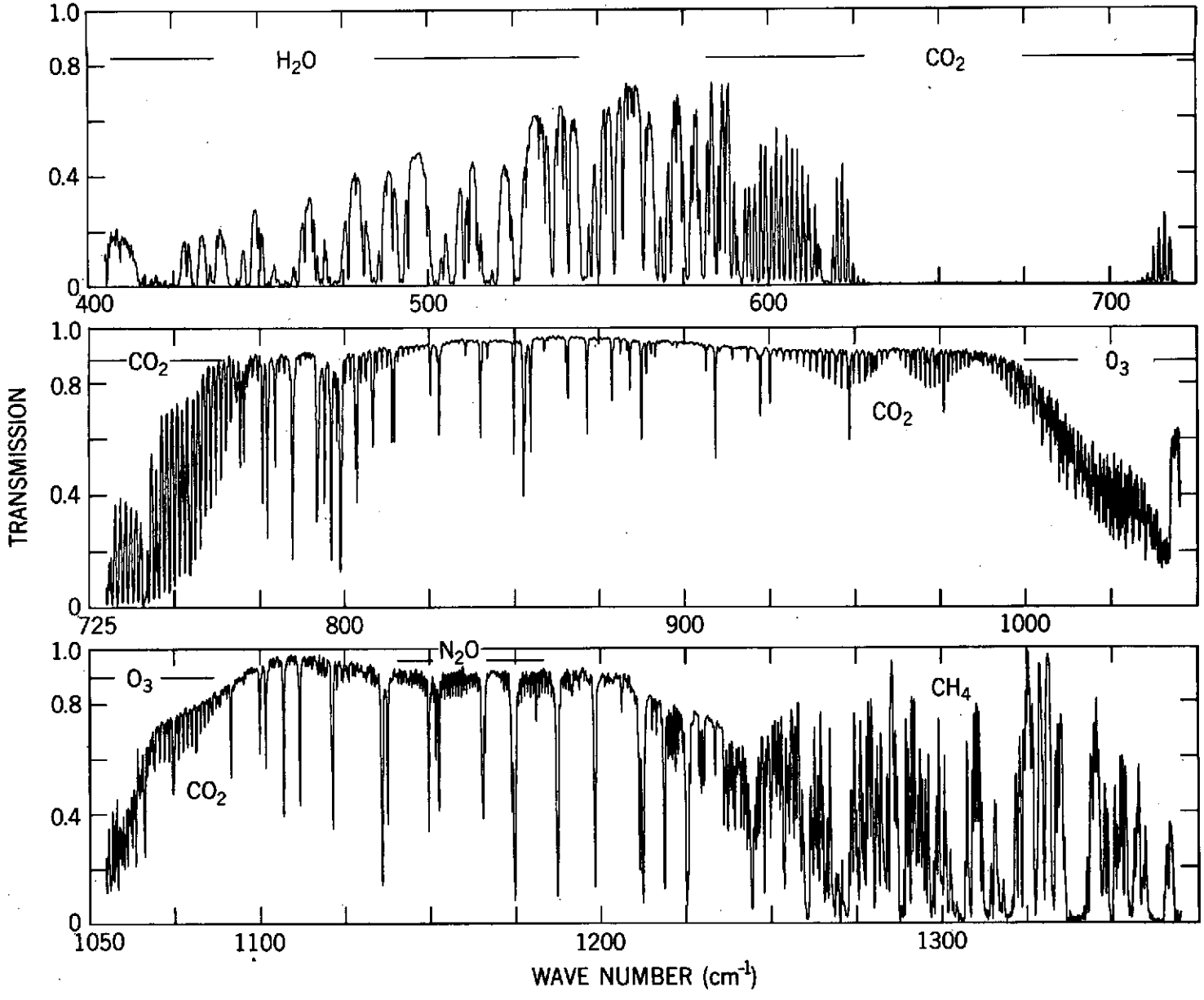
TRANSMISSION
1.0
0.8
0.4
0
H_2O
CO_2
400
500
600
700
CO_2
O_3
CO_2
725
800
900
1000
N_2O
O_3
CH_4
CO_2
1050
1100
1200
1300
WAVE NUMBER (cm^{-1})

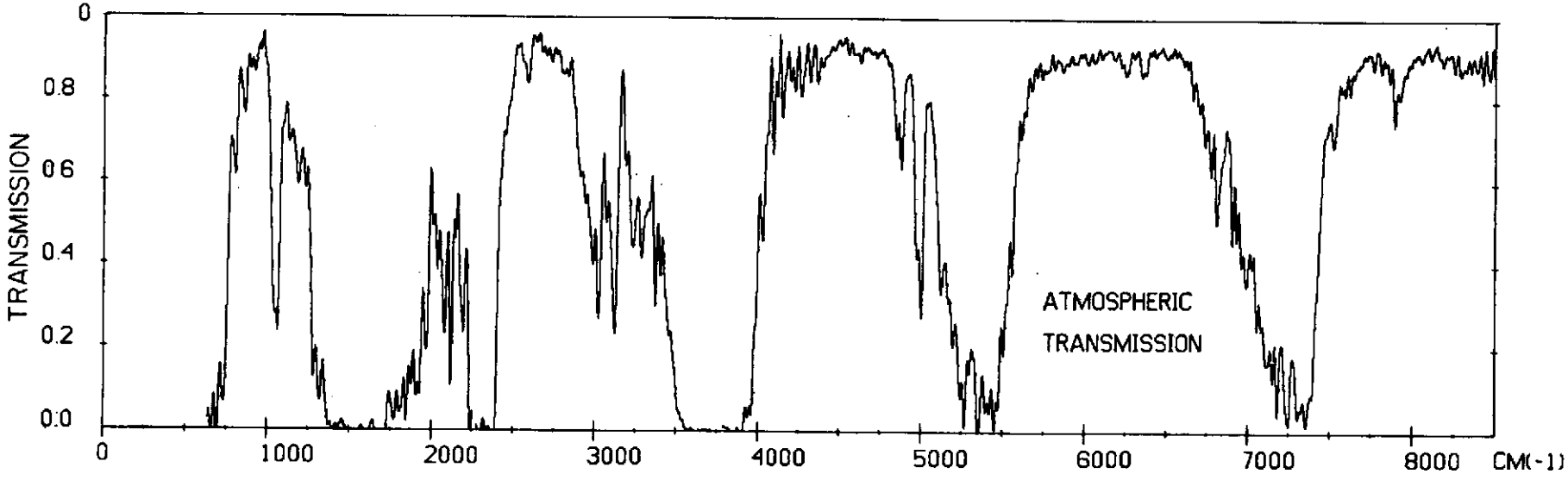
TRANSMISSION
0
0.8
0.6
0.4
0.2
0.0
0
1000
2000
3000
4000
5000
6000
7000
8000
CM(-1)
ATMOSPHERIC
TRANSMISSION

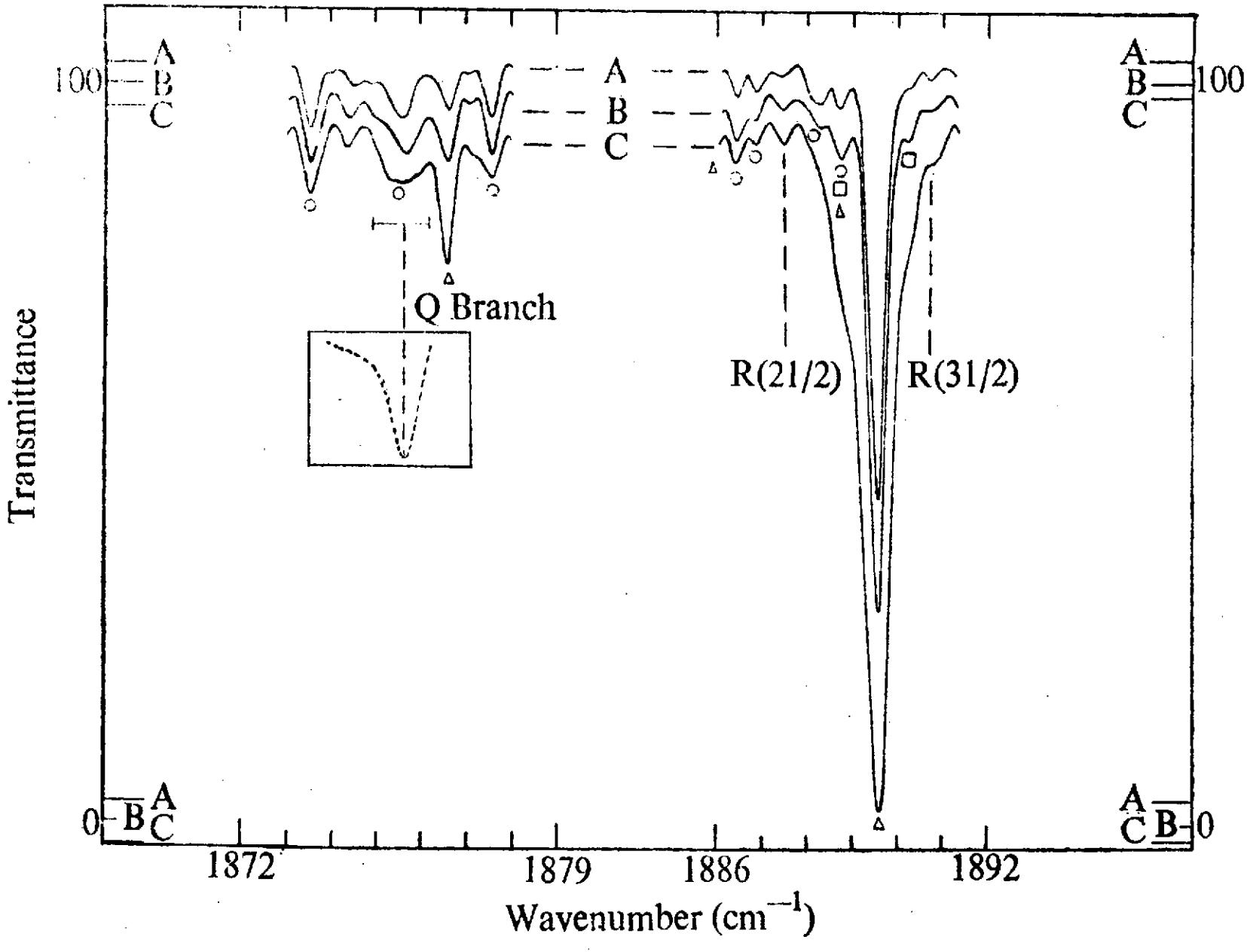
100
A
B
C
0
A
B
C
Transmittance
Q Branch
R(21/2)
R(31/2)
1872
1879
1886
1892
Wavenumber (cm^{-1})

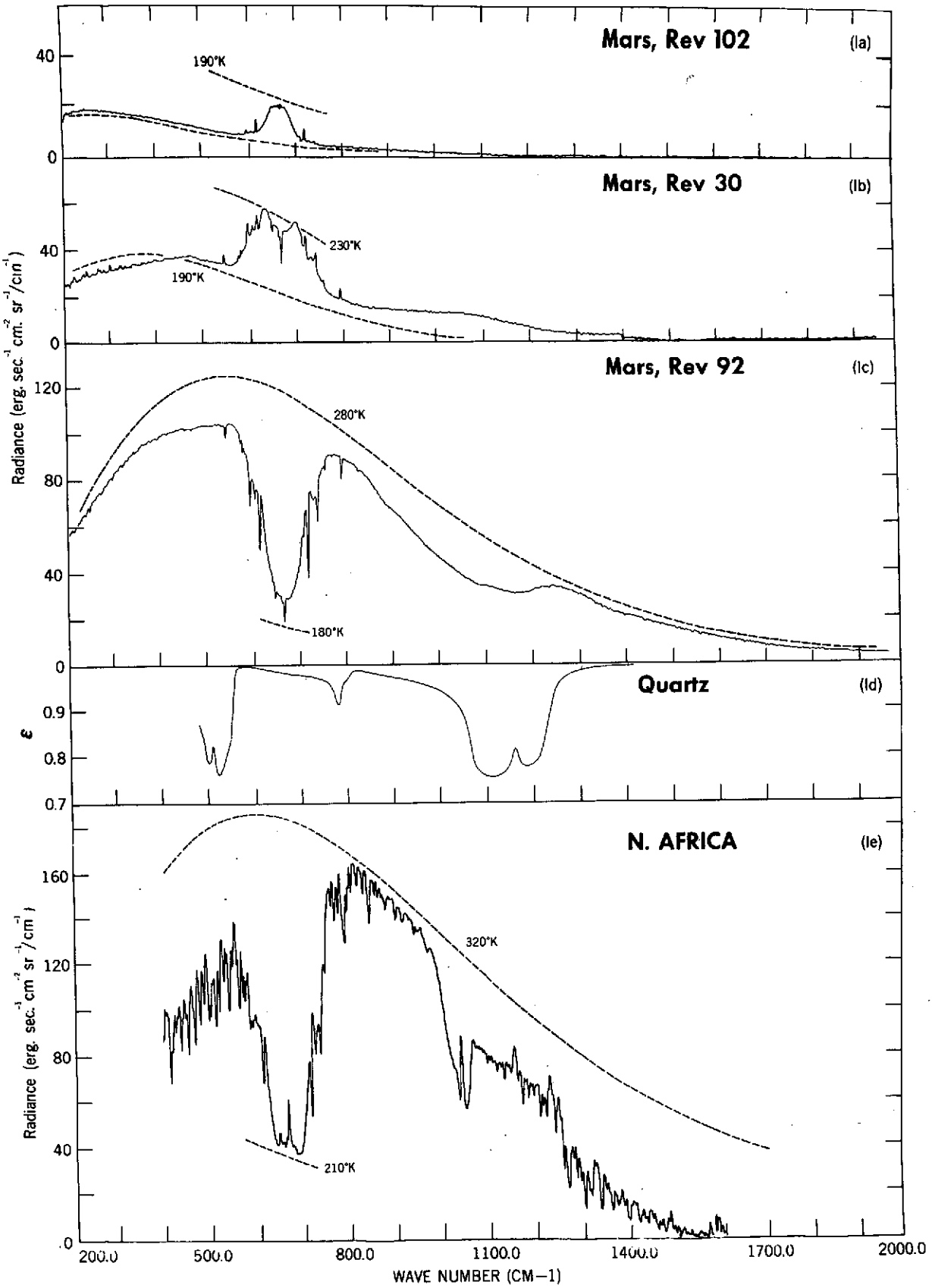
Mars, Rev 102
(Ia)
190°K
Mars, Rev 30
(Ib)
230°K
190°K
Mars, Rev 92
(Ic)
280°K
180°K
Quartz
(Id)
ε
N. AFRICA
(Ie)
320°K
210°K
Radiance (erg. sec.⁻¹ cm.⁻² cm. sr⁻¹/cm⁻¹)
Radiance (erg. sec.⁻¹ cm⁻² sr⁻¹/cm⁻¹)
WAVE NUMBER (CM−1)
200.0
500.0
800.0
1100.0
1400.0
1700.0
2000.0

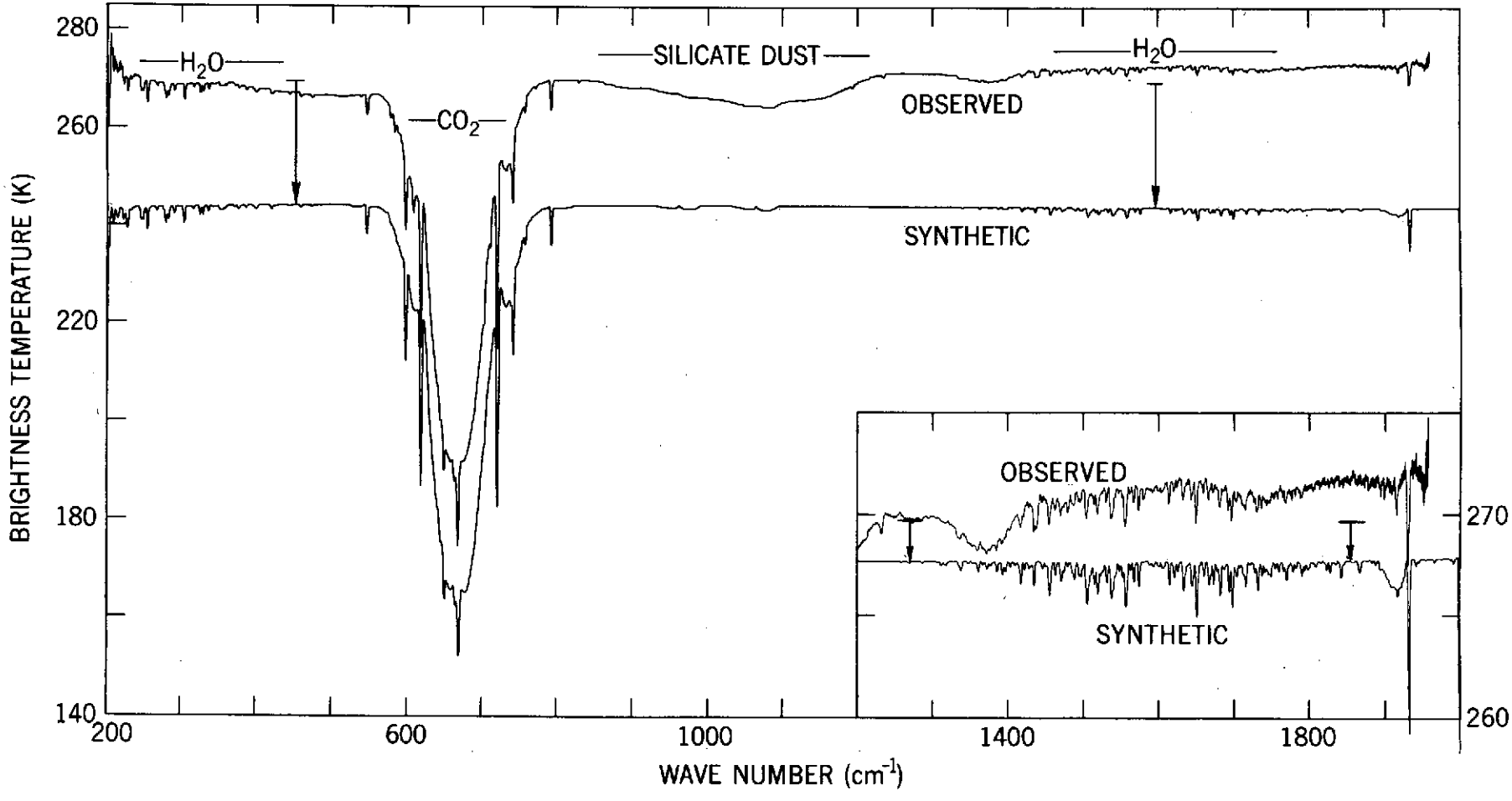
280
260
220
180
140
BRIGHTNESS TEMPERATURE (K)
H_2O
CO_2
SILICATE DUST
H_2O
OBSERVED
SYNTHETIC
OBSERVED
SYNTHETIC
270
260
200
600
1000
1400
1800
WAVE NUMBER (cm^{-1})

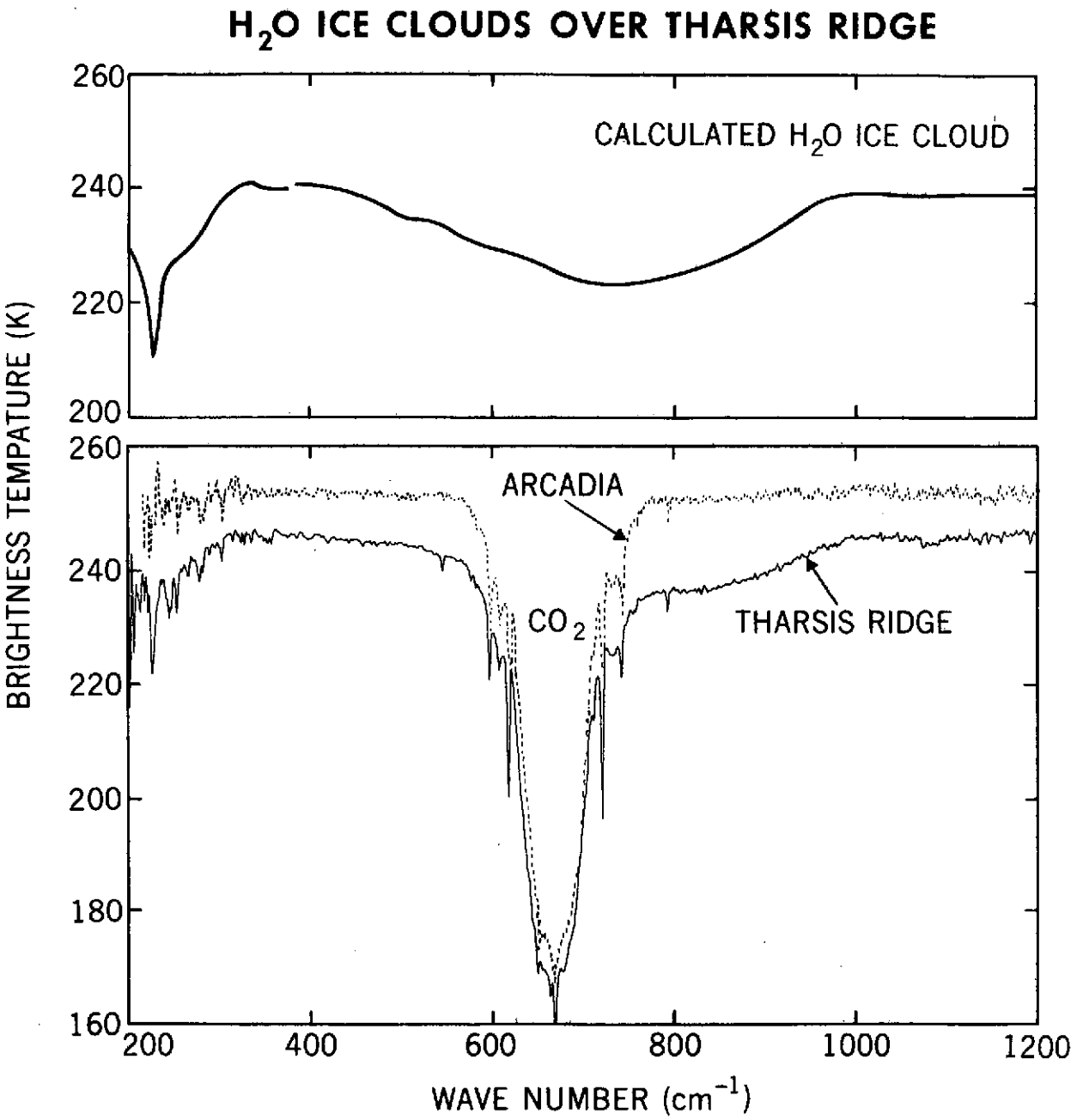
H2O ICE CLOUDS OVER THARSIS RIDGE
CALCULATED H2O ICE CLOUD
ARCADIA
CO2
THARSIS RIDGE
BRIGHTNESS TEMPATURE (K)
WAVE NUMBER (cm-1)
260
240
220
200
180
160
200
400
600
800
1000
1200

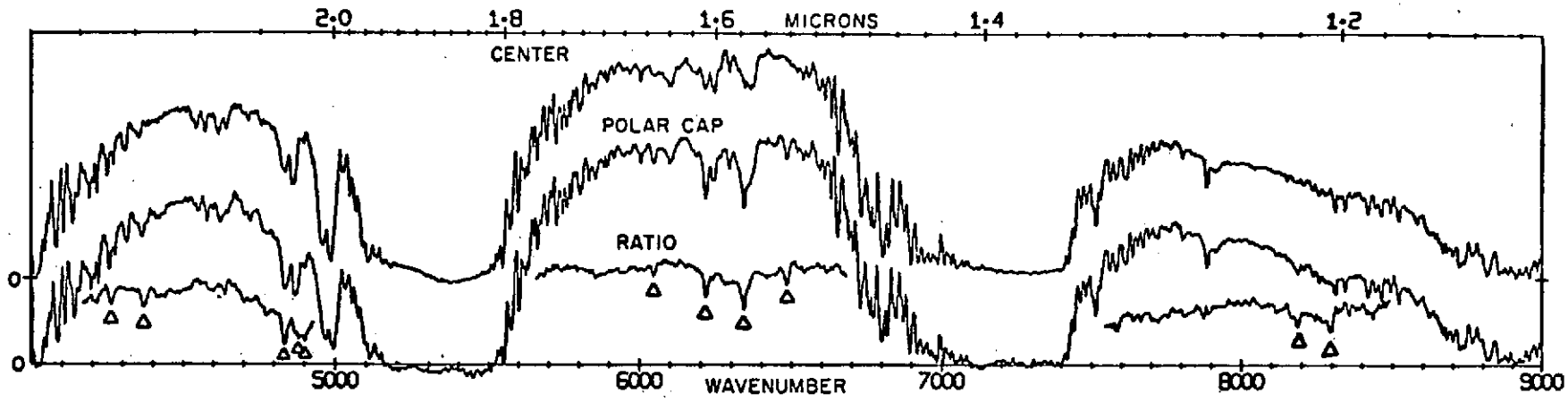
2·0
1·8
1·6
MICRONS
1·4
1·2
CENTER
POLAR CAP
RATIO
0
0
5000
6000
WAVENUMBER
7000
8000
9000

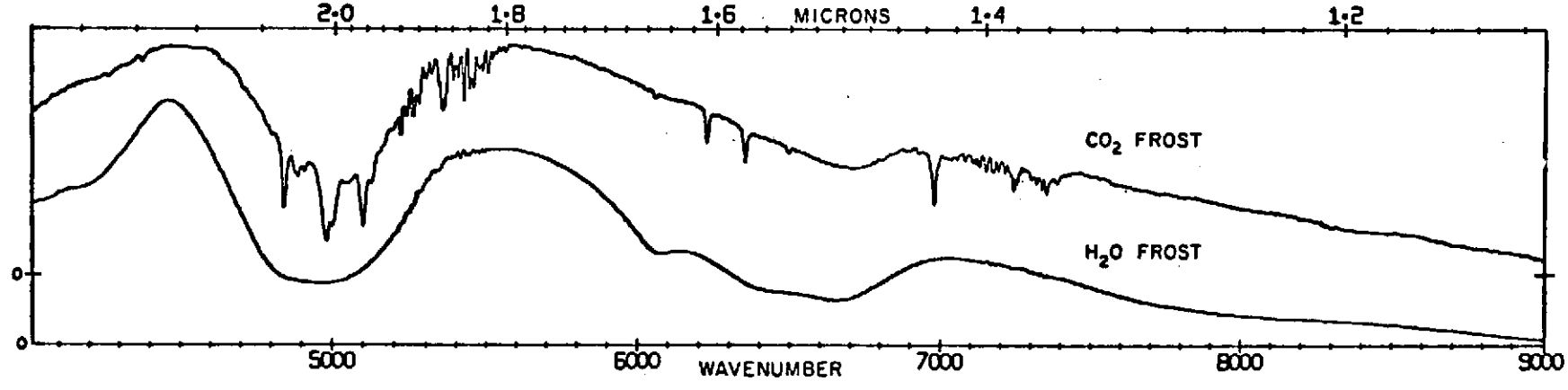
2·0
1·8
1·6
MICRONS
1·4
1·2
CO_2 FROST
H_2O FROST
0
0
5000
6000
WAVENUMBER
7000
8000
9000

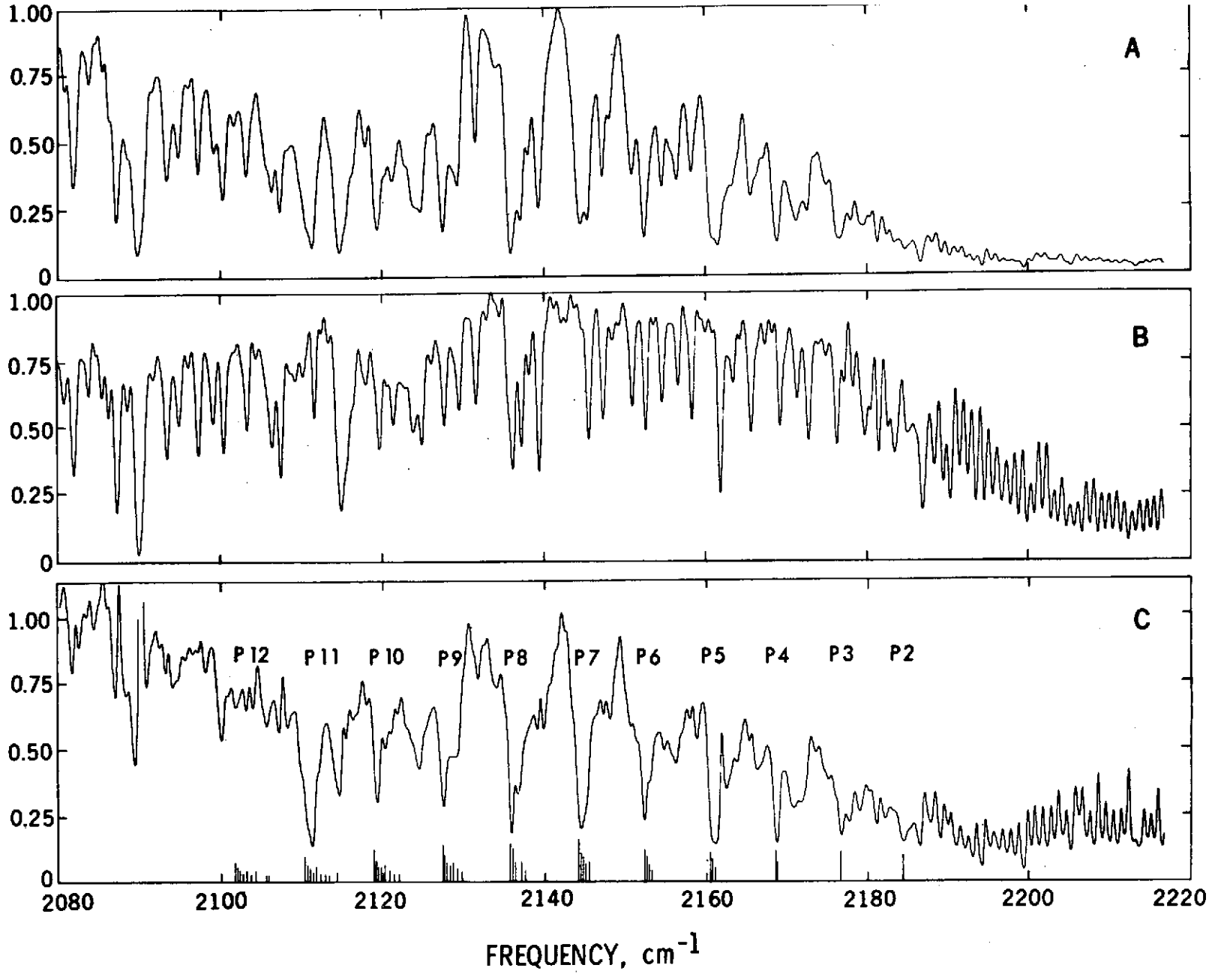
1.00
0.75
0.50
0.25
0
A
B
C
P 12
P 11
P 10
P9
P8
P7
P6
P5
P4
P3
P2
2080
2100
2120
2140
2160
2180
2200
2220
FREQUENCY, cm-1

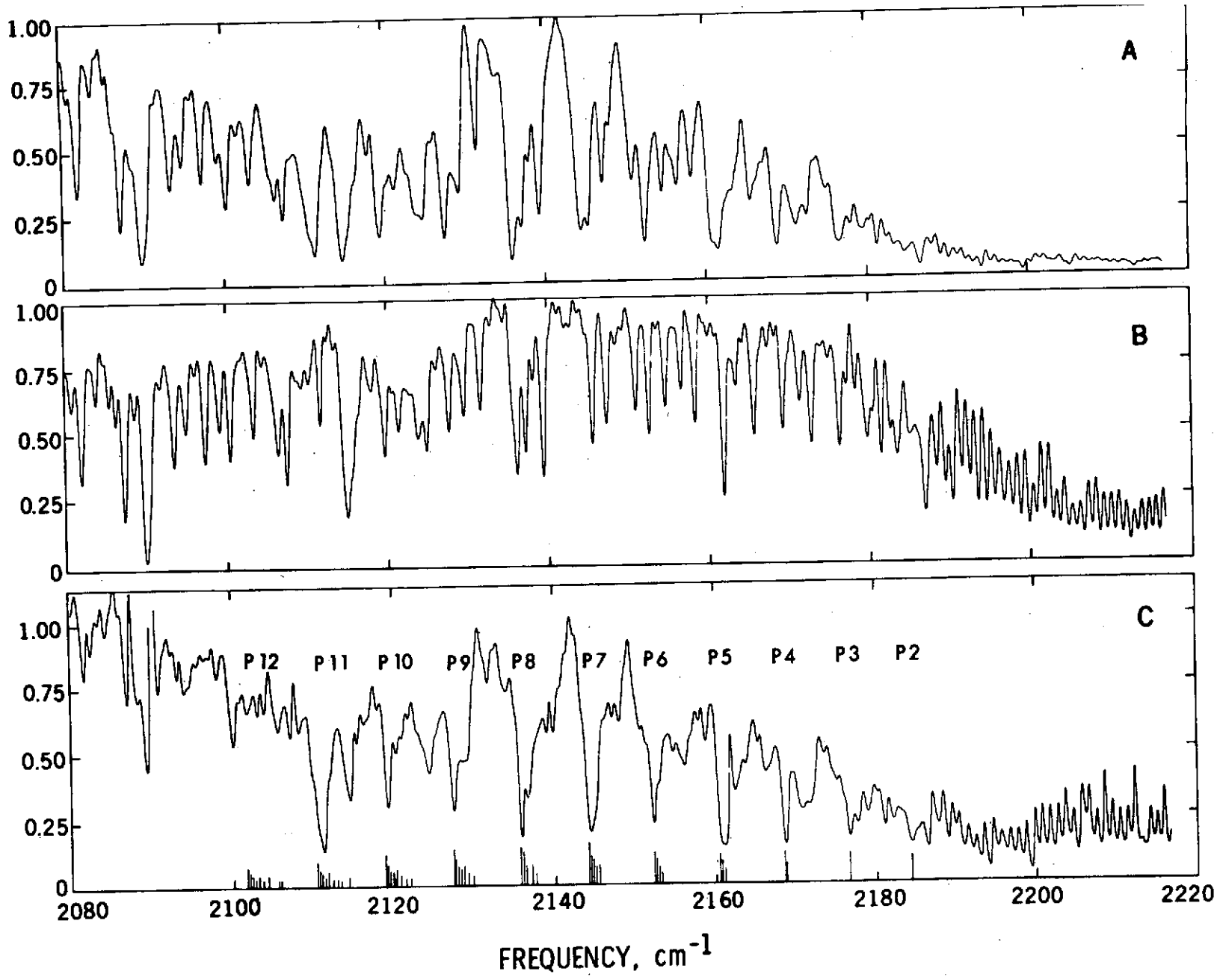
1.00
0.75
0.50
0.25
0
A
B
C
P 12
P 11
P 10
P9
P8
P7
P6
P5
P4
P3
P2
2080
2100
2120
2140
2160
2180
2200
2220
FREQUENCY, cm-1

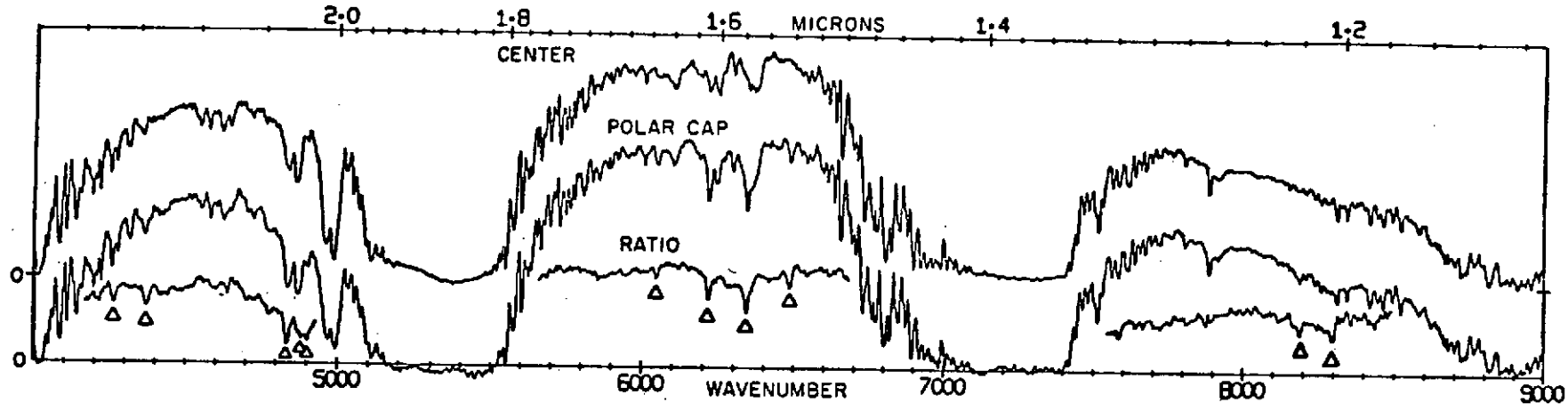
2·0
1·8
1·6
MICRONS
1·4
1·2
CENTER
POLAR CAP
RATIO
0
0
5000
6000
WAVENUMBER
7000
8000
9000

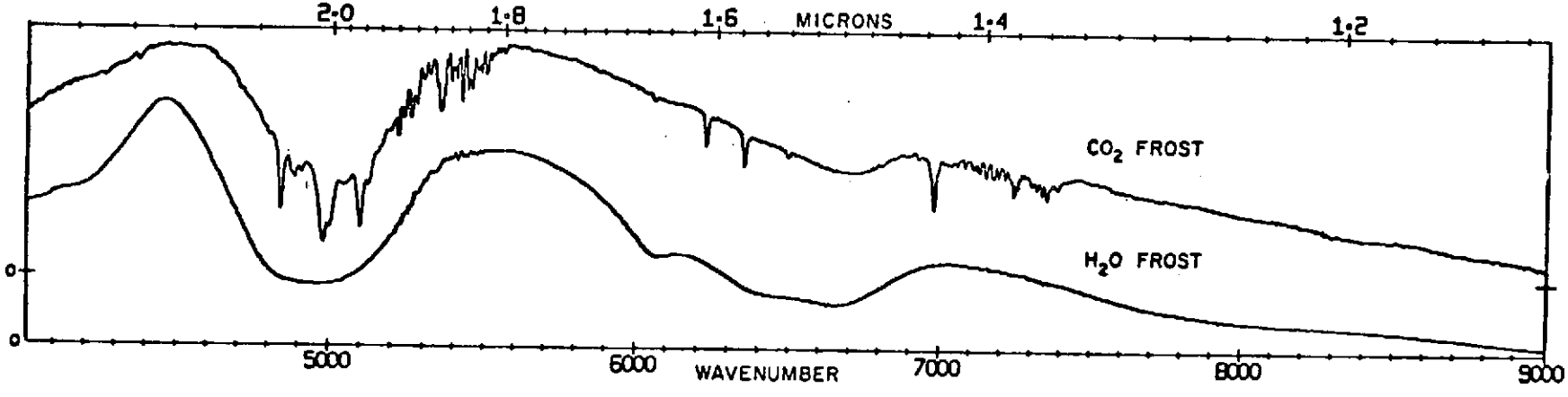
2·0
1·8
1·6
MICRONS
1·4
1·2
CO_2 FROST
H_2O FROST
0
0
5000
6000
WAVENUMBER
7000
8000
9000

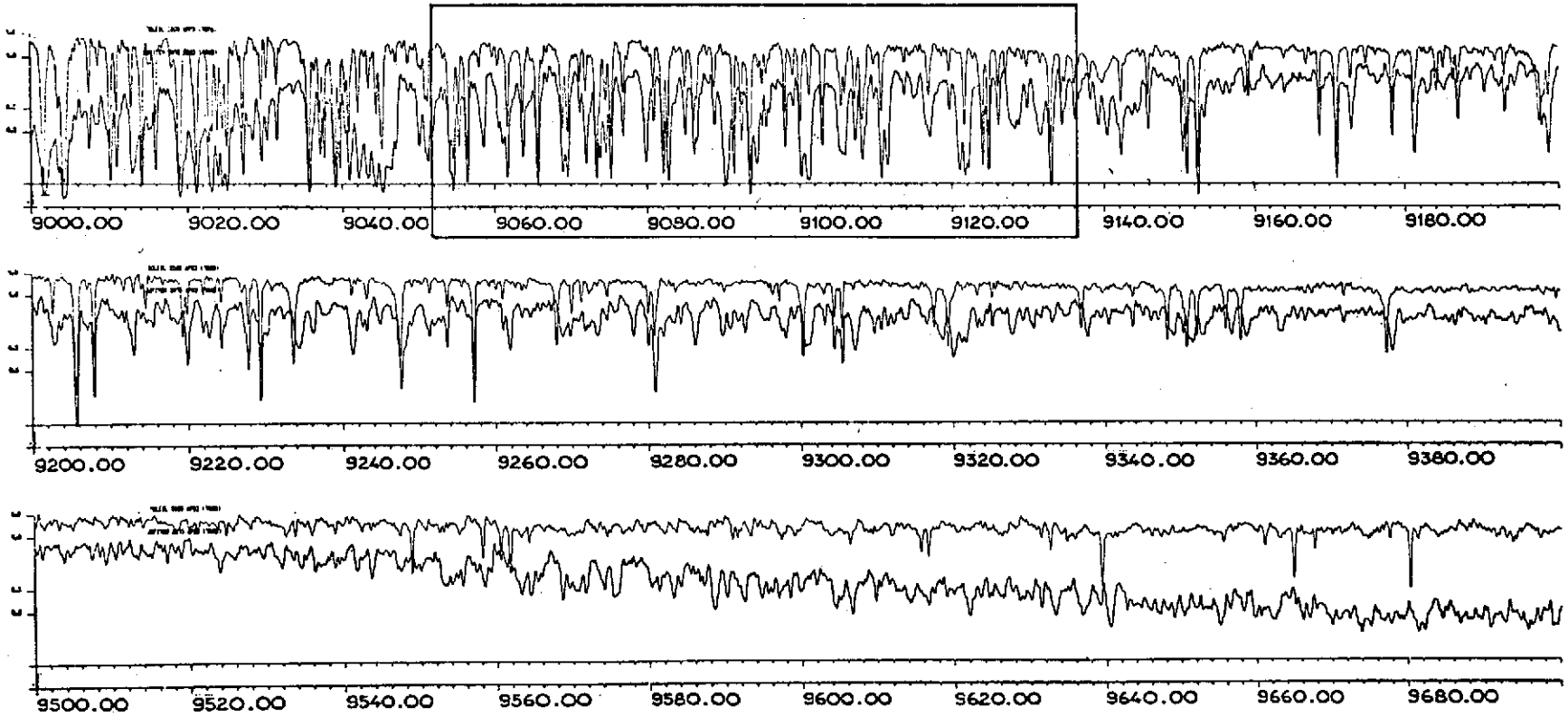
9000.00
9020.00
9040.00
9060.00
9080.00
9100.00
9120.00
9140.00
9160.00
9180.00
9200.00
9220.00
9240.00
9260.00
9280.00
9300.00
9320.00
9340.00
9360.00
9380.00
9500.00
9520.00
9540.00
9560.00
9580.00
9600.00
9620.00
9640.00
9660.00
9680.00

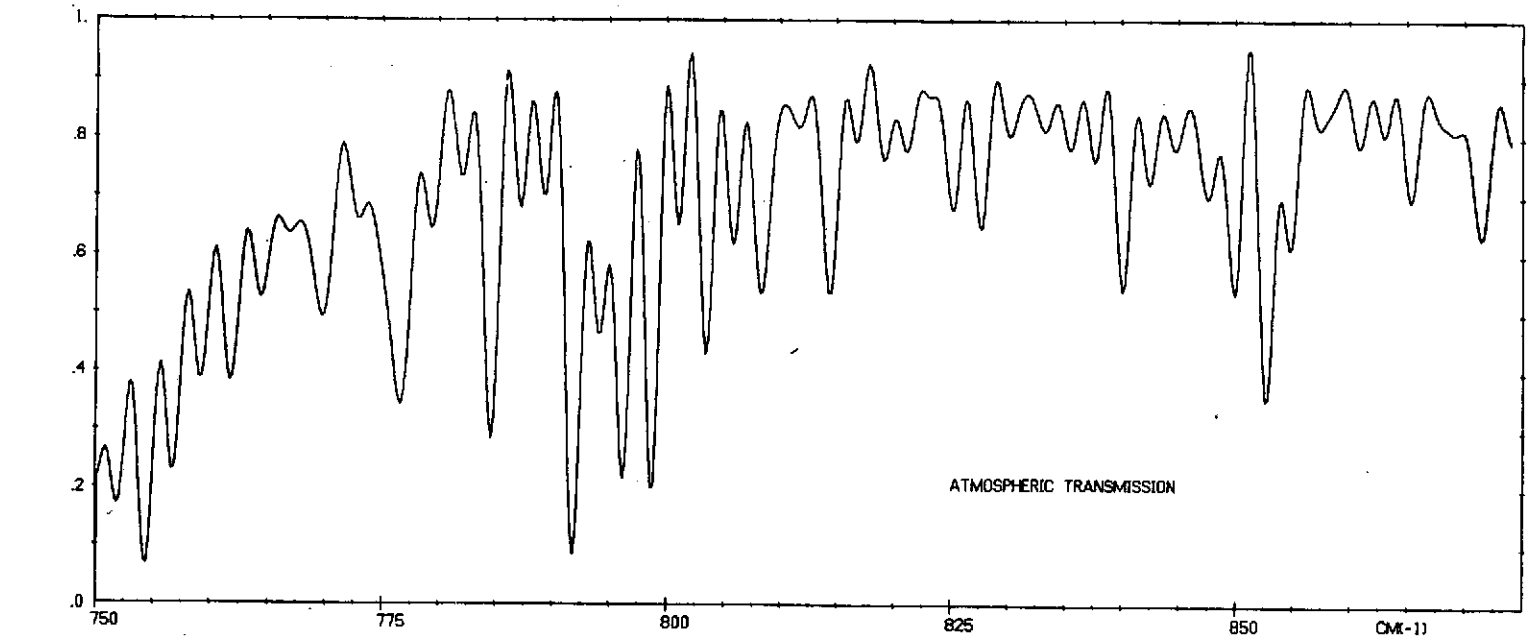
1.
.8
.6
.4
.2
.0
ATMOSPHERIC TRANSMISSION
750
775
800
825
850
CM(-1)

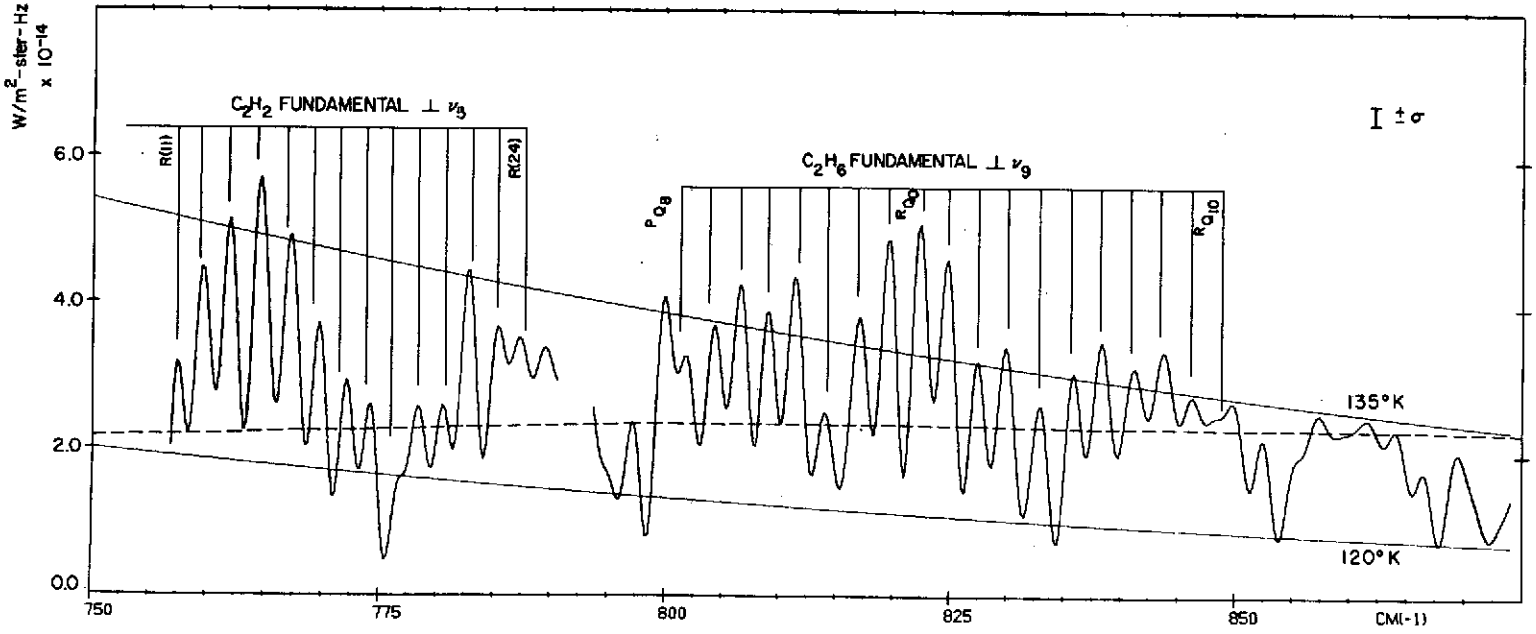
W/m²-ster-Hz
x 10⁻¹⁴
C₂H₂ FUNDAMENTAL ⊥ ν₅
R(1)
R(24)
C₂H₆ FUNDAMENTAL ⊥ ν₉
P Q8
R Q9
R Q10
I ± σ
135°K
120°K
6.0
4.0
2.0
0.0
750
775
800
825
850
CM(-1)

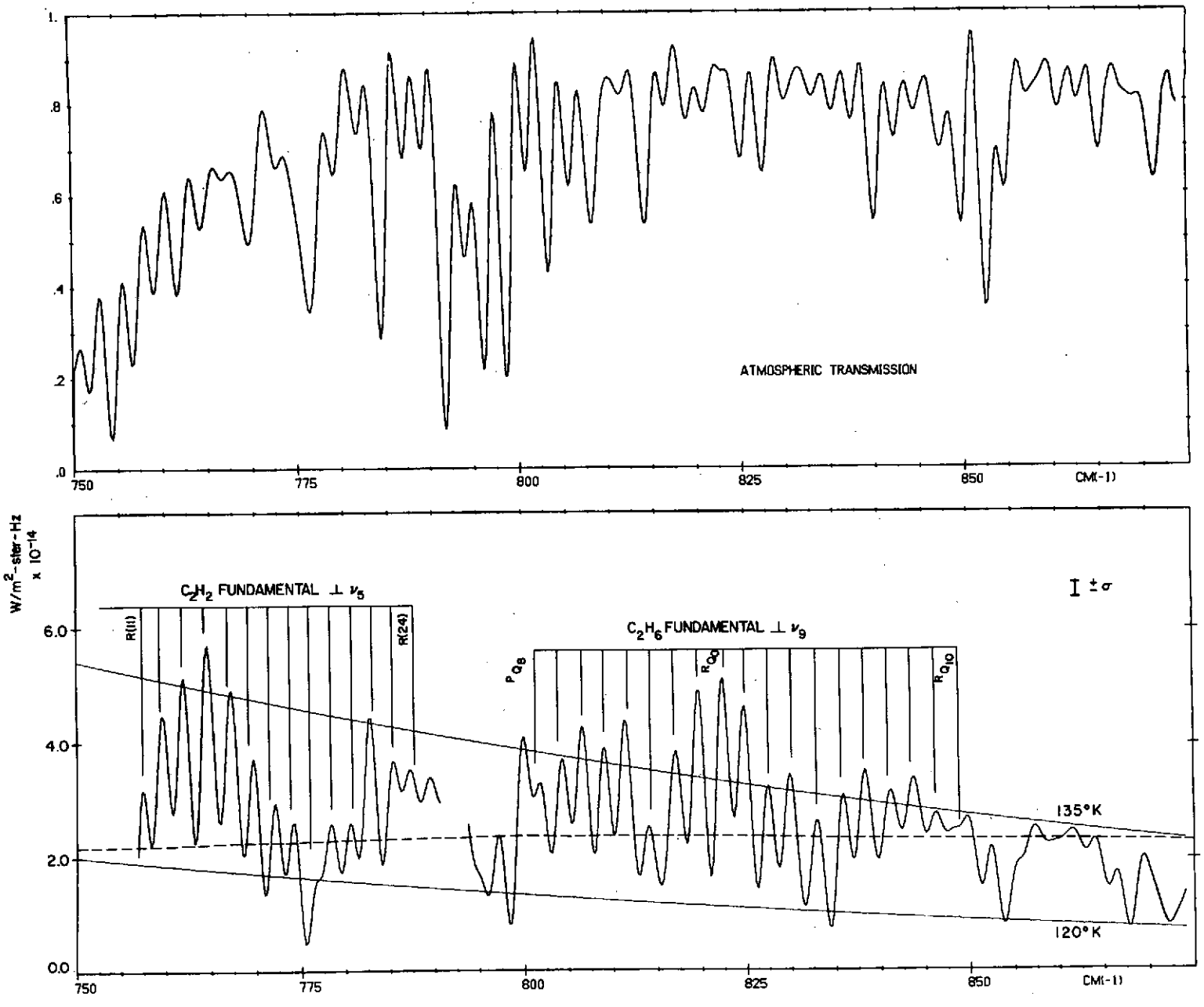
1.
.8
.6
.4
.2
.0
ATMOSPHERIC TRANSMISSION
750
775
800
825
850
CM(-1)
W/m²-ster-Hz
x 10⁻¹⁴
C₂H₂ FUNDAMENTAL ⊥ ν₅
R(1)
R(24)
C₂H₆ FUNDAMENTAL ⊥ ν₉
PQ8
RQ9
RQ10
I ± σ
6.0
4.0
2.0
0.0
135°K
120°K
750
775
800
825
850
CM(-1)

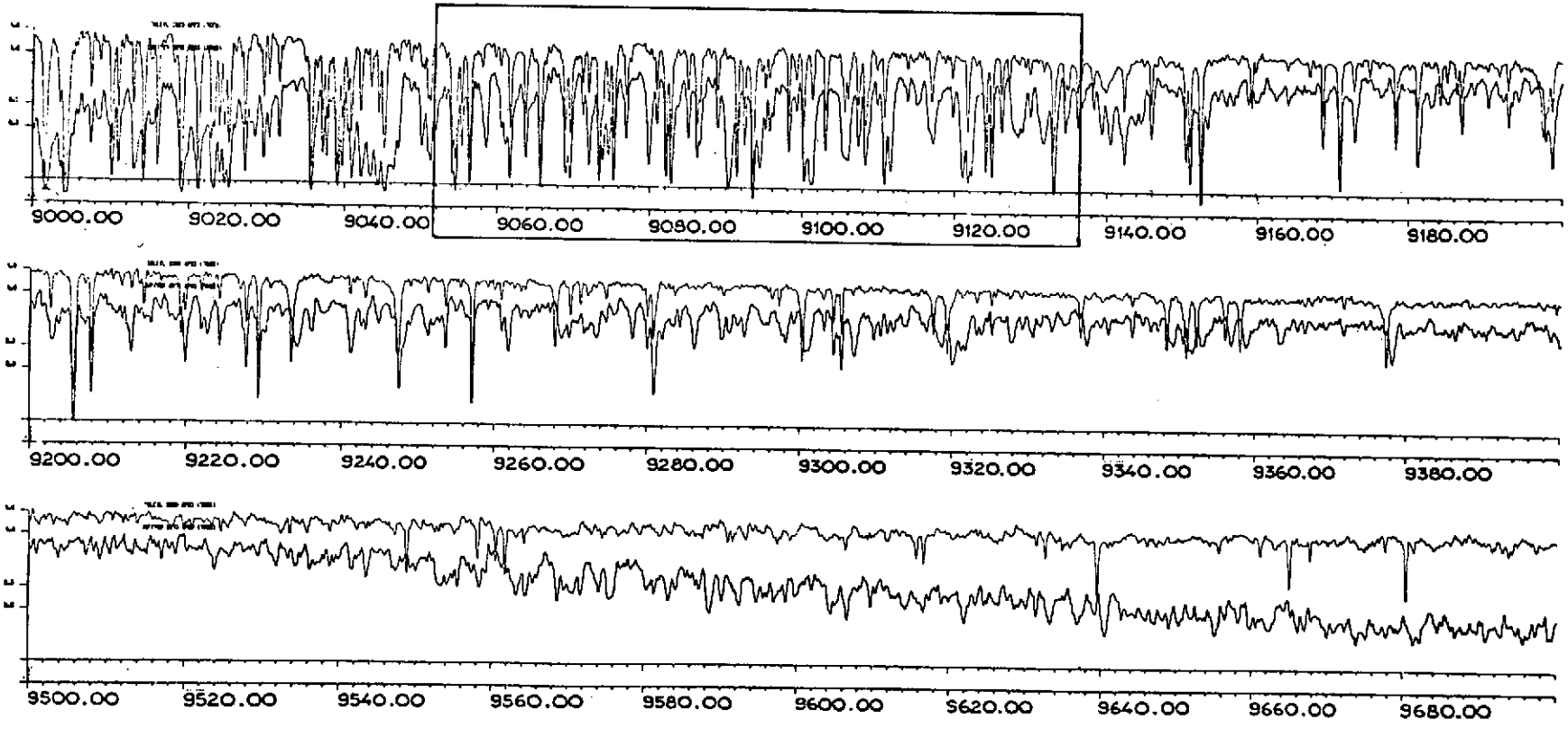
9000.00
9020.00
9040.00
9060.00
9080.00
9100.00
9120.00
9140.00
9160.00
9180.00
9200.00
9220.00
9240.00
9260.00
9280.00
9300.00
9320.00
9340.00
9360.00
9380.00
9500.00
9520.00
9540.00
9560.00
9580.00
9600.00
9620.00
9640.00
9660.00
9680.00

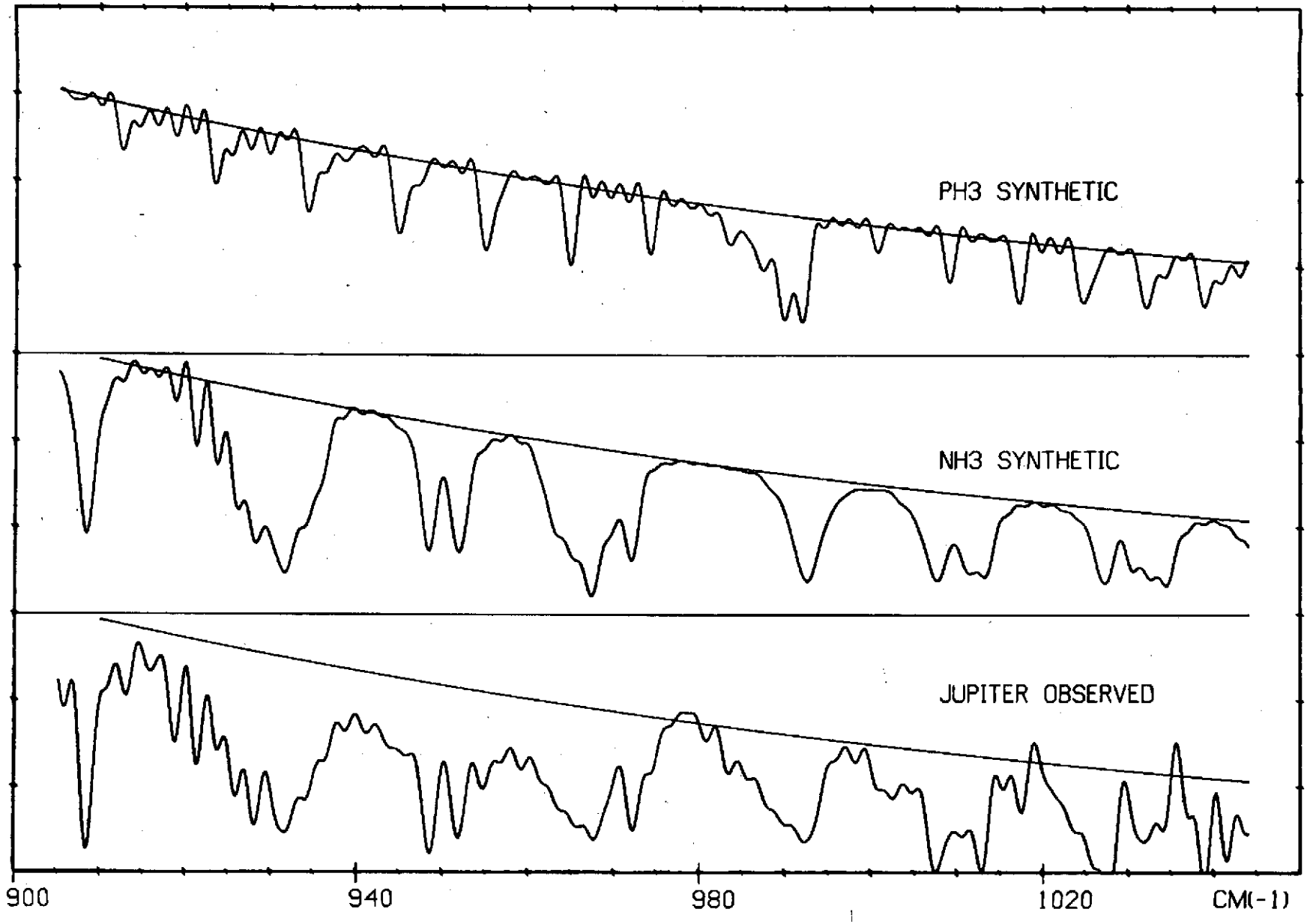
PH3 SYNTHETIC
NH3 SYNTHETIC
JUPITER OBSERVED
900
940
980
1020
CM(-1)

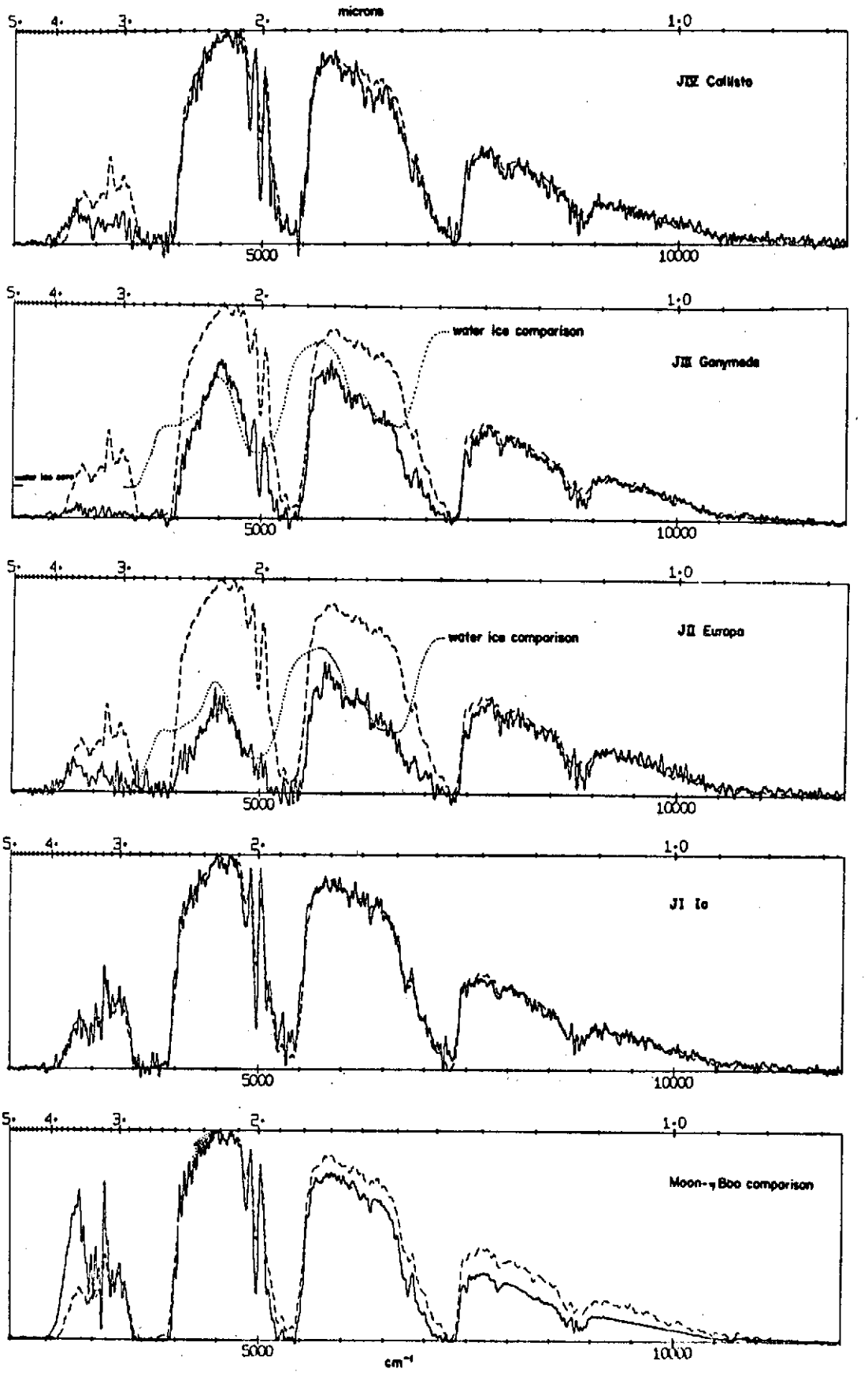
microns
5·
4·
3·
2·
1·0
JIV Callisto
5000
10000
water ice comparison
JIII Ganymede
JII Europa
JI Io
Moon-γ Boo comparison
cm⁻¹

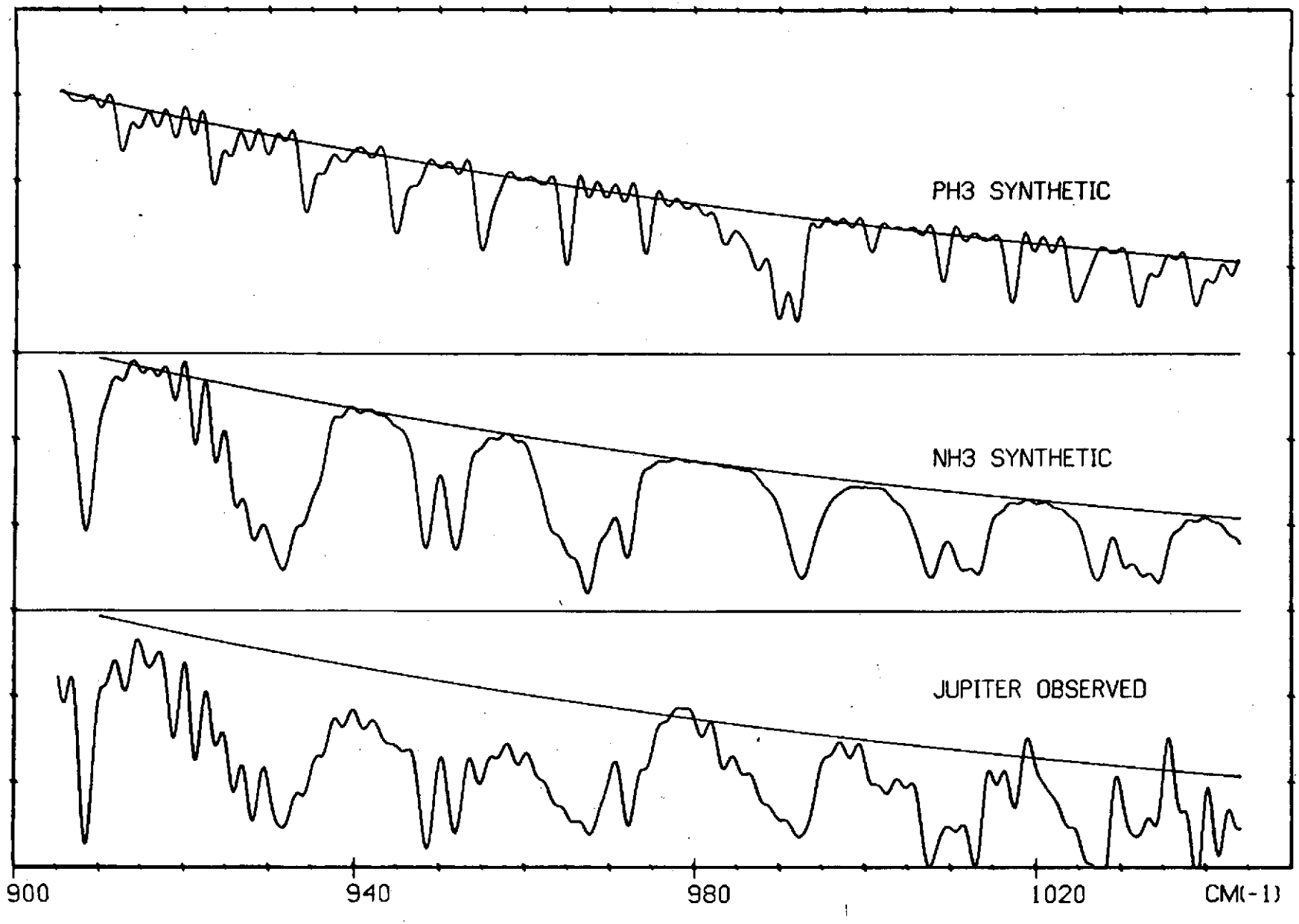
PH3 SYNTHETIC
NH3 SYNTHETIC
JUPITER OBSERVED
900
940
980
1020
CM(-1)

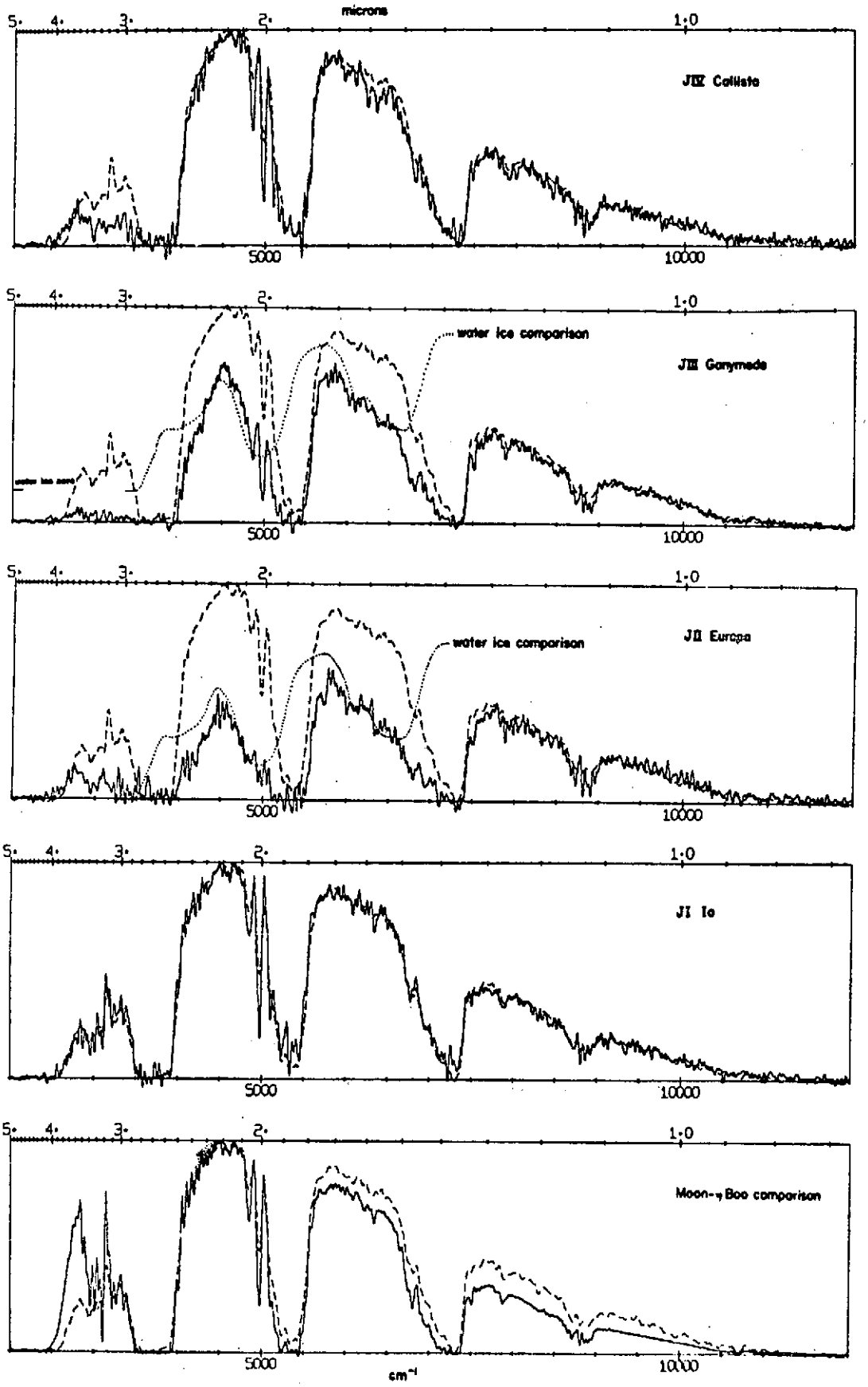
microns
5. 4. 3. 2. 1.0
JIII Callisto
5000
10000
water ice comparison
JIII Ganymede
JII Europa
JI Io
Moon-γ Boo comparison
cm⁻¹

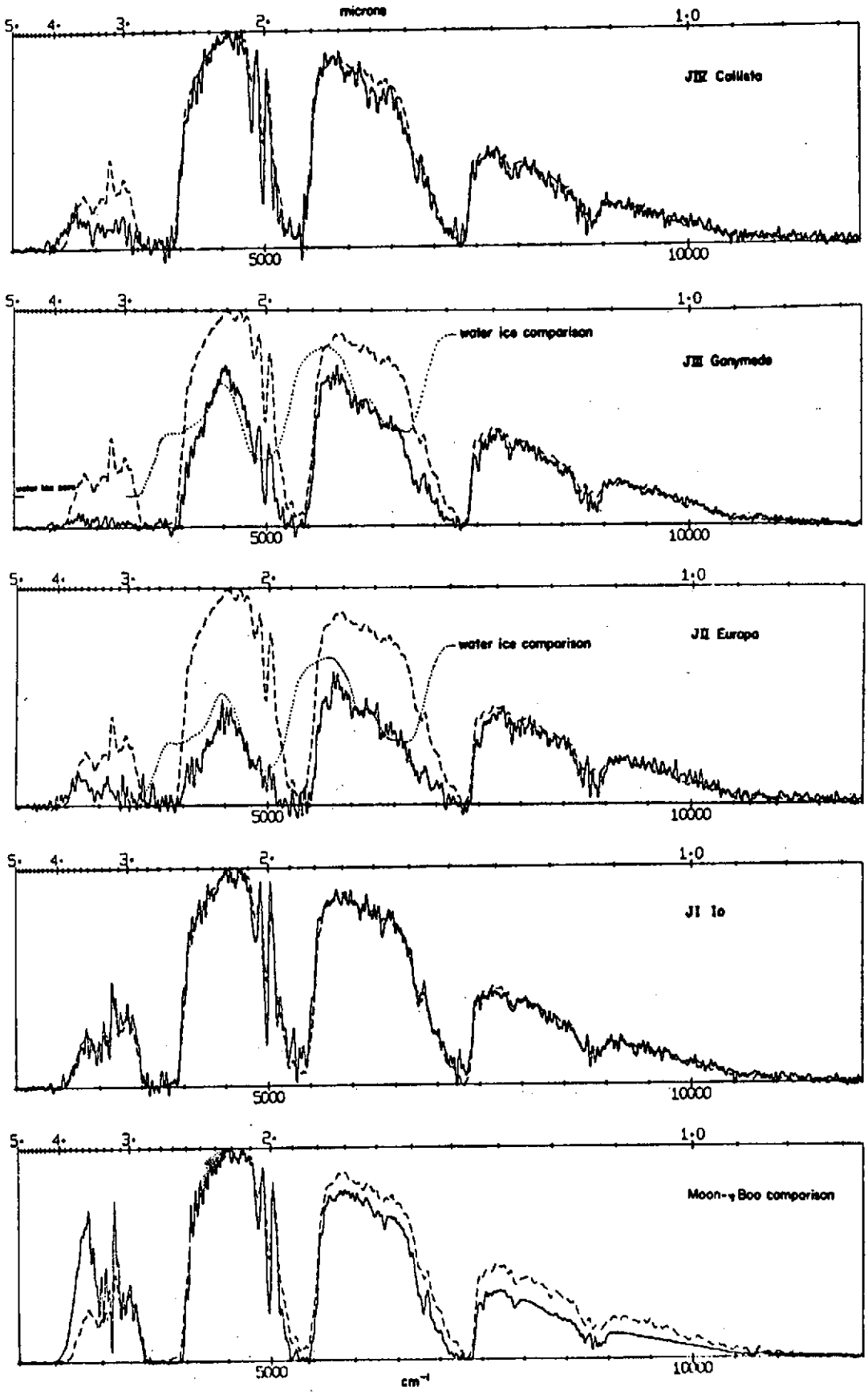
microns
5. 4. 3. 2. 1.0
JIII Callisto
5000
10000
water ice comparison
JIII Ganymede
JII Europa
JI Io
Moon-γ Boo comparison
cm⁻¹

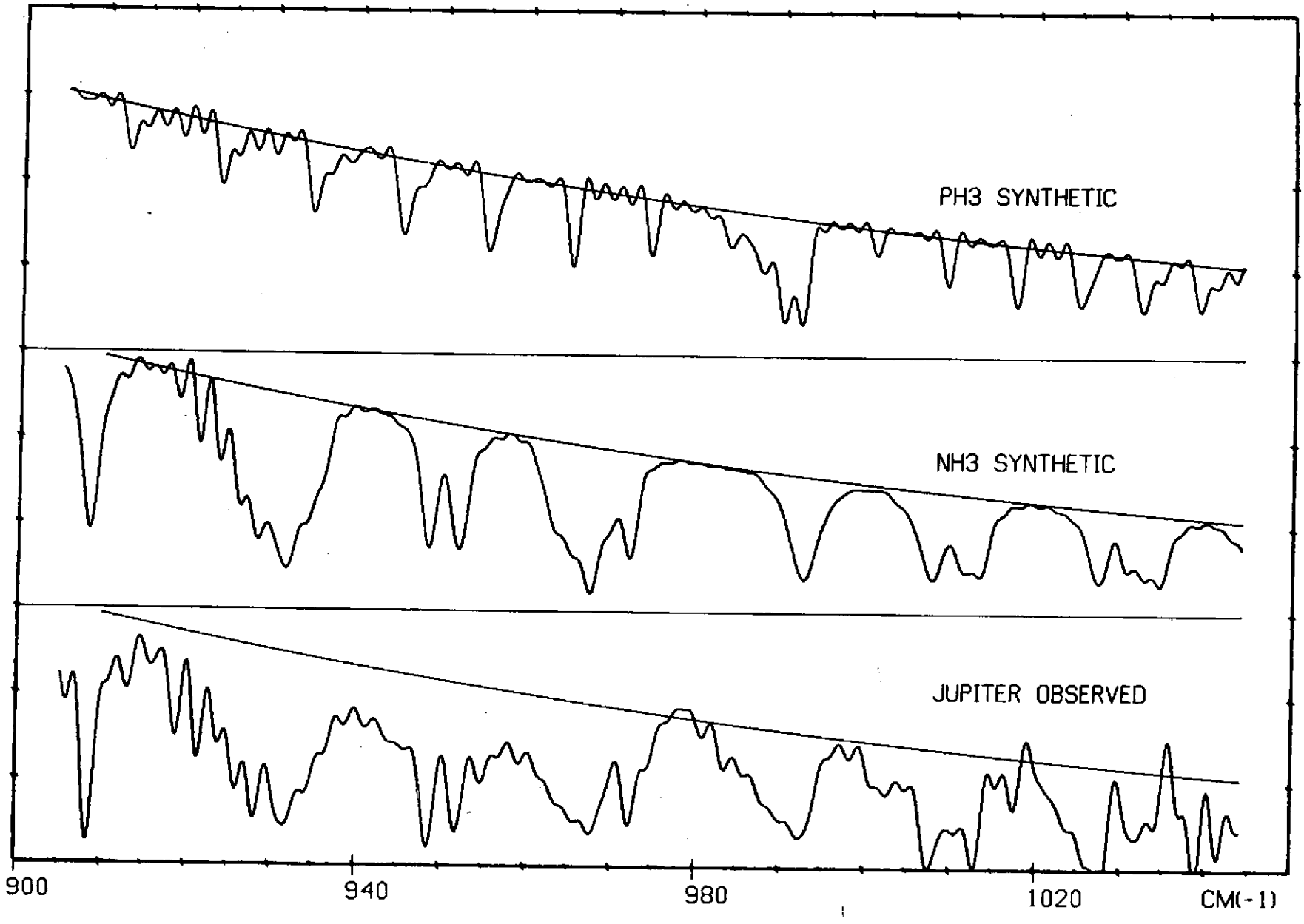
PH3 SYNTHETIC
NH3 SYNTHETIC
JUPITER OBSERVED
900
940
980
1020
CM(-1)

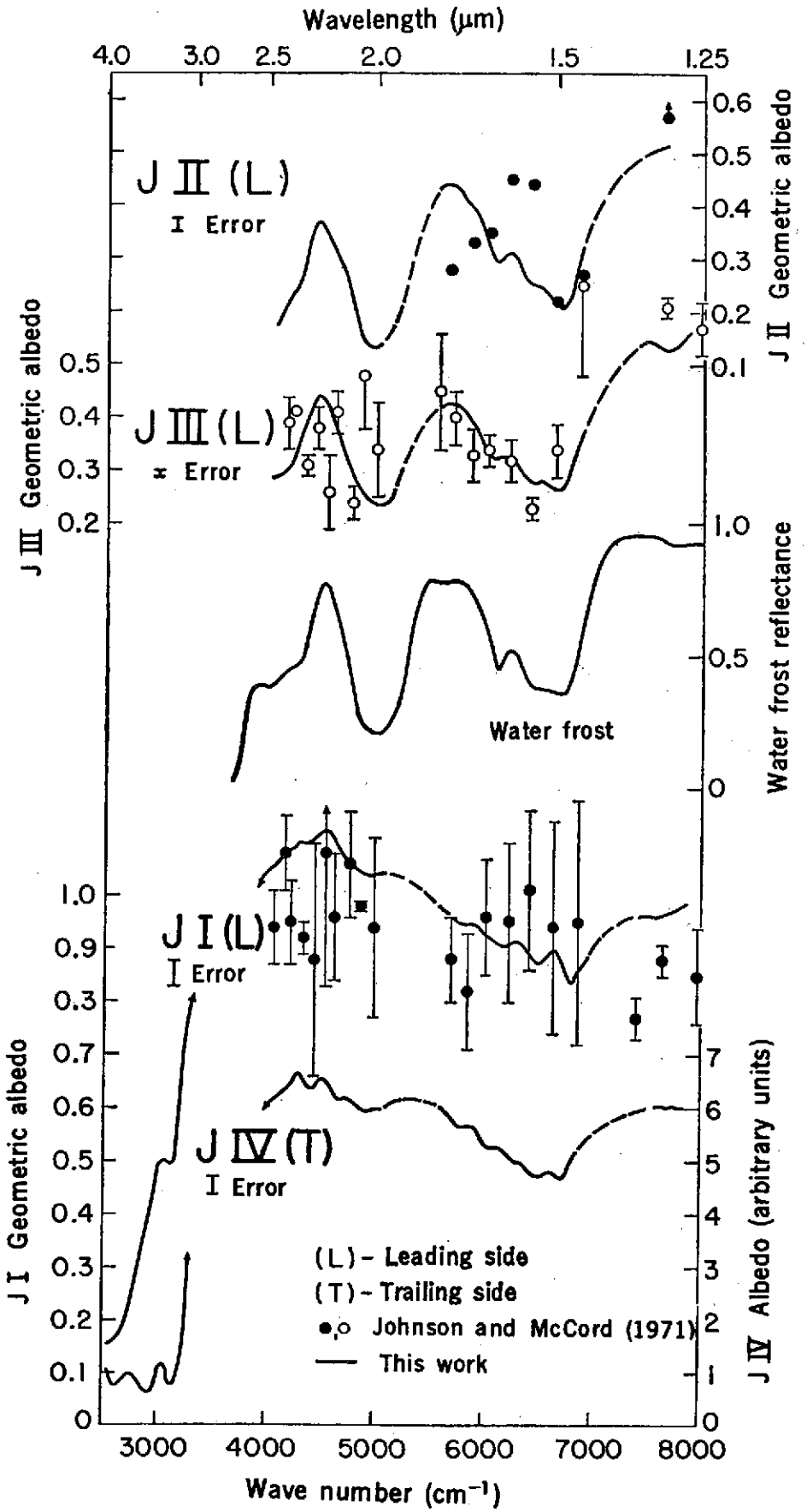
Wavelength (μm)
4.0
3.0
2.5
2.0
1.5
1.25
J II (L)
I Error
J III (L)
± Error
J I (L)
I Error
J IV (T)
I Error
Water frost
(L) - Leading side
(T) - Trailing side
Johnson and McCord (1971)
This work
J III Geometric albedo
J II Geometric albedo
Water frost reflectance
J I Geometric albedo
J IV Albedo (arbitrary units)
Wave number (cm⁻¹)
3000
4000
5000
6000
7000
8000

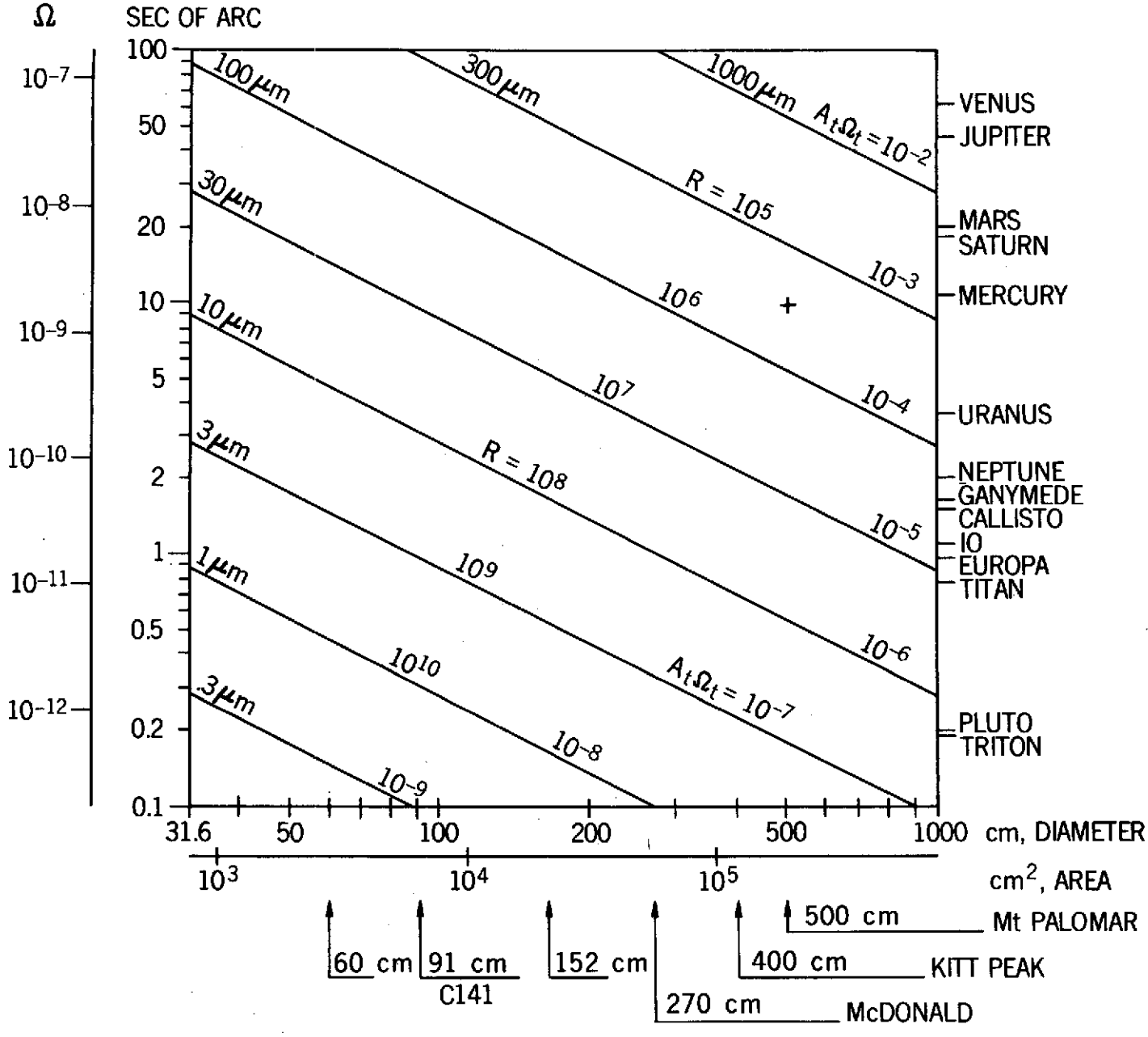
Ω
SEC OF ARC
100
50
20
10
5
2
1
0.5
0.2
0.1
10⁻⁷
10⁻⁸
10⁻⁹
10⁻¹⁰
10⁻¹¹
10⁻¹²
100 μm
300 μm
1000 μm
A_tΩ_t = 10⁻²
R = 10⁵
10⁻³
30 μm
10⁶
10⁻⁴
10 μm
10⁷
10⁻⁵
3 μm
R = 10⁸
10⁻⁶
1 μm
10⁹
A_tΩ_t = 10⁻⁷
.3 μm
10¹⁰
10⁻⁸
10⁻⁹
VENUS
JUPITER
MARS
SATURN
MERCURY
URANUS
NEPTUNE
GANYMEDE
CALLISTO
IO
EUROPA
TITAN
PLUTO
TRITON
31.6
50
100
200
500
1000
cm, DIAMETER
10³
10⁴
10⁵
cm², AREA
60 cm
91 cm
C141
152 cm
270 cm
McDONALD
400 cm
KITT PEAK
500 cm
Mt PALOMAR